

Dynamic Behaviour and Stability Analysis of an Accelerator Driven System (ADS)

Marco Jovanovich

ET-2165, Delft, November 2004

Members of the examination commission:

Prof. dr. ir. A.H.M. Verkooijen

Dr. Ir. J.L. Kloosterman

Ir. C. Ceballos

Abstract

Accelerator Driven Systems (ADS) represent an attractive way for the transmutation of high-level waste.

The concept consists of coupling a high energy particle accelerator with a sub-critical reactor core. Therefore, the neutron kinetic and the dynamic behaviour of an ADS is significantly different from those of conventional power reactors currently used for the production of power.

This project has studied the dynamic behaviour of the ADS by means of analytical models and linear stability theory. The objective was to characterize the reactor dynamic behaviour and to identify the most important parameters in driving the system response during the transients.

The work includes a parametric analysis of the reactor response to different perturbations and the stability analysis under source fluctuations during normal and accident conditions.

The results have shown that ADS is stable in operating conditions and in most of the analysed transients. Instability risk is only present under severe accident conditions. The proper choice of the sub-criticality level may reduce the risk of instability and allow a safer control on the system.

Abstract

L'ADS, acronimo di "Accelerator Driven System", costituisce una prospettiva interessante per la trasmutazione delle scorie ad alta radioattività.

L'idea di base consiste nell'accoppiare un acceleratore di particelle ad alta energia con un reattore sotto-critico. La cinetica e la dinamica dell'ADS e' dunque molto diversa rispetto a quella dei reattori convenzionali, utilizzati per la produzione di energia

Questa tesi ha studiato il comportamento dinamico dell'ADS attraverso modelli analitici e la teoria per la stabilita' dei sistemi lineari, con l'obiettivo di caratterizzare il comportamento dinamico del reattore ed identificare i parametri piu' importanti nel determinare la risposta del sistema durante i transitori.

Il lavoro comprende anche un'analisi parametrica della risposta del reattore a diversi tipi di perturbazioni e l'analisi di stabilita' quando il sistema e' sottoposto a fluttuazioni della sorgente, sia in condizioni normali, sia incidentali.

I risultati hanno dimostrato che l'ADS e' stabile in condizioni normali e in molti dei transitori analizzati. Il rischio di instabilita' e' presente soltanto nelle piu' severe condizioni incidentali. Un'adeguata scelta del livello di sotto-criticita' puo' ridurre il rischio di instabilita' e garantire un piu' sicuro controllo del sistema.

Acknowledgements

This assignment was done under the supervision of Prof. dr. ir. A.H.M. Verkooijen and Ir. C. Ceballos.

I would like to thank both of them to their help and advices in improving my work.

Many other people have contributed in different ways to this work.

Special thanks to Lisa and to my brother Paolo, who have improved the layout of the report and of the presentation.

I want also to thank all my friends who have lived or are still living in Delft for their support and precious advices.

Finally, I would like to thank my family and my friends in Italy for their support during my years at the University.

Contents

<i>Introduction</i>	1
---------------------------	---

Chapter 1 The sustainable Nuclear Fuel Cycle

1.1 Nuclear energy and nuclear waste.....	3
1.2 The role of ADS in the nuclear fuel cycle.....	4
1.3 Activities on ADS worldwide.....	5

Chapter 2 The ADS Concept

2.1 The accelerator.....	8
2.2 The spallation module.....	8
2.3 The fuel and the fuel cycle.....	9
2.4 The sub-critical reactor.....	10
2.5 Kynetic and dynamic behaviour.....	14

Chapter 3 Dynamics of critical reactors

3.1 Point Kinetics Theory.....	15
3.2 The inhour equation.....	17
3.3 Response to a step-wise reactivity insertion.....	19
3.4 Approximate dynamic equations.....	21
3.5 Frequency response and transfer function.....	23
3.6 Reactivity feedback.....	25
3.7 The Nordheim-Fuchs model.....	26

Chapter 4 Stability of critical systems

4.1 Feedback and Transfer Function.....	29
4.2 Criteria for linear stability analysis.....	30

4.3	Stability of critical reactors: forward-loop transfer function.....	34
4.4	Feedback transfer function.....	36
4.5	Reactor system with feedback.....	37
4.6	Two-path feedback model.....	38
4.7	Considerations for fast reactors analysis.....	41

Chapter 5 *Dynamic behaviour of sub-critical systems*

5.1	System response to a step-wise change in the source.....	43
5.2	The Prompt Jump approximation.....	51
5.3	The Fuchs Model for sub-critical system.....	55

Chapter 6 *Stability analysis of sub-critical systems*

6.1	Reactor core transfer function.....	59
6.2	Six groups approximations.....	66
6.3	Temperature feedback.....	71
6.4	Six groups and lumped model.....	76
6.5	The feedback transfer function with delay.....	82
6.6	Six groups approximation and delayed feedback.....	85
6.7	Stability in case of reactivity fluctuations.....	91

Chapter 7 *Conclusions and Recommendations*.....95

***Appendix*.....97**

***References*.....101**

Introduction

As part of the curriculum at Politecnico di Milano a final assignment has to be completed by each student. It is in this framework that the present report on Dynamic Behaviour and Stability Analysis of an Accelerator Driven System has been written. Since one of the possibilities offered by Politecnico is to write the thesis in a foreign university, this work has been performed at TU Delft, in the section Energy Technology of the Faculty of Mechanical Engineering.

Studies on thermal-hydraulics of Accelerator Driven Systems (ADS) at TU Delft are currently driven by Prof. Verkooijen and by Ir. Ceballos, with the aim of studying the thermal-hydraulic behaviour during steady state and transient conditions and thus propose and evaluate enhancing mechanisms that could improve ADS' safe operation.

The availability of a wide range of reliable software has often decreased the interest in finding analytical solutions, which can be a flexible tool and can help understanding a complex problem by looking at simple cases.

The interest of the author in this field and the fruitful discussion with Ir. Ceballos and Prof. Verkooijen has been the starting point of this Master Thesis, which should provide a complementary work within the project and an understanding on aspects that cannot be directly handed by the permanent researchers.

The goals of the thesis are:

1. Characterize the dynamic behaviour of a sub-critical reactor by means of analytical models and study the influence of various parameters in reactor response to source and reactivity fluctuations.
2. Study the stability of the system in case of both source and reactivity fluctuations, in presence and absence of feedback.

The interest in these topics is increased by their novelty. A wide literature research has shown that no books currently exist on ADS and that and not so many papers concerning analytical studies or stability analysis have been published.

Chapter 1 of this report is an introduction on the nuclear fuel cycle and the problem of nuclear waste while Chapter 2 provides a general description of the ADS.

Since the theory on critical systems is robust and experimentally validated, it is an important starting point in developing the one for ADS. Therefore, in chapter 3 and 4 the concepts of critical reactor theory relevant to study the ADS are presented. In particular, chapter 3 gives an overview on critical reactors dynamics, with a focus in the most used models and approximations while chapter 4 briefly presents the most important stability criteria and gives an overview on their application to critical reactors. The linear stability theory is used.

The theory on sub-critical systems is derived in chapter 5: point kinetics system with source is solved and transients at different sub-criticality levels and for different

values of the parameters are studied. The complexity of the equations defines the limit in finding analytical solutions: only a few simple cases can be manually handed.

Chapter 6 is entirely dedicated to stability analysis of ADS, mostly in case of source fluctuation and at different level of complexity: with or without feedback and with or without delay. Matlab codes are used to study the transients. A comparison of the results at different complexity levels gives an understanding on the importance of the approximations and the magnitude of the various effects.

Results are discussed in Chapter 7, where a few recommendations for further research are also suggested.

Chapter 1 The sustainable Nuclear Fuel Cycle

1.1 Nuclear energy and nuclear waste

The search for high living standards, together with the growth of the population worldwide has led to a continuous increase of energy consumption.

In the last decade, the massive use of fossil fuels has been questioned for the limited availability of these sources, for the political instability in most of the supplying countries and for environmental concerns, especially related to the greenhouse induced global warming.

The possibility for alternative energy sources (sun, wind, tides, biomass ...) has been investigated and interesting results have been reached but an extensive use is not yet possible in a market economy with the current technological level.

Nuclear energy, which is Greenhouse free, attracted a lot of interest in the 60s and 70s, when many nuclear power plants were built. The impossibility in giving compelling responses to the public's safety concerns, somehow validated by a few accidents (TMI, Chernobyl), has decreased the popularity of nuclear energy so that nowadays nuclear power only accounts for 4.5% of the total energy production [Nifenecker et al, 2001]. Nevertheless, the interest in nuclear energy has never ceased and an increase in the nuclear power share up to 15% is still considered one of the possible scenarios to reduce Greenhouse emission [WEC, 2002].

The most pronounced problem with the use of nuclear power is how to safely take care of wastes, mostly consisting in the spent fuel elements extracted from operating reactors. Only wastes with lifetimes exceeding about 10 years are considered a significant storage problem; all the others, after a proper treatment, can be safely stored in specialized centres till their radio-toxicity becomes negligible.

Different strategies to ensure that these long life wastes will not interplay with the biological life on earth have been proposed through the years; the most important are:

1. Direct underground storage of spent fuel elements, without any reprocessing.
2. Partitioning, incineration and transmutation to reduce the amount, the radio-toxicity and the half-life before disposing the remaining waste in a geological repository.

The option currently adopted is the first but the difficulties in finding a suitable site, the enormous cost in building it and the very long time horizon to reduce the radio-toxicity level have made the second one very attractive.

If Plutonium and Minor Actinides (MA), which are mainly responsible for the long-term radio-toxicity, are removed from the waste (partitioning) and fissioned (incineration) or transformed into stable elements by neutron absorption (transmutation) the remaining waste loses most of its long term radio-toxicity. The half-life and the amount of waste can be reduced by a factor higher than 1000 and 100 respectively [Roadmap, Enea, 2001]. As shown in Fig.1.1, the reference radio-

toxicity level would be reached in about 700 years. The process has also a reasonably good efficiency, because losses during reprocessing can be kept well below 1%. In addition, incineration leads to energy production.

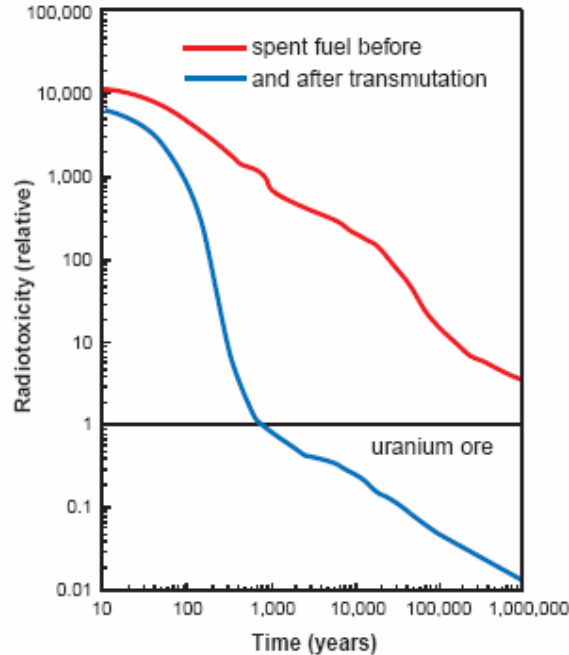


Fig 1.1: Ingestion radio-toxicity of spent nuclear fuel. With a separation efficiency of 99.9% of the long-lived by-products from the waste, followed by transmutation, reference radio-toxicity level can be reached within 700 years. [Roadmap, Enea, 2001]

1.2 The role of ADS in the nuclear fuel cycle

Neutron's fission and absorption cross sections suggest that fast neutrons, and thus fast reactors, are required to perform incineration and transmutation. While the reliability and safety of PWRs has been widely demonstrated in industrialized western countries, the experience with fast breeder or converter reactors is still more limited.

For this reason, the idea of a sub-critical system driven by an accelerator proposed by C. Rubbia in 1995 has encountered a lot of interest in the scientific community.

The possibility of accelerator based transmutation has been discussed as a concept since the 40s mostly for breeding fissile material from fertile Thorium and Uranium [Brookhaven National Laboratory, 1977] but the high power accelerators needed for this purpose were not technically available until fairly recently.

In contrast to conventional critical reactors in which there are enough neutrons to sustain a chain reaction, a sub-critical system used in accelerator driven system (ADS) needs an external neutrons source to sustain the chain reaction. These extra neutrons come from spallation reactions induced by high energy protons from an accelerator.

The ADS concept thus consists of coupling a high energy particle accelerator with a sub-critical reactor core.

The advantage in building such a new system is that ADS has more control and flexibility, which is required when the reactor is used to transmute a large amount of nuclear waste in the form of MAs. In fact the mixture of Actinide waste and native Thorium that should be used as a fuel for ADS has a delayed neutrons emission twice as low than ^{235}U : this causes control problems that cannot be efficiently handled in a critical assembly.

In sub-critical systems the neutrons source strength plays a major role because without its extra neutrons the reaction cannot sustain itself and the power level will thus be lowered. The possibility of switching off the source at any time, thus stopping the chain reaction, should provide high safety standards.

The first Conceptual Design [Rubbia et al, 1995] is based on a 1500 MW_{th} reactor driven by an accelerator able to produce a proton current up to 20mA in order to cope with the inevitable variation of performance during fuel lifetime. The coolant medium is molten natural lead operating at a maximum temperature of $600\text{ }^{\circ}\text{C}$; such a high temperature is possible because of the high boiling temperature of lead and allows achieving efficiency up to 45%.

A most relevant feature in the design is the possibility of using natural convection alone to remove all the heat produced inside the core. Elimination of all pumps in the primary loop is an important simplification and a contribution towards safety since, unlike pumps, natural convection cannot fail.

A more detailed description of the reactor in all its components is given in Chapter 2.

1.3 Activities on ADS worldwide

The promising characteristics of the first Conceptual Design have required further studies and validation. For this reason, the research on ADS for waste incineration/transmutation and energy production has considerably expanded during the last few years. The focus on the present ADS research worldwide is on incineration and transmutation while the production of nuclear energy by ADS, using fresh Thorium, is on a longer time scale.

The funds available for partitioning and transmutation research have increased by a factor of 10 going from the 4th to the 5th Framework Program of the European Commission and by another factor of 3 from the 5th to the 6th [Roadmap, Enea, 2001]. The support now covers several research projects involving studies on partitioning, fuel, spallation, sub-critical reactors and nuclear data.

The research ministries of France, Italy and Spain have agreed on collaboration on research of ADS. Several other European countries, like Belgium and The Netherlands, have joined this effort on a working-group level. This technical working group, chaired by C. Rubbia, has presented in April 2001 a “roadmap” report on research and development leading to an European ADS demonstration facility (XADS) in year 2015, and a prototype (XADT) around 2030 [Roadmap, Enea, 2001]. At the moment three prototypes are being studied: a 80 MW LBE-Cooled

concept, a 80 MW Gas-Cooled concept and a 50 MW LBE-Cooled concept (MYRRHA). These three concepts have been developed at a sufficient level as to allow the identification of critical issues and, in several cases, to propose some effective solutions [Cinotti et al, 2003].

Accelerator Driven Systems have encountered a lot of interest also outside Europe. In the USA a new project (AAA = Advanced Accelerator Applications) has been initiated and several other studies are carried on in Russia, Japan (OMEGA project) and in Korea.

In the Netherlands the activity on ADS is mainly concentrate in four institutes, often cooperating together and involved in many national and international projects: NRG (Petten), KVI (Eindhoven), NIKHEF (Amsterdam) and IRI/TU Delft (Delft). In the latter the emphasis is put on dynamics and thermal-hydraulics of ADS, on the fundamental aspects of sub-critical reactor physics and on the measurement and calculation of the reactivity and kinetic parameters. The latter research has been performed in collaboration with the other partners in the MUSE project, concluded at the end of 2003 [5th Framework Program, 1998-2002].

Chapter 2 The ADS Concept

In this chapter a basic description of ADS in all its components is given. A wide literature survey has shown that a lot of work has already been done but much more has still to be done. Neither a comprehensive work nor full agreements on the design have been reached by the different research groups.

Therefore the purpose of this chapter is to describe the structure of the system and to provide the reader with an overview on the discussion within the scientific community and the different options that are currently under evaluation.

As discussed in more details in the following sections, the key issues and main technical and safety options to be investigated are related to the following ADS components:

- Accelerator
- Spallation module
- Fuel and fuel cycle
- Sub-critical reactor

In addition, the interfaces and coupling of these components need to be studied and they sometimes constitute one of the most challenging parts in the research.

A schematic view of ADS is drawn in the figure below.

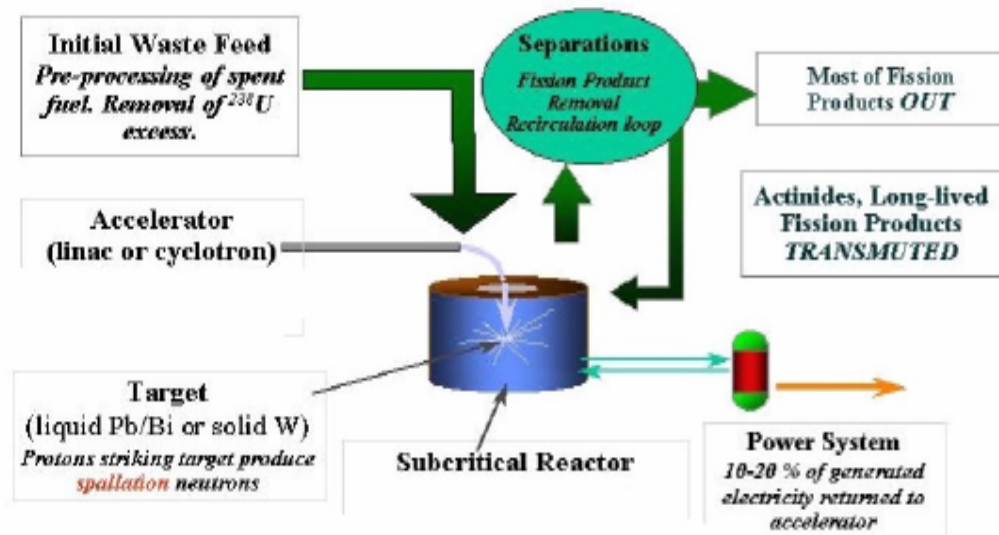


Fig 2.1: Main components of an ADS transmutation facility [Conde', 2002]

The main focus in the project is on the sub-critical reactor; nevertheless a brief overview on the other components will be given for completeness.

2.1 The accelerator

In the Conceptual Design [Rubbia et al., 1995] the novelty and the key role played by the accelerator had already been understood.

The accelerated particles are protons and the physics of spallation reactions and of energy depositions favours the choice of a kinetic energy of about 1 GeV [Roadmap, Enea, 2001].

While such a kinetic energy is well within the state of the art, the related beam intensity from 10 up to 20 mA requires an increase of presently available capability [Roadmap, Enea, 2001].

Nevertheless, results obtained at PSI and the experience accumulated at CERN and elsewhere suggested this goal to be perfectly achievable [Rubbia et al., 1995]. Further studies have confirmed this optimistic prevision [Roadmap, Enea, 2001].

The accelerator design, formerly based on a three stages cyclotron accelerator [Rubbia et al., 1995] has more recently been changed into a three stages LINAC accelerator [Roadmap, Enea, 2001] where a low energy but high intensity proton beam is first created and after accelerated at medium energy (second stage) and at high energy (last stage). The optimal solution is still under study and evaluation [Roadmap, Enea, 2001].

Besides the desired energy and intensity, the accelerator should fulfil the highest standard of reliability and safety. The former requirements are essentially related to the number of allowable beam trips: frequently repeated and long duration beam trips can damage the reactor structure, the spallation target or the fuel in the sub-critical core. The available results show that the allowable duration of beam trip is about 1s and that in the existing accelerator the number of beam trips still exceed ADS requirements [Roadmap, Enea, 2001].

Safety issues are mainly related to power control: the accelerator should be quickly shut down in any accident scenarios and not restarted until a safe mode operation is set up. Other safety concerns imply the containment of radioactive materials in the spallation target and the radiological protection of the operators.

2.2 The spallation module

The spallation module or target is probably the most important component of the ADS because it represents the coupling between the accelerator and the sub-critical core.

It is very sensitive since it is subjected both to severe thermal-mechanical loads and damage due to high energy particles (protons, spallation and fission neutrons, irradiation and spallation products). Therefore, its optimum design should be based on a compromise between neutron efficiency, material properties and thermal-hydraulic performances. Moreover, a suitable lifetime, ranging from a few months to one year, should be achieved.

The physics of spallation reactions suggests that the highest conversion efficiency is reached with high-Z nuclei target material and high kinetic energy of colliding protons. The required high beam power poses significant problems in cooling the target: a low melting heavy metal mixture, like LBE (Lead-Bismuth eutectic), has been considered the best option so far [Roadmap, Enea, 2001]. One of the

advantages in using LBE is that this mixture should also be used as a coolant, thus allowing a full compatibility between the target and the coolant. Nevertheless, corrosion-erosion problems have to be carefully considered [Roadmap, Enea, 2001].

Another design choice to be made is to either couple the proton beam into the LBE through a solid window (window option) or directly (windowless option). The original design by Rubbia proposed the use of a thin Tungsten window; other materials, like ferritic-martensitic steel are currently under study [Cinotti et al, 2003]. Such a wide and fruitful discussion highlights the importance of this component for the whole system; nevertheless, according to the XADS Roadmap [Enea, 2001], the final choice has to be made around the year 2006.

2.3 The fuel and the fuel cycle

The first ADS concept was thought to be operated with a variety of different fuels with the double purpose of both transmuting the spent fuel elements of thermal reactor and of producing energy. The proposed mixture was about 16% MA waste and 84% Thorium by weight [Rubbia et al, 1995]. The use of Thorium and MA and of breeder or converter reactors could extend the duration of the reserves of Thorium and Uranium considerably [Nifenecker et al, 2001].

The technical difficulties encountered in realizing the ideas in the Conceptual Design have led to a different choice at least in the near future.

The experimental reactor XADS will first operate with conventional fuel while in a second phase advanced fuel pins or fuels, characterized by a high content of Plutonium and Minor Actinides will be introduced. Therefore, ADS will be used only as a transmutation facility; energy production will be considered afterwards.

Separation techniques for MA and long-lived fission products, necessary to produce advanced fuel materials, are still on a laboratory research [Conde', 2002]. Two different types of processes can be applied: hydro-chemical (wet) and pyro-chemical (dry).

The PUREX process is the most important hydro-chemical reprocessing technique to separate Uranium and Plutonium from spent fuel elements and it is based on the fuel dissolution in nitric acid; for the extraction of MA the process should be modified/extended.

An alternative to hydro-chemical processes are pyro-chemical processes in which refining is carried out in molten salt. The mayor advantages in using this technique are the higher compactness of the equipment and the possibility to form an integrated system between irradiation and reprocessing facility. In addition, the higher stability of the salt is an important advantage when dealing with high active spent fuel elements.

Once partitioning has been performed, the fuel has to be incinerated: two different routes can be followed: the "double strata" and the "single strata". In the former U and Pu are first extracted from the spent fuel elements and the remaining MA and long lived products are sent to an independent partitioning and transmutation facility.

In the other route all the products are transmuted together. This strategy is preferred and several studies are in progress [Conde', 2002].

To close the fuel-cycle, a short description on how to deal with extracted fuel elements from ADS is necessary. At replacement time the fuel itself is still sound and it could continue to burn much further if it were not for the neutron absorption due to accumulated fission fragments. Hence, after reprocessing the fuel can be used again: this process can be better called "fuel regeneration", and it consists of Fission Fragments removal and adding of fresh Thorium.

This idea of course works only if ADS is considered as a system for energy production.

2.4 The sub-critical reactor

Several different designs have been proposed through the years for the sub-critical core.

While an industrial assembly for waste transmutation requires a power level of about 1000 MW_{th}, it was thought that a reference level of 80 MW_{th} was much better for an experimental facility like XADS, in which the generated thermal power has to be discarded. Nevertheless, many simulations and experiments, especially regarded Thermal-Hydraulics, are based on larger reactors. A power level of 1500 MW_{th}, as proposed in the Conceptual Design [Rubbia et al, 1995], has been selected for this project [Ceballos, 2004].

The general layout of the reactor core according to the first Conceptual design is shown in Fig 2.2.

The sub-critical unit consist of a main vessel, about 6m in diameter and 30 m tall, filled with molten Lead and Bismuth (LBE).

A high energy proton beam is injected through the top and made to interact in the LBE near the core: it provides the extra neutrons for the chain reaction to be sustained. The heat produced by the nuclear cascade is extracted by the Heat Exchangers. Most of the inside of the vessel is free of obstruction to permit a healthy circulation of the cooling liquid; circulation is ensured exclusively by natural convection.

Heat extraction from the Primary Loop is guaranteed by four Heat Exchanger (HX), designed to introduce only a small pressure drop in order not to slow down to much the convective cooling flow.

Once cooled by the HXs, the liquid descends along the periphery and feeds the lower part of the core and the target region. A thermally insulated wall separates the two flows. A temperature gradient across the core of about 250 °C guarantees an effective circulation at the selected power level [Rubbia et al, 1995].

In case that the normal heat removal and safety systems fail, the ultimate emergency decay heat removal system is a Reactor Vessel Auxiliary cooling system (RVACS), based on the principle of thermal radiation and natural air convection around the reactor vessel.

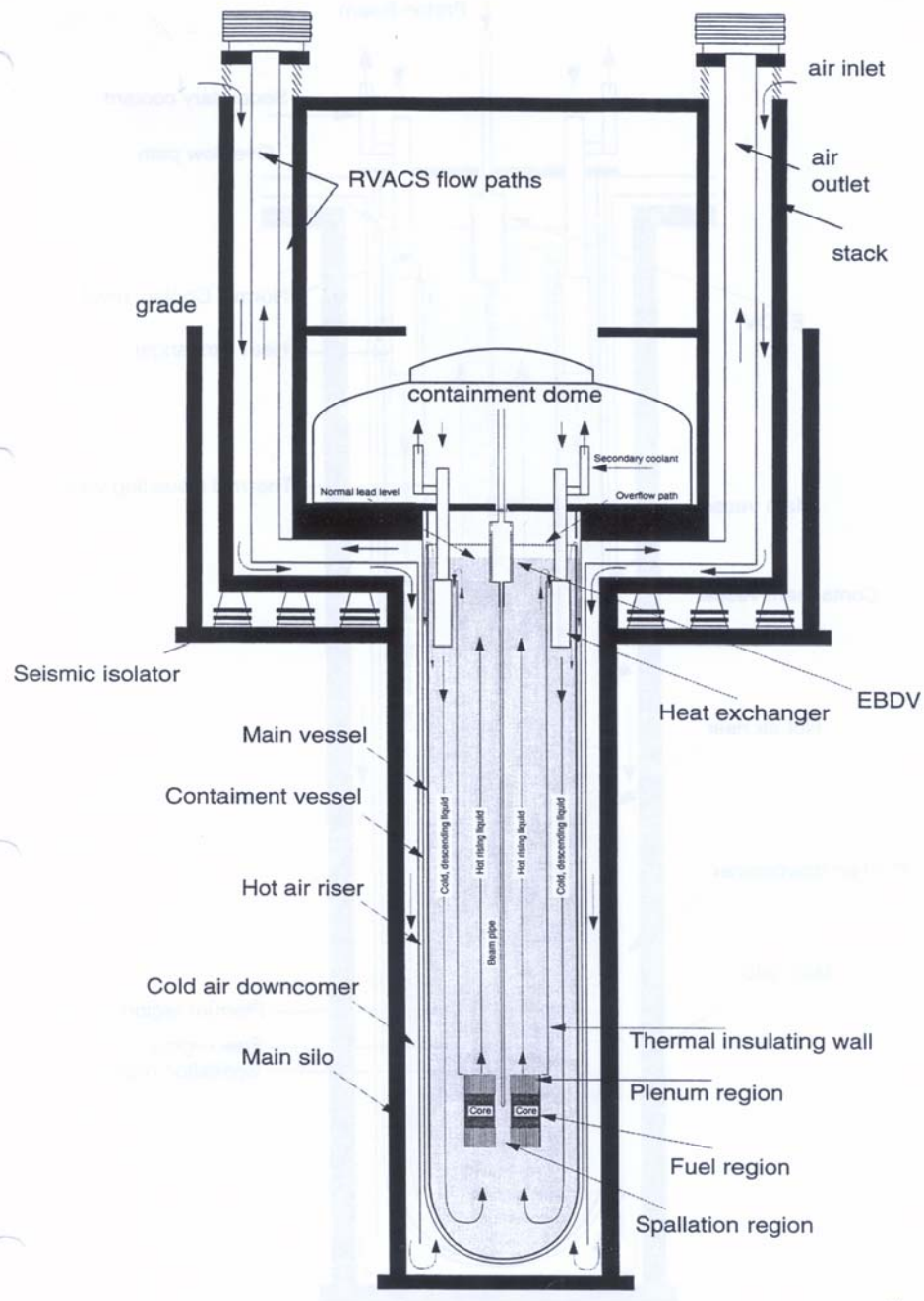


Fig 2.2: General structure of the sub-critical system [Rubbia et al, 1995]

Fig. 2.3 describes one of the experimental XADS, the 80 MW LBE-cooled system designed by Ansaldo: compared with Rubbia's Conceptual design, many particulars have been better studied and implemented, but the general structure stay the same.

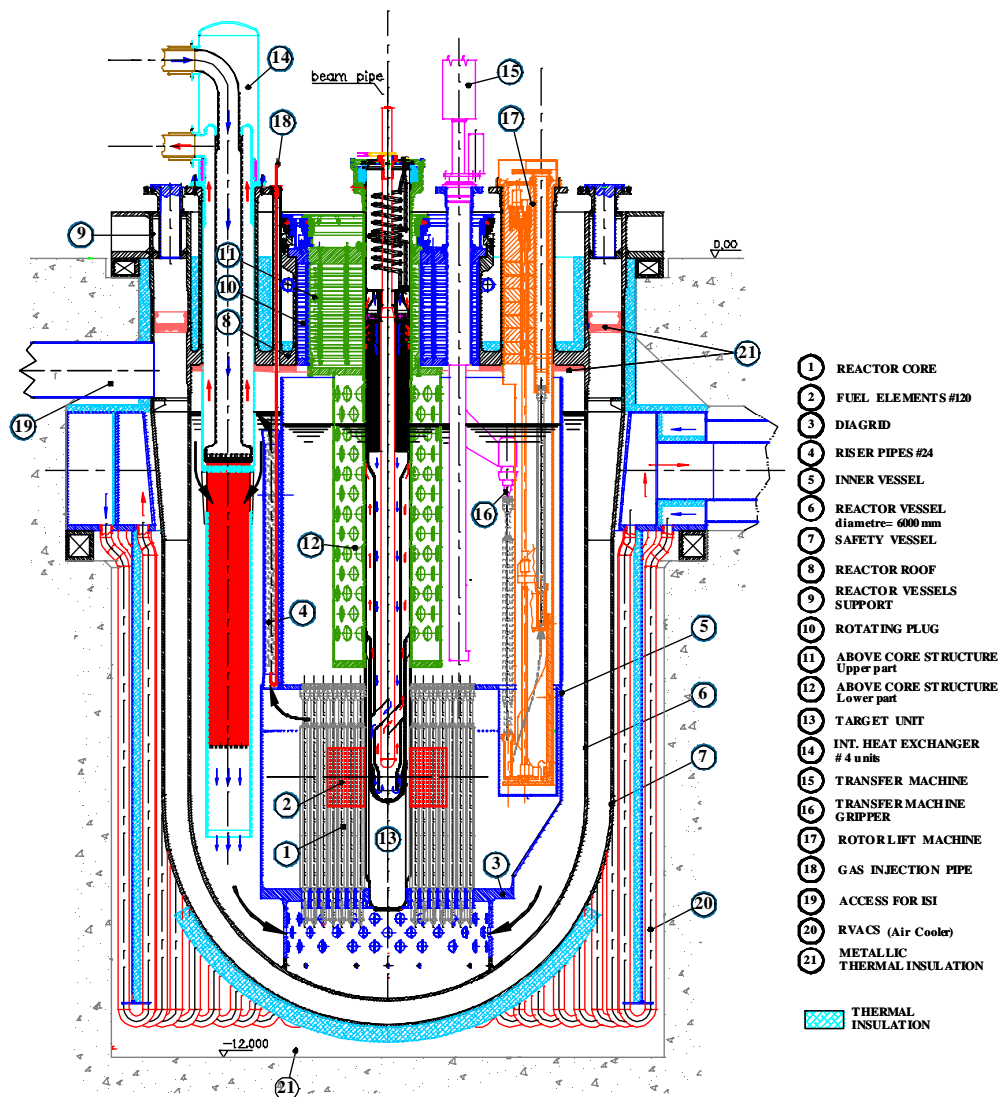


Fig 2.3: schematic view of the Ansaldo XADS [Cinotti et al, 2003]

Fuel elements are loaded in the form of pins, clustered in hexagonal fuel sub-assemblies. Pins are made of small pellets inserted in a robust steel cladding. Each pin has two extended void regions, called “plenums”, one at each end, intended to accumulate the gaseous fission fragments. The Pin-Pitch diameter is larger in the inner core and smaller in the outer core to guarantee a flatter profile of the neutrons flux. Sub-critical systems normally reach high fluxes ($\approx 5 \cdot 10^{15} \text{ n/cm}^2 \text{ s}$), high burn up, high power density and they thus have small core dimensions.

There are neither shutoff rods nor control assemblies disposed in the core; some design includes dummy assemblies (“empty” assemblies filled with inert fuel pins) or a set of neutron absorbers, which are kept parked at the periphery during operation [Mansani et al, 2002].

To complete the description of the system a few remarks about the different coolant options have to be added; moreover the most important physical parameter – the sub-criticality level- must be introduced.

Coolant options

In order to obtain a fast neutron spectrum the choice of the primary coolant medium is restricted to liquid metals (Pb, LBE and Na) or gas (He, CO_2). More “exotic” coolants, like molten salts, are presently considered well beyond the state of the art [Roadmap, Enea, 2001]. Liquid metals are eligible candidates because they have good thermal properties and offer the possibility to operate close to atmospheric pressure. The disadvantages are mainly related to chemical properties, like corrosion and to the difficulties in in-service inspection (metals are opaque). LBE is normally preferred to Na because the latter has a positive feedback coefficient from voiding.

The use of gases facilitates the in-service inspection and repair but requires high primary system pressure that causes a mechanical loading of the vessel and the target assembly, with a consequent increase in the probability of failures.

Liquid metals are thus usually preferred.

Sub-criticality level

The degree of sub-criticality can be expressed by the parameter k or by the reactivity ρ , both defined as for critical reactors: in sub-critical system k will be of course smaller than 1 and ρ will always be negative.

The sub-criticality level directly affects key accelerator system parameters (e.g: proton beam current) required to sustain the predefined power level.

Low sub-criticality levels imply low proton beam current but increased risk of approaching or attaining criticality under abnormal or accidental conditions. Higher sub-criticality levels require more demanding accelerator performances to provide a higher beam current but the risk of approaching criticality is reduced.

From the safety point of view, it is mandatory that the nuclear design ensures that criticality conditions are not attained, with adequate margin, under any foreseeable occurrence pertaining either to design basis conditions or beyond design basis conditions. The required sub-criticality level must be thus determined by a properly balanced approach between excessively demanding accelerator system performances and risk of accidental criticality. The selected range in most of the experiments is $0.95 < k < 0.99$; the optimum level has still to be determined but it is around 0.98, as initially proposed in the Conceptual Design.

One of the goals of this project is to determine the influence of the sub-criticality level in the power response to source fluctuations and in the stability analysis. Further considerations will be therefore presented after the simulations.

The physics of the system is a lot more complex than presented so far: the presence of a proton beam generates a non-uniform neutron flux, so that in accurate simulations the core has to be divided in zones [Schikorr, 2001].

Moreover, a careful transient analysis allows a better understanding on the role of k and on differences and similarities between critical and sub-critical systems.

A basic understanding on the problems can be gained in the following section.

2.5 Kinetic and Dynamic behaviour

The presence of a neutrons source driving the system is probably the most innovative feature in ADS compared to critical systems. While in the latter power response to reactivity fluctuation is driven by delayed neutrons, in ADS power response is almost instantaneous and it is driven by the source.

Chapter 3 and 4 will widely show how kinetic equations are derived and solved for both critical and sub-critical reactors. The basic assumption, supported by Schikorr, is the applicability of the point kinetic equation for sub-critical system with an external source. This is justified by the fact that point kinetics equations can be derived in a more general fashion from the transport equation; therefore the assumptions made for critical reactors are not necessary (1-speed diffusion and time independence of the spatial flux shape) [Schikorr, 2001].

A few numerical codes have been implemented to solve this set of equations and, if coupled with Thermal Hydraulics, complete simulations describing reactor behaviour in normal or accidental condition can be run.

So far it has been demonstrated that dynamic behaviour of sub-critical systems is substantially different from that of critical reactors to typical plant transient initiators. The state of sub-criticality is an important parameter, that needs constant monitoring during the various burn-up stages in the fuel cycle.

The preferred state of sub-criticality of ADS is not clear-cut, since for some transient a relative low k (≈ 0.95) is preferable while for other transient, like underpower excursion, a rather high k (≈ 0.99) guarantees safer operation [Schikorr, 2001].

It has also been demonstrated that design with large positive reactivity coefficient can exhibit unfavourable dynamic characteristics even if the assembly is made relatively large sub-critical. The dependency of some reactivity coefficients on the state of sub-criticality requires a careful monitoring of the system as the burn up proceeds, and thus k changes [Schikorr, 2001].

Simulations show that natural circulation can be successfully implemented in the primary cooling system of an ADS but some calculated transients, like ULOHS (Unprotected Loss of Heat Sink) prove that limit values are exceeded and some materials are subjected to high thermal stresses, which may eventually lead to failure [Ceballos, 2004].

The above discussion clearly demonstrates that simply making a critical assembly sub-critical will not assure automatic safety. On the contrary, careful analysis and assessment is required for each different ADS core design to assure that its combination of reactivity coefficients and selected sub-criticality level does not lead to unacceptable dynamic behaviour.

Chapter 3 *Dynamics of critical reactors*

In this chapter an overview on the most important theoretical aspects of critical reactor physics is given, with a main focus on reactor's dynamic behaviour.

Some methods to describe the response to reactivity fluctuations of different amplitude and time scale are also presented.

The theory described, developed by several authors in the 50s and 60s, has been experimentally proved and accepted worldwide. Its critical understanding represents the starting point to cope successfully with sub-critical systems, for which a solid theory has not been developed yet.

This justifies the quite extensive description provided in this chapter and mostly taken from the book "Dynamics of Nuclear Reactor" by D.L.Hetrick.

3.1 Point Kinetics Theory

The derivation of reactor's dynamic equations for homogeneous material starts from a time dependent diffusion equation of neutrons, including a source q :

$$\frac{\partial N}{\partial t} = Dv\nabla^2 N - \Sigma_a vN + q \quad (3.1)$$

where

$$\begin{aligned} N(\vec{r}, t)dV &= \text{number of neutrons in a volume } dV \text{ at a point } \vec{r} \text{ at time } t; \\ Dv\nabla^2 NdV &= \text{number of neutrons diffusing into } dV \text{ per unit time at time } t; \\ \Sigma_a vNdV &= \text{number of neutrons absorbed into } dV \text{ per unit time at time } t; \\ q(\vec{r}, t)dV &= \text{number of neutrons produced in } dV \text{ per unit time at time } t; \end{aligned}$$

The coefficients D , v and Σ_a are respectively the diffusion constant, the neutron speed and the macroscopic neutrons' absorption cross section.

Equation (3.1) is derived under the following assumptions:

1. The neutron current density is given by Fick's law ($\vec{J} = -Dv\nabla n$).
2. All the coefficients are independent on position and their numerical values represent suitable averages over the neutron velocity distribution.
3. The effect of different energy levels is simplified by assuming one average energy group.

Neutrons can be separated into prompt and delayed; the latter are produced by radioactive decay of certain fission fragments (precursors), described by the balance equations:

$$\frac{\partial C_i}{\partial t} = -\lambda_i C_i + \Sigma_f Nv\beta \quad (3.2)$$

where C_i and λ_i are respectively the density and the decay constant of the i^{th} type of precursor, β is the fraction of delayed neutrons and Σ_f is the macroscopic neutrons' fission cross section.

Equations (3.1) and (3.2) fully describe the physics of the problem. In this approximate treatment, it is next assumed that N and C_i are separable in space and time:

$$N(\vec{r}, t) = f(\vec{r})n(t)$$

$$C_i(\vec{r}, t) = g_i(\vec{r})c_i(t)$$

The removal of spatial dependency requires the functions f and g_i to have the same shape and f to satisfy a Helmholtz equation.

Introducing a few parameters the set of point kinetic equations is obtained in the well-known formulation:

$$\frac{dn}{dt} = \frac{\rho - \beta}{l} n + \sum_i \lambda_i c_i + q \quad (3.3a)$$

$$\frac{dc_i}{dt} = \frac{\beta_i}{l} n - \lambda_i c_i \quad (3.4a)$$

where ρ is the reactivity and l the neutron generation time, that represents the time interval between two subsequent neutrons generations.

For one group of delayed neutrons the system is:

$$\frac{dn}{dt} = \frac{\rho - \beta}{l} n + \lambda c + q \quad (3.3)$$

$$\frac{dc}{dt} = \frac{\beta}{l} n - \lambda c \quad (3.4)$$

In the point kinetic model spatial dependency can be neglected because suitable integral quantities over the reactor volume are chosen. In fact, an alternative procedure to derive equations (3.3a) and (3.4a) is based on the integration of equations (3.1) and (3.2) over the reactor volume. For this reason, the main limit of this model is its inability to describe spatially dependent dynamic effects, considered as changes in the spatial distribution during transients.

The solution of this equation has been worked out with different approximations in order to understand the physics of critical (chapter 3) and sub-critical systems (chapter 5). A few techniques are described in the following paragraphs.

3.2 The inhour equation

The solutions of (3.3a) and (3.4a) for constant reactivity and without source are linear combinations of $m+1$ exponentials $e^{\omega_j t}$, where m is the number of precursors' groups. The ω_j depend upon the reactivity through the characteristic equation, which is called "the inhour equation".

The case of constant reactivity level ρ_0 for positive time is now considered.

Let $N(s)$ be the Laplace transform of $n(t)$; using the Laplace Transform method to solve the system, $N(s)$ can be expressed as:

$$N(s) = \frac{l \left[n(0) + \sum_i \frac{\lambda_i c_i(0)}{s + \lambda_i} \right]}{ls + \beta - \rho_0 - \sum_i \frac{\beta_i \lambda_i}{s + \lambda_i}} \quad (3.5)$$

where $n(0)$ and $c_i(0)$ are respectively the neutrons and precursors concentration at time $t=0$.

Equation (3.5) can be seen as a ratio of two polynomials, the numerator degree being m , the denominator one being $m+1$. The back Laplace Transform is an equation of the form:

$$n(t) = \sum_{j=1}^{m+1} A_j e^{\omega_j t} \quad (3.6)$$

where ω_j are the roots $s=\omega_j$ of the denominator and A_j are coefficients.

In other words, each ω_j satisfies the equation:

$$\rho_0 = l\omega + \sum_i \frac{\beta_i \omega}{\omega + \lambda_i} \quad (3.7)$$

It can be shown that the inhour equation has m negative real roots and one root of the same sign as ρ_0 .

A few more features on the inhour equation can be gained from the qualitative plot in Fig. 3.1. Two asymptotes can be distinguished, one for very large ω and one for ω values very close to zero. Moreover, for large time one term may eventually dominate, that is the greatest algebraically ω_j ; for positive reactivity level this dominant term is a growing exponential and its reciprocal is called the reactor period. The crossover $\rho_0=\beta$ is called prompt critical because at this point the chain reaction is self-sustaining on prompt neutrons alone.

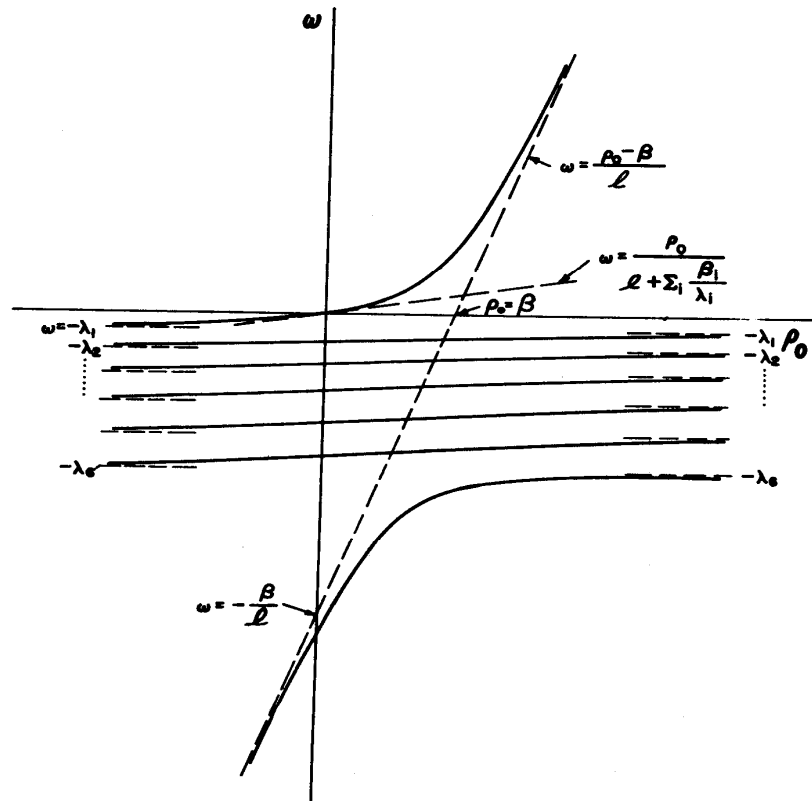


Fig. 3.1: Qualitative plot of the inhour equation for six groups of delayed neutrons. In practice, $\beta/l \gg \lambda_6$ and the asymptote for large ω has much steeper slope than shown [Hetrick, 1993]

The neutron generation time is one of the driving parameters in reactor dynamics and thus deserves further considerations. Since l is normally very short, especially for fast reactors, a good approximated solution can be obtained by setting it to 0: this is the so called “prompt jump approximation”. Equation (3.6) is thus simplified into:

$$\rho_0 = \sum_i \frac{\omega \beta_i}{\omega + \lambda_i} \quad (3.8)$$

According to this approximation the system exhibit a step wise change of ω while approaching the level of prompt criticality.

A further simplification can be introduced by neglecting the different decay constants of the precursors. Accurate simulations normally use 6 groups of delayed neutrons but a simpler one group representation allows a better physical understanding. The inhour equation is reduced to a second order one and the two eigenvalues are one negative and the other one has the same sign of ρ_0 .

Some authors have proposed 2 or 3 group approximations to improve the results but the 6 groups’ approximation is still the most widely used system.

3.3 Response to a step-wise reactivity insertion

The system of equations (3.3a) and (3.4a) is now solved in the special case of source free equilibrium followed by a step input of reactivity from 0 to $\rho=\rho_0$ at time $t=0$. This case is of special interest because many accidental conditions can be simulated by giving a step-wise increase in the reactivity level.

Provided that $n=n_0$ for $t \leq 0$, equation (3.6) can be written in a convenient way as:

$$n(t) = n_0 \rho_0 \sum_{j=1}^{m+1} \frac{e^{\omega_j t}}{\omega_j \left[l + \sum_i \frac{\beta_i \lambda_i}{(\omega_j + \lambda_i)^2} \right]} \quad (3.9)$$

This equation is derived from equation (3.5), using the residues method and with the aid of (3.7).

For one delayed group approximation, equation (3.9) becomes:

$$n(t) = n_0 \rho_0 \left\{ \frac{e^{\omega_1 t}}{\omega_1 \left[l + \frac{\beta \lambda}{(\omega_1 + \lambda)^2} \right]} + \frac{e^{\omega_2 t}}{\omega_2 \left[l + \frac{\beta \lambda}{(\omega_2 + \lambda)^2} \right]} \right\} \quad (3.10)$$

A few algebraic steps and substitutions lead to:

$$n(t) = \frac{n_0}{\omega_1 - \omega_2} \left[\left(\frac{\rho_0}{l} - \omega_2 \right) e^{\omega_1 t} + \left(\omega_1 - \frac{\rho_0}{l} \right) e^{\omega_2 t} \right] \quad (3.11)$$

Equation (3.11) represents the time evolution of the neutron density for a step input of reactivity of any sign.

If ρ_0 is positive then ω_1 is positive and ω_2 is negative.

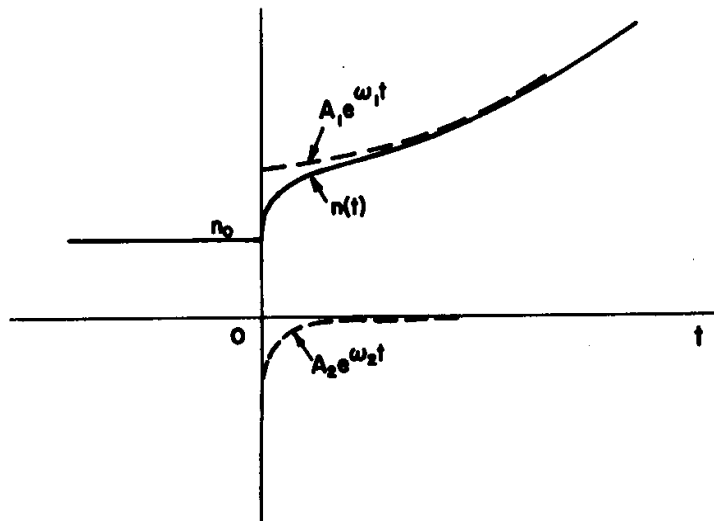


Fig. 3.2: Neutron density as a function of time for a step input of reactivity [Hetrick,1993]

Fig 3.2 shows that neutron population undergoes a rapid initial rise, “the prompt jump”, followed by a flatter increase. The prompt jump is due to the fact that delayed neutrons depend on the past history of $n(t)$ and for a short time they are still being produced at a rate basically determined by n_0 , because precursors don't have enough time to decay. The chain reaction then adjust itself until both $n(t)$ and $c(t)$ are rising with the same time dependence. It takes thus some time before the population of delayed neutrons plays a significant role in the response.

If a negative reactivity step is given, the relation $\omega_2 < \rho_0/l < \omega_1 < 0$ is satisfied and both the coefficients in equation (3.11) are positive. The solution consists of two superposed decaying exponential, the one with ω_2 being more rapid.

Equation (3.11) can be further simplified in some limiting cases.

Using the properties of the sum and product of the roots of a second order equation, assuming ρ_0 small ($\omega_1 \ll \omega_2$) and not too close to β ($\lambda l \ll \beta - \rho_0$), a simple expression for ω_1 and ω_2 can be derived:

$$\begin{aligned}\omega_2 &\cong -\frac{\beta - \rho_0}{l} \\ \omega_1 &\cong \frac{\lambda \rho_0}{\beta - \rho_0}\end{aligned}\quad (3.12)$$

Plugging into (3.11) the following equation is obtained:

$$n(t) = \frac{n_0}{\beta - \rho_0} \left[\beta \exp\left(\frac{\lambda \rho_0}{\beta - \rho_0} t\right) - \rho_0 \exp\left(-\frac{\beta - \rho_0}{l} t\right) \right] \quad (3.13)$$

This equation shows that:

1. the prompt jump in n/n_0 is approximately from 1 to $\frac{\beta}{\beta - \rho_0}$
2. the duration of the rapidly decaying transient is of the order of $\frac{l}{\beta - \rho_0}$

In the prompt-jump approximation ($l \rightarrow 0$) the negative exponential term in equation (3.13) is negligible; the neutron density evolution is thus:

$$n(t) = \frac{n_0}{\beta - \rho_0} \left[\beta \exp\left(\frac{\lambda \rho_0}{\beta - \rho_0} t\right) \right] \quad (3.14)$$

3.4 Approximate dynamic equations

The Point Kinetic system has been analyzed so far neglecting a general time dependency of the reactivity. Should it be taken into account, the differential equations have time-dependent coefficients, because $\rho=\rho(t)$.

Several simplifying approximations often lead to analytical solutions that provide a physical insight not readily available otherwise.

Looking at the purpose of this project the most interesting approximation is the “prompt jump approximation” (PJ), also called “zero-lifetime approximation” and already introduced in chapter 3.2 and 3.3.

In this section, another viewpoint is suggested.

Expansion in powers, small reactivity changes

The Point Kinetic model with time dependent reactivity is described by the system:

$$\frac{dn}{dt} = \frac{\rho(t) - \beta}{l} n + \sum_i \lambda_i c_i + q(t) \quad (3.15)$$

$$\frac{dc_i}{dt} = \frac{\beta_i}{l} n - \lambda_i c_i \quad (3.16)$$

If $\rho \ll \beta$ and l is small, with values typical of fast systems, the right hand side of equation (3.15) contains a large term compared to the derivative dn/dt so that the derivative can be retained.

The neutron density n can be written as an expansion in power of the parameter l :

$$n = n_1 + n_2 l + \dots \quad (3.17)$$

and the same holds for its derivative.

Substitution into equation (3.15) yields:

$$\frac{dn_1}{dt} + l \frac{dn_2}{dt} = \frac{\rho - \beta}{l} n_1 + (\rho - \beta) n_2 + \sum_i \lambda_i c_i + q + \dots \quad (3.18)$$

The solution of the system (3.15) and (3.16) in equilibrium conditions, which requires c and q to assume constant values, shows that they both have a $1/l$ dependence with respect to n . In addition, it can be inferred that this remains true during slow transients.

The first term in the power expansion can be obtained equating all the term of order $1/l$ and assuming time derivatives to be small. The result is:

$$n_1 = \frac{\sum_i \lambda_i l c_i + l q}{\beta - \rho} \quad (3.19)$$

which is identified as the neutron density in the prompt jump approximation.

The neutron density given by (3.19) satisfies equation (3.15) provided the derivative to be small enough to be ignored; n_1 thus satisfies a system of differential equations whose order has been reduced by one. This physically means that one initial

condition has been lost, and can be interpreted by the fact that in the fast decaying transient the approximate neutron density is only a part of the complete solution. Using an iterative procedure n_2 and higher order terms are obtained.

A few interesting remarks on the prompt jump approximation can be made by looking at the simpler one group approximation. Equation (3.19) becomes:

$$n_1 = \frac{\lambda c + l q}{\beta - \rho} \quad (3.20)$$

Solving for c and substituting in the precursor equation (3.4) it is found that:

$$(\beta - \rho) \frac{dn_1}{dt} - \left(\lambda \rho + \frac{d\rho}{dt} \right) n_1 = \lambda l q + l \frac{dq}{dt} \quad (3.21)$$

This equation expresses neutrons density evolution in the prompt jump approximation with time dependent source.

A criterion to establish the validity of this approximation is to consider the magnitude of the successive terms in the equation to be small.

The result, for one delayed group and no source is:

$$\beta - \rho \gg \sqrt{l \left| \lambda \rho + \frac{d\rho}{dt} \right|} \quad (3.22)$$

This criterion expresses the permissible approach to prompt criticality for the prompt jump approximation to be valid. If l is small, this approach can be quite close.

If ρ and its derivative are small, the PJ approximation reduces to an important special case; in the source free case equation (3.21) becomes:

$$\frac{dn}{dt} = \frac{\lambda \rho}{\beta} n \cong \frac{\rho}{l'} n \quad (3.23)$$

where l' is the effective lifetime. This parameter is much bigger than the neutron generation time l and reflects the dominance of delayed neutrons for small reactivity.

Prompt jump from a second order differential equation

To complete the discussion on the prompt jump approximation a full description of the one delayed group model can be provided by transforming the point kinetic system (3.15) and (3.16) into an ordinary second order differential equation:

$$l \frac{d^2 n}{dt^2} + (\beta + \lambda l - \rho) \frac{dn}{dt} - \left(\lambda \rho + \frac{d\rho}{dt} \right) n = \lambda l q + l \frac{dq}{dt} \quad (3.24)$$

The prompt jump approximation can be seen to be the limit of equation (3.24) when $l \rightarrow 0$, whenever the second derivative is sufficiently small so that the first term can be neglected.

Expansion in powers, large reactivity

An expansion in powers of l can also be used in the case of large reactivity insertion and fast excursions but different assumptions have to be made on the relative magnitude of the terms. The derivative dn_1/dt is now taken of order $1/l$, while c and q are of order l^0 .

Equating the terms of order $1/l$, equation (3.18) becomes:

$$\frac{dn_1}{dt} = \frac{\rho - \beta}{l} n_1 \quad (3.25)$$

which is called the Nordheim-Fuchs model for fast excursions.

n_1 is the neutron density that satisfies (3.3) when the neutron population is growing so rapidly that the precursor's concentration and the source can be neglected.

Once again n_1 satisfies a system of reduced order differential equations.

Using the same iterative procedure described for small reactivity the higher order terms can be calculated.

3.4 Frequency response and transfer function

Transfer Functions represent one of the most powerful mathematical "objects" to analyze systems' stability. They are widely used in many fields, for example in electronics.

A transfer function is defined as the ratio of Laplace transform of output and input to a system and it thus describes the properties of the system itself.

In this paragraphs transfer functions will be introduced using a few examples related to sub-critical systems to understand their importance in stability analysis.

Let's consider a subcritical reactor, with a reactivity level $\rho = \rho_0 < 0$ in equilibrium with a steady source q_0 . Solution of point kinetics under steady state conditions leads to:

$$n_0 = -lq_0 / \rho_0 \quad (3.26)$$

If the source is oscillating around its mean value q_0 and the reactivity is constant, neutron population will oscillate about its time average n_0 with the same frequency as the source.

This can be easily proved using the method of transfer function.

In fact the Laplace transform of the source and of the inhomogeneous part of the point kinetics system have a simple relationship. This suggests a source to response relation that can be expressed by the following scheme:

$$F_0(s) = H(s)F_i(s) \quad (3.27)$$

where $F_0(s), F_i(s)$ are respectively the Laplace transform of the output and of the input and $H(s)$ is the transfer function.

If the source has a sinusoidal dependence, the result is:

$$F_0(s) = \frac{\omega_0}{s^2 + \omega_0^2} H(s) \quad (3.28)$$

$$f_0(t) = \frac{1}{2\pi j} \int_c \frac{\omega_0}{s^2 + \omega_0^2} H(s) e^{st} ds$$

where the contour of integration is to the right of all the singularities of the integrand. By employing the residues method the output becomes:

$$f_0(t) = |H(j\omega_0)| \sin(\omega_0 t + \mathcal{G}) + T(t) \quad (3.29)$$

where all the decaying transients are lumped together in the function $T(t)$.

Two assumptions are needed for the validity of (3.29):

1. The singularities of $H(s)$ are in the left half plane. If this condition is not satisfied the system is not stable and $T(t)$ may contain diverging terms.
2. $H^*(j\omega_0) = H(-j\omega_0)$: this is always verified in a real coefficients system.

Equation (3.29) clearly expresses that, under certain assumptions, the response to a sinusoidal input is a sinusoidal output with the same frequency ω_0 whose amplitude and phase shift are determined by the transfer function of the system.

Since the response to an arbitrary periodic input can be seen as a Fourier series in which superposition principle is valid, the general solution is nothing but a superposition of Laplace transformed harmonic components.

Another interesting case is to study a point reactor response to an oscillating source. Let's assume:

$$n = n_0 + \delta n$$

$$c_i = c_{i0} + \delta c_i$$

$$q = q_0 + \delta q$$

$$\rho = \rho_0$$

By solving point kinetics, the equilibrium conditions are:

$$c_{i0} = \frac{\beta_i n_0}{\lambda_i l}$$

$$n_0 = -\frac{l q_0}{\rho_0}$$

Substitution into (3.3a) and (3.4a), followed by Laplace Transform, leads to:

$$\delta N(s) = \frac{l \left[\delta n(0) + \sum_i \frac{\lambda_i \delta c_i(0)}{s + \lambda_i} + \delta Q(s) \right]}{ls + \beta - \rho_0 - \sum_i \frac{\beta_i \lambda_i}{s + \lambda_i}} \quad (3.30)$$

The steady-state part of the response is just:

$$\delta N(s) = \frac{l\delta Q(s)}{ls + \beta - \rho_0 - \sum_i \frac{\beta_i \lambda_i}{s + \lambda_i}} \quad (3.31)$$

The ratio between equation (3.30) and (3.31) gives the so called source transfer function $H(s)$ which describes reactor response to source fluctuations. This equation will be widely used in chapter 6 to study the stability of an ADS.

3.5 Reactivity feedback

A complete analysis on reactor dynamics requires the point reactor model to be extended in order to include the effects on fission energy production on the reactivity. That portion of reactivity change arising from energy production is called reactivity feedback.

Feedback effects can be determined by temperature and density changes (intrinsic feedback) or by automatic control systems (external feedback).

In this paragraph an overview on the feedback effects for different reactors will be given in order to understand why feedback is so important also for sub-critical systems.

Changes in the power level are always related to temperature variation in the fuel, the coolant and the structural material. For this reason feedback effects are normally expressed through a temperature feedback coefficient:

$$\alpha_T = \frac{d\rho}{dT} \quad (3.32)$$

where ρ is the reactivity and T is the temperature.

Recalling the relation:

$$\rho = \frac{k-1}{k} = 1 - k^{-1} \quad (3.33)$$

if k is close to 1 equation (3.32) becomes:

$$\alpha_T = \frac{1}{k^2} \frac{dk}{dT} \cong \frac{1}{k} \frac{dk}{dT} \quad (3.34)$$

Assuming α_T to be the only feedback coefficient, the stability of the system is possible only if this coefficient is negative.

For an unreflected homogeneous thermal reactor, the reactivity feedback coefficient can be expressed in terms of reactors physical and geometrical parameters. In particular, the feedback coefficient is directly proportional to the buckling B^2 and, since buckling is inversely proportional to the geometrical dimensions, larger reactors imply less negative feedback

Heterogeneous systems represent a more realistic case.

The basic idea to analyze these systems is the separation between prompt and

delayed effects: the former are mostly related to the fuel and derived from the energy released by fission fragments while the latter include effects from moderator, coolant and supporting structures, driven by heat-transfer processes and thus delayed. Therefore, the temperature reactivity coefficient may be split into prompt and delayed components.

Fast reactors show a different mechanism: neutrons are not slow down and their spectrum exhibits only weak temperature dependence. Most neutrons are absorbed or leak out of the system at energies far higher than thermal, and there are no neutrons in thermal equilibrium with the reactor material.

Nevertheless even in this case prompt reactivity effects, that arise from fuel thermal expansion (longitudinal and radial) and fuel bowing can be separated from delayed effects, due to structural heating, thermal expansion of the coolant or coolant expulsion.

Since in fast reactors time scales are very much shorter than in thermal ones, it may happen that feedback, even if negative, may not be sufficient to quench a reactivity change and avoid a dangerous overpower excursion.

3.6 The Nordheim Fuchs model

Several approximated methods have been developed to describe reactivity insertions of any magnitude on different time scales. The Nordheim-Fuchs model, developed in the 40s, is appropriate for fast self-limiting power excursions with large reactivity insertion.

The essential approximation is that all neutrons' sources except the production of prompt neutrons are neglected: this is meaningful only for sufficiently large reactivity.

As already introduced in chapter 3.3, the reactor power follows the equation :

$$\frac{dn}{dt} = \frac{\rho - \beta}{l} n \quad (3.35)$$

The physical meaning is that power is so large and changes are so fast that delayed or external neutrons may be entirely neglected.

This model normally describes a critical or sub-critical reactor operating at low power level and quickly made supercritical by step input reactivity $\rho_0 > \beta$. Step input means that the reactivity change is so rapid that for some time the value is kept at ρ_0 before any significant change due to reactivity feedback can play a role.

It can be inferred that the system's evolution mostly depends on the step input and not on the level of reactivity present at the beginning.

Reactivity is normally described by the relation:

$$\rho = \rho_0 - \alpha T \quad (3.36)$$

where $-\alpha$ is the negative temperature feedback coefficient.

Since transients are very short, energy losses can be neglected and an adiabatic

model can be used to describe heat transfer:

$$\frac{dT}{dt} = Kn \quad (3.37)$$

where K is the reciprocal of reactor heat capacity and n is the power, proportional to the number of neutrons.

Using equations (3.35), (3.36) and (3.37) a relation between power and reactivity can be worked out.

The most interesting value is the maximum power level, which is reached when $\rho = \beta$. Its value is:

$$n_{peak} = \frac{(\rho_0 - \beta)^2}{2\alpha Kl} = \frac{l\omega^2}{2\alpha K} \quad (3.38)$$

where $\omega = \frac{\rho_0 - \beta}{l}$ is the inverse of reactor period.

Equation (3.38) shows that fast reactors, having a shorter l , are subjected to higher peak values and thus to more severe accidents.

Since delayed neutrons are not taken into account, power distribution is symmetric and “falls down” to 0 power level.

A slightly modified model including delayed neutrons can be easily developed. The main difference is that after the fast burst the reactor power does not fall to zero, but approaches a small asymptotic value, dependent on delayed neutrons properties, feedback coefficient and thermo-dynamical properties

Chapter 4 *Stability of critical systems*

This chapter presents a summary of the theoretical background required to study the stability of sub-critical systems.

After an overview on the most used criteria to analyze linear systems' stability, the main focus will be on critical reactors, for which the theory has been already validated by experimental results. The book "Dynamics of Nuclear Reactor" by D.L.Hetrick has been the main reference.

In reality, the equations of reactors dynamics are non-linear if the reactivity depends on the power. Therefore, the analysis performed in this chapter is just a first approximation of the more complex real problem. Nevertheless, it offers in many cases very good results.

4.1 **Feedback and transfer function**

The central problem in stability analysis is to understand if a system at equilibrium, when perturbed in some manners throughout a finite time interval, is able to return to its equilibrium state.

A system is stable when it satisfies this requirement.

In the case of linear systems, the stability problem can be formulated in a convenient way using transfer functions and block diagrams, as shown in Fig 4.1.

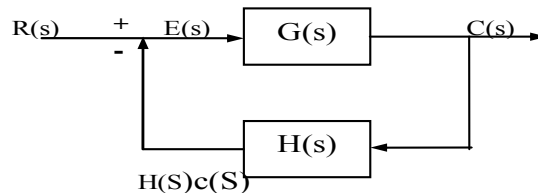


Fig 4.1: linear system with feedback in the frequency domain

The block $G(s)$ represents the forward-loop transfer function while all the feedback effects are summarized in the block $H(s)$.

$R(s)$, $C(s)$, $E(s)$ are respectively the input signal, the output of the system and the difference between the input to the system and the output of the feedback element, also called "error signal". All the quantities are already in the frequency domain.

If this general scheme is specialized to nuclear reactors, $G(s)$ is the transfer function for the reactor core while $H(s)$ takes into account feedback effects.

For the closed-loop system in Fig 4.1 the transfer function is:

$$Y(s) = \frac{C(s)}{R(s)} = \frac{G(s)}{1 + G(s)H(s)} \quad (4.1)$$

A stability analysis is based on the positions of the poles and the zeros of $Y(s)$. The poles are the roots of the characteristic equation:

$$1 + G(s)H(s) = 0 \quad (4.2)$$

A system is stable when all the poles have negative real parts, because in the time domain this is translated in an exponentially decaying behaviour. If at least one of the root has positive real part the system is unstable while a border line condition appears when there's at least one zero real part. In the latter case time response contains decaying transient together with constant terms: this type of system is called "critical".

4.2 Criteria for linear stability analysis

In this section four of the most used criteria for stability analysis of linear systems will be briefly described: the Routh Criterion, the Bode diagrams, the Nyquist Criterion and the Root Locus method.

The Routh Criterion

The Routh criterion gives necessary and sufficient conditions for all the roots of the characteristic equation to be negative or with at least a negative real part.

Equation (4.2) can be written as the so-called "Characteristic Polynomial" in this general form:

$$D(s) = a_n s^n + a_{n-1} s^{n-1} + a_{n-2} s^{n-2} + \dots + a_1 s + a_0 \quad (4.3)$$

where the coefficients a_i are real numbers and are normally a combination of physical parameters that can vary within a certain range.

Using the coefficient in equation (4.3) the Routh array, formed by $n+1$ rows, can be build up:

$$\begin{pmatrix} a_n & a_{n-2} & a_{n-4} & \dots \\ a_{n-1} & a_{n-3} & a_{n-5} & \dots \\ b_1 & b_2 & b_3 & \dots \\ \vdots & & & \end{pmatrix}$$

where the coefficients b_i are proper combinations of the a_i ; moreover, the last term in the first column is a_0 .

The necessary and sufficient condition for stability is that all the terms in the first column have the same sign.

If a zero is encountered in building the array, one can investigate an auxiliary polynomial constructed by adding a parameter ε in equation (4.3).

If the second last Routh number is zero, there's a pair of characteristic roots equal in magnitude and opposite in sign.

Once defined the stability region, it is important to consider the boundaries. If equation (4.3), specialized at the boundaries, gives a zero characteristic root the

stability boundary is called “static”, while the name “dynamic” is given when there are two conjugate imaginary roots.

The Bode diagrams

The Bode Diagrams are one of the easiest and most effective criteria to study stability analysis. They represent system’s response in magnitude and phase to a sinusoidal input of any frequency through a log-log plot of the magnitude or phase versus the frequency itself.

The amplitude is normally expressed in decibel (db).

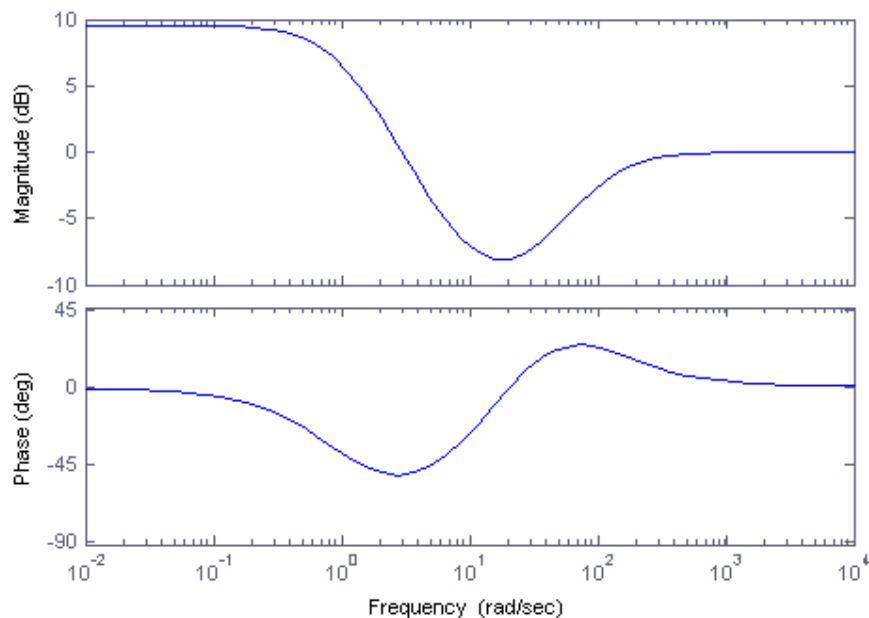


Fig 4.2: example of Bode Diagrams: the transfer function has two poles and two zeros

The example of Bode diagrams given in Fig 4.2 shows that, once the poles and the zeros of the transfer function are placed, the diagrams can be easily drawn following a few rules. Every negative pole introduces a decrease in the amplitude of 20db/decade and a phase shift of -90^0 while for the zeros the same rule hold, but with positive sign. A couple of complex conjugate poles cause a decrease of 40 db/decade and a phase shift of -180^0 .

If poles and zeros are close in frequency they will interact with each other and the rules described above give the asymptotic behaviour: this is clear for the phase diagram in Fig 4.2.

The stability of the system is determined by the phase: the system is stable until the phase crosses -180^0 and the value of the amplitude at that point represents the “gain margin”.

Since the Bode Diagrams do not give any information about the time scale of the transient, the stability analysis is often completed by adding system’s response to a step.

The Nyquist criterion

Another method to determine if the zeros of (4.2) are in the left half plane was developed by Nyquist and it is based on a theorem of complex analysis that can be explained as follows.

Let's consider a function $f(s)$ analytic and different from zero on a simple closed contour C and analytic inside C except for a finite number of poles; the following relation can be proved to be valid:

$$\frac{1}{2\pi j} \int_C \frac{f'(s)}{f(s)} ds = Z - P \quad (4.4)$$

where Z and P are the number of zeros and poles respectively, counted with their multiplicity. The contour is traversed counter clockwise, and $f'(s)$ is the derivative df/ds . $f(s)$ may be regarded as a mapping and thus the contour C in the s -plane corresponds to the mapped contour C' in the f -plane.

Since:

$$\frac{f'}{f} ds = d(\log f)$$

each counter clockwise encirclement of the origin in the f -plane gives a contribution of $2\pi j$ to the integral.

If E is the number of counter clockwise encirclement in the f -plane per each traversal of the C contour in the s -plane equation (4.4) becomes:

$$E = Z - P \quad (4.5)$$

These results can be applied to linear stability analysis as follows.

First of all, $1 + G(s)H(s) = f(s)$ and the contour in the s -plane is in general a half semicircle in the positive half of the plane including the imaginary axis. If any pole is present on the imaginary axis, it must be excluded from the contour introducing a small circle around it.

Instead of the f -plane it may be convenient to use the GH plane, considering that the origin in the f -plane is the point -1 in the GH plane.

If the system is stable, than $f(s)$ has no zeros inside the surface Γ limited by the contour C , because otherwise some poles would have positive real part. This means: $Z=0$.

The Nyquist criterion for stability can thus be expressed as:

$$E = -P \quad (4.6)$$

The system is stable if there is an encirclement of the point -1 in the f -plane for each pole of GH in the right half plane.

The locus in the GH plane is called Nyquist plot: an example is shown in Fig 4.3 for a stable system.

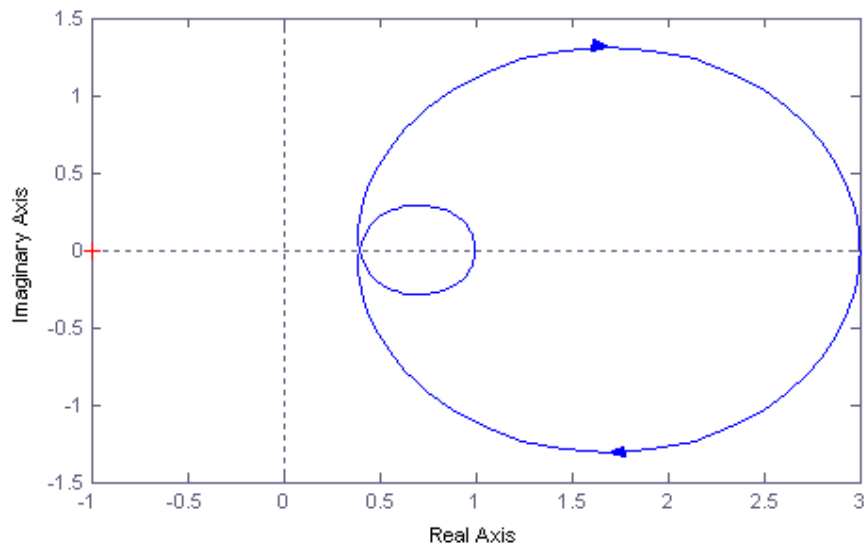


Fig 4.3: example of Nyquist plot for a stable system: since there are no poles for GH in the right half plane, the point -1 is never encircled

Since the Nyquist plot is drawn in the complex plane, it gives in just one graph the same information of the Bode Diagrams.

The Root-Locus method

The Root-Locus method is based on a plot of the roots of the characteristic equation in the s -plane as a function of a parameter - usually the gain K -. The stability “border” is reached when a root or a pair of complex conjugate roots cross the imaginary axis and enter the positive half plane.

The locus can be sketched in the s -plane following a few rules.

First of all, the poles and the zeros of the open-loop must be placed in the correct position in the s -plane, and then the “asymptotes” must be drawn.

For positive K , the locus contains the real axis to the left of an odd number of poles and zeros. Moreover, in analogy with the “field lines” from positive to negative charges the zeros act as sinks and the poles as sources. The poles and zeros move along the locus if the value of the gain is changed: the stability boundaries are reached when one of the poles enters the positive half plane.

If the poles have negative real part the system is stable but it can show an oscillatory behaviour when, for particular values of K , a couple of complex conjugate poles appears.

4.3 Stability of critical reactors: forward-loop transfer function

In this and in the following sections the general model described in Fig 4.1 will be specialized to the case of critical reactors and the use of stability criteria will lead to an understanding of the most important parameters that determines the stability range.

If the system “reactor” is perturbed with reactivity oscillations, using the method of transfer function introduced in chapter 3.5, the forward-loop transfer function is:

$$G(s) = \frac{\delta N(s)}{\delta R(s)} = \frac{n_0}{ls + \beta - \rho_0 - \sum_i \frac{\beta_i \lambda_i}{s + \lambda_i}} \quad (4.7)$$

where $\delta R(s)$ is the Laplace Transform of the reactivity oscillations $\delta \rho(t)$.

Considering only one group of delayed neutrons, equation (4.7) can be rewritten as:

$$G(s) = \frac{\delta N(s)}{\delta R(s)} = \frac{n_0}{\left(l + \frac{\beta}{s + \lambda}\right) s - \rho_0} = \frac{n_0 (s + \lambda)}{l(s - \omega_1)(s - \omega_2)} \quad (4.8)$$

where ω_1 and ω_2 are the roots of the inhour equation.

These equations represent the reactor core in the model described in Fig 4.1.

Since for critical systems the reactivity level is zero, one pole is at the origin, while if $\rho_0 < 0$ the two poles have both negative real part and the system is thus stable.

For the critical case, equation (4.8) becomes:

$$G(s) = \frac{n_0}{\left(l + \frac{\beta}{s + \lambda}\right) s} = \frac{n_0 (s + \lambda)}{ls \left(s + \lambda + \frac{\beta}{l}\right)} \quad (4.9)$$

A sketch of the Bode diagram for the amplitude is given in Fig 4.4.

Considering different frequency range and different order of magnitude for the neutron generation time l , very simple approximated expressions describing the forward-loop transfer function are obtained. In these cases, the stability analysis can be performed analytically by solving rather simple equations.

For low frequency (s small) equation (4.9) becomes:

$$G(s) \approx \frac{n_0}{\left(l + \frac{\beta}{\lambda}\right) s} = \frac{n_0}{sl'} \quad (4.10)$$

where l' is the “effective lifetime”.

The Bode diagram is just a straight line with negative slope of 20db/decade as it can be seen if the left part of Fig 4.4; the phase is negative ($-\pi/2$).

For high frequency (s large), the asymptotic behaviour is:

$$G(s) \approx \frac{n_0}{(ls + \beta)} \quad (4.11)$$

The high frequency pole is at $s = -\beta/l$ and the parameter β reflects the presence of delayed neutrons. This case is shown in the right part of Fig 4.4 because the values $s = -\beta/l$ and $s = -(\beta/l + \lambda)$ are very close, especially for fast systems.

Finally, if the parameter l is very small the PJ approximation is valid and equation (4.9) becomes:

$$G(s) \approx \frac{n_0 (s + \lambda)}{ls \left(\frac{\beta}{l}\right)} = \frac{n_0 (s + \lambda)}{\beta s} = \frac{n_0}{\beta} \frac{(s + \lambda)}{s} \quad (4.12)$$

$G(s)$ has now only a pole at $s=0$ and a zero; this case is often called “the infinite bandwidth”, as it can be inferred from the Bode diagram in Fig 4.4. The stability of such a system is normally not an issue because feedback effects are dominant.

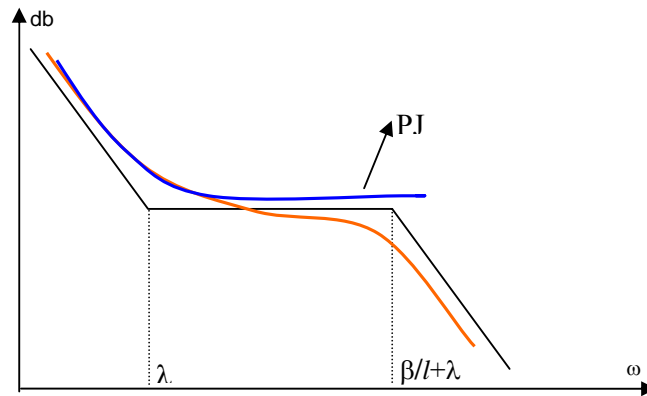


Fig 4.4: Bode diagram for critical reactor with 1 group of delayed neutrons and in the prompt jump approximation

If a neutrons' source is present, the typical Bode Diagram for the forward loop transfer function is given in Fig 4.5: since the low frequency pole is not in the origin anymore, the Bode diagram for the amplitude starts flat and the initial value of the phase is 0 and not $-\pi/2$,

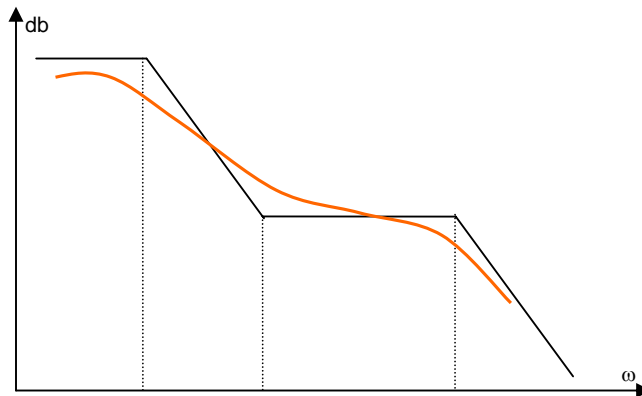


Fig 4.5 Bode diagram in the presence of source

4.4 Feedback transfer function

The Feedback Transfer Function can be studied in a few simple cases but also in its general form by means of the so called “Linear Feedback Kernel”.

The starting point is the general equation of reactivity:

$$\rho = \rho_0 - \rho_f \quad (4.13)$$

ρ_f is the feedback reactivity that in case of linear temperature feedback can be written as:

$$\rho_f = \alpha(T - T_0) \quad (4.14)$$

where α is the opposite of the temperature feedback coefficient, T is an average temperature for the reactor and T_0 is a reference temperature, often referred to stable equilibrium operation. Equation (4.14) represents the first order term of a more general non linear relation between reactivity and temperature.

Since temperature depends on power P and often also on the previous “history of power”, the relation T - P is generally non linear.

Nevertheless, it is possible to consider for the T - P relation a simpler linear equation expressed by Newton’s law of cooling:

$$\frac{dT}{dt} = Kn - \gamma(T - T_c) \quad (4.15)$$

where K is the reciprocal of the heat capacity C , n is the power, $1/\gamma$ is the mean time for heat transfer and T_c is the coolant temperature.

According to this model, the reactor is considered as a unique block with a characteristic average temperature T and temperature variations due to any kind of perturbation are adequately represented by assuming a single averaged coolant temperature T_c .

This model is very simple and assumes that suitable effective values for the parameters can be obtained.

Equation (4.14) and (4.15) can be combined to derive a direct relation between the power and the reactivity.

In addition, from equation (4.15) it is possible to derive other simple linear models, like the adiabatic model, valid for fast excursions during which heat losses are negligible.

All these models are special cases of a more general relation between the reactivity and the power level:

$$\rho_f(t) = \int_0^t h(t-t') [n(t') - n_0] dt' \quad (4.16)$$

This equation is valid for linear systems and describes the dependency of the reactivity on the past history of power. $h(t)$ is called “feedback kernel”. It is determined by the feedback mechanism and it is formally a weighting function in a linear superposition. Since equation (4.16) is a convolution integral, it is convenient to use Laplace Transform and get the equation:

$$R_f(s) = H(s)\delta N(s) \quad (4.17)$$

where $H(s)$ is the feedback transfer function.
For Newton's law of cooling the Feedback Kernel is:

$$H(s) = \frac{\alpha K}{s + \gamma} \quad (4.18)$$

4.5 Reactor systems with feedback

Using the results derived in chapter 4.3 and 4.4 and one of the stability criteria described in chapter 4.2 the stability of the complete reactor with feedback can be studied. The use of one of the approximations introduced in chapter 4.3 for the forward-loop transfer function makes the problem easy to handle.
 $H(s)$ is expressed by equation (4.18).

Effective lifetime model

According to this model, valid at low frequency, $G(s)$ is given by equation (4.10). Hence the characteristic equation is:

$$D(s) = s^2 + \gamma s + K_0 \lambda = 0 \quad (4.19)$$

where

$$K_0 = \frac{\alpha K n_0}{\beta}.$$

The system is stable if K_0 and γ are positive, that means $\alpha > 0$.

Prompt jump approximation

Since $G(s)$ is expressed by equation (4.12) and has just one pole, the characteristic equation is still of second order and it is given by:

$$D(s) = s^2 + (K_0 + \gamma)s + K_0 \lambda = 0 \quad (4.20)$$

The stability condition is the same as in the effective lifetime model because they have equal behaviour at low frequencies.

Second order zero-power transfer function

This model, mostly valid for fast systems, assumes l to be small; a good approximation of $G(s)$ is now:

$$G(s) \approx \frac{n_0(s + \lambda)}{ls \left(s + \frac{\beta}{l} \right)} \quad (4.21)$$

$G(s)$ has now two poles; therefore, the characteristic equation is a third order one:

$$D(s) = \left(\frac{l}{\beta}\right)s^3 + \left(1 + \frac{\gamma l}{\beta}\right)s^2 + (K_0 + \gamma)s + K_0\lambda = 0 \quad (4.22)$$

According to the Routh criterion the system is stable if the following two conditions are satisfied:

$$\alpha > 0$$

$$K_0 \left(\gamma - \lambda + \frac{\beta}{l} \right) + \gamma \left(\gamma + \frac{\beta}{l} \right) > 0$$

Being l small compared to the other coefficients, it can be inferred that the second condition is always satisfied if $K_0 > 0$, which means again $\alpha > 0$.

In other words, the second order model does not add any further information about stability compared with the prompt jump. As described in Fig 4.4 the second order model only adds the high frequency pole.

In the examples analyzed so far only a single feedback loop has been considered: this means that all the feedback effects are of the same nature and act at the same time scale. A more complex model is presented in the following section.

4.6 Two-path feedback model

The point reactor model with two independent reactivity feedbacks, as described in Fig. 4.7, has been the subject of much attention.

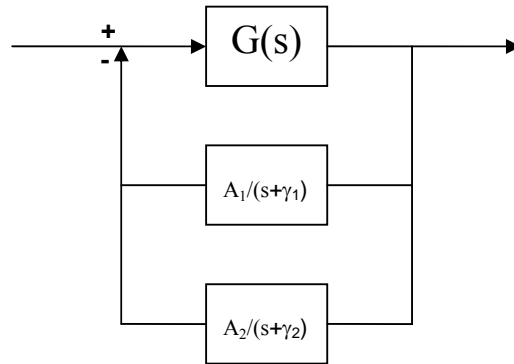


Fig. 4.7: two path feedback model

A_1 and A_2 are coefficients while γ_1 and γ_2 are two different time constants. Since feedback is described by two loops completely independent to each other, this model seems quite unrealistic. Nevertheless it can be demonstrated, making use of transformation matrices formalism, that this decoupled system can represent infinitely many coupled system; hence this is not just a particular case.

The simpler case is the effective lifetime model:

$$H(s) = \frac{A_1}{s + \gamma_1} + \frac{A_2}{s + \gamma_2} \quad (4.23)$$

$$G(s) = \frac{n_0}{l's} \quad (4.10)$$

The characteristic equation is of third order and, assuming the poles of $H(s)$ to be negative, the Routh criterion gives two conditions to be satisfied for stability:

$$(n_0 \lambda / \beta)(A_1 \gamma_1 + A_2 \gamma_2) + \gamma_1 \gamma_2 (\gamma_1 + \gamma_2) > 0 \quad (4.24)$$

$$A_1 \gamma_2 + A_2 \gamma_1 > 0 \quad (4.25)$$

If both conditions are verified the system is unconditionally stable, which means stable at any power level, while if only the second one is satisfied the system is conditionally stable, which means stable up to a certain critical power level.

A zero value for equations (4.24) and (4.25) gives respectively the dynamic and the static stability boundary.

Defining the parameters:

$$\begin{aligned} x &= A_1 n_0 / \beta \\ y &= A_2 n_0 / \beta \end{aligned} \quad (4.26)$$

the stability range can be plotted in the x-y plane, as shown in Fig. 4.8.

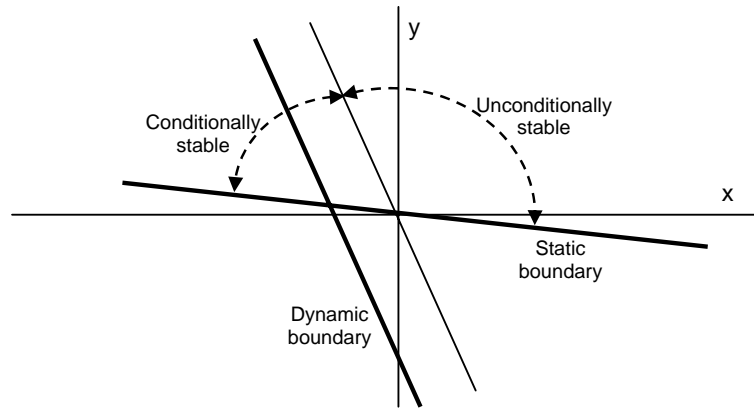


Fig. 4.8: conditional and unconditional stability in the effective lifetime model

In the previous section it has been shown how delayed neutrons play an important and sometimes unexpected role in the stability analysis.

Their role in the “two path feedback model” can be understood using equation (4.12) for the forward loop transfer function.

The characteristic equation is still a third order one and the Routh criterion implies three conditions to be satisfied for stability.

Using equation (4.26) it is possible to draw the stability region in the x-y plane and compare the results with the effective lifetime model.

4.7 Considerations for fast reactors analysis

As mentioned in chapter 3.5, stability in fast reactors shows different features compared to thermal systems: prompt-positive feedback coefficients may arise from Doppler effect and from fuel rod bowing. The Doppler effect is caused by the broadening of many closely-spaced high energy resonances in both the fission and the parasitic-absorption region. The net result of these two competing effects can be either positive or negative.

A stability model can be built up considering the following expression for reactivity [Hetrick, 1993]:

$$\rho = -\alpha_1 T_1 - \alpha_2 T_2 \quad (4.27)$$

where 1 and 2 represent the two regions the system can be divided in: 1 is the fuel region with its near surroundings and 2 is the remaining part of the reactor.

The stability problem is still described by a third order characteristic equation and the construction of the Routh array leads to a variety of cases similar to those analyzed in chapter 4.5.

A remarkable fact is that fast reactor with both negative feedback coefficients may show instability, when the prompt coefficient is small and the delayed one sufficiently large.

In this case, the stability boundaries can enter the first quadrant in the parameters space representation [Hetrick, 1993].

Chapter 5 *Dynamic behaviour of sub-critical systems*

In this chapter, the point kinetics model with source for one group of delayed neutrons is solved for a few cases and under different approximations.

The interest in finding analytical solutions when reliable and powerful numerical methods can solve any kind of system is justified by several reasons. First of all, an exact solution provides better understanding in the physics of the problem and in the importance of the various parameters. Moreover, analytical solutions are often used to evaluate the reliability of numerical methods and the use of different approximations gives information on the validity of the approximations themselves compared to the complete solution. Furthermore, the complexity of the problem states the limit of the analytical analysis.

5.1 System response to a step-wise change in the source

Let us consider the complete system with constant source q_0 in the one group approximation:

$$\frac{dn}{dt} = \frac{\rho - \beta}{l} n + \lambda c + q_0 \quad (5.1)$$

$$\frac{dc}{dt} = \frac{\beta}{l} n - \lambda c \quad (5.2)$$

Looking at equilibrium condition, which means setting to zero the two derivatives, and substituting (5.1) into (5.2), it is found:

$$0 = \frac{\rho - \beta}{l} n_0 + \frac{\beta}{l} n_0 + q_0 \quad (5.3)$$

that means:

$$q_0 = -\frac{\rho}{l} n_0 \quad \text{or} \quad q_0 l = -\rho n_0 \quad (5.4)$$

According to the definition given by equation (5.4), q_0 is the strength of the external source per unit time.

Initial conditions can be set by assuming equilibrium for $t < 0$ so that at the instant $t = 0$ the concentration of neutron and precursors are expressed by:

$$n(t = 0) = n_0$$

$$c(t = 0) = c_0$$

The relation between c_0 and n_0 can be worked out by solving (5.2) under equilibrium conditions.

Study of transients consists in analysing what happens to the system if either the strength of the neutrons source or the reactivity level change in time.

The easiest cases are a step-wise change of the neutron source or of the reactivity level; the strength of the source thus varies from q_0 to q_{new} or the reactivity changes from ρ to $\rho + \rho_0$. The former case is now considered in details.

Let us suppose the system to be in equilibrium condition at a certain power level; at $t=0$, the source is brought step-wise from q_0 to q_{new} and it is then kept to the new value.

In the Laplace domain, for $t > 0$, (5.1) and (5.2) are transformed into:

$$\begin{aligned} Ns - n_0 &= \frac{\rho - \beta}{l} N + \lambda \Gamma + \frac{q_{new}}{s} \\ \Gamma s - c_0 &= \frac{\beta}{l} N - \lambda \Gamma \end{aligned} \quad (5.5)$$

where N and Γ are the Laplace transform of n and c respectively. Solving for Γ in the second equation leads to:

$$\Gamma = \frac{c_0 + \frac{\beta}{l} N}{s + \lambda} \quad (5.6)$$

The relation (5.6) can be plugged into the first equation of the system (5.5); after a few steps it is found that :

$$N(s) = \frac{n_0}{s} \frac{\left[s^2 + \left(\frac{n_0 \lambda + \frac{\beta}{l} n_0 + q_{new}}{n_0} \right) s + \frac{q_{new} \lambda}{n_0} \right]}{\left[s^2 + \left(\frac{l\lambda - \rho + \beta}{l} \right) s - \frac{\rho \lambda}{l} \right]} \quad (5.7)$$

Looking at the denominator it can be noticed that the term between mayor brackets is exactly the same as in the critical case and it thus gives the same two poles $s = \omega_1$ and $s = \omega_2$, while the presence of the source is reflected in a third pole $s = 0$.

Therefore, in the time domain the solution has the following expression:

$$n(t) = A + B e^{\omega_1 t} + C e^{\omega_2 t} \quad (5.8)$$

Equation (5.7) can be rewritten in a more convenient way as:

$$N(s) = \frac{n_0 s}{(s - \omega_1)(s - \omega_2)} + \frac{(n_0 \lambda + \frac{\beta}{l} n_0 + q_{new})}{(s - \omega_1)(s - \omega_2)} + \frac{q_{new} \lambda}{s(s - \omega_1)(s - \omega_2)} \quad (5.9)$$

This expression is now back Laplace transformed; after a few steps it is found that:

$$n(t) = \frac{q_{new} \lambda}{\omega_1 \omega_2} - \left(\frac{n_0 \omega_1^2 + \omega_1 C + q_{new} \lambda}{\omega_1 (\omega_2 - \omega_1)} \right) e^{\omega_1 t} + \left(\frac{n_0 \omega_2^2 + \omega_2 C + q_{new} \lambda}{\omega_2 (\omega_2 - \omega_1)} \right) e^{\omega_2 t} \quad (5.10)$$

where C is a constant.

Applying the rule of the product of the roots in a second order equation the first term

of equation (5.10) becomes:

$$\frac{q_{new}\lambda}{\omega_1\omega_2} = -\frac{q_{new}\lambda l}{\rho\lambda} = -\frac{q_{new}l}{\rho} \quad (5.11)$$

The expressions for the second and third term can be simplified by using the same assumptions introduced for the critical case: $\lambda l \ll \beta - \rho$ and ρ small; the assumptions about ρ are satisfied in slightly sub-critical systems, where the reactivity has negative values not very far from 0. With the aid of these assumptions ω_1 and ω_2 are expressed by equation (3.12); substituting these values, after a few steps equation (5.10) takes the approximated form:

$$n(t) = -\frac{q_{new}l}{\rho} + \left(\frac{l\lambda\rho n_0}{(\beta - \rho)^2} + A + \frac{q_{new}l}{\rho} \right) e^{\frac{\lambda\rho t}{\beta - \rho}} + \left(n_0 - A + \frac{l^2\lambda q_{new}}{(\rho - \beta)^2} \right) e^{\frac{\rho - \beta}{l}t} \quad (5.12)$$

where

$$A = \frac{n_0 l}{\beta - \rho} \left(\lambda + \frac{\beta}{l} + \frac{q_{new}}{n_0} \right)$$

A first insight on the results can be obtained by looking at the asymptotes for $t \rightarrow \infty$ and at the value of the prompt jump ($l \rightarrow 0$).

For simplicity, the source is redefined as:

$$\begin{aligned} q_0 l &= Q_0 \\ q_{new} l &= Q_{new} \end{aligned} \quad (5.13)$$

so that the source has the same dimensions as the power n . With this choice equation (5.12) becomes:

$$n(t) = -\frac{Q_{new}}{\rho} + \left(\frac{l\lambda\rho n_0}{(\beta - \rho)^2} + A' + \frac{Q_{new}}{\rho} \right) e^{\frac{\lambda\rho t}{\beta - \rho}} + \left(n_0 - A' + \frac{l\lambda Q_{new}}{(\rho - \beta)^2} \right) e^{\frac{\rho - \beta}{l}t} \quad (5.14)$$

where

$$A' = \frac{n_0}{\beta - \rho} \left(l\lambda + \beta + \frac{Q_{new}}{n_0} \right)$$

Considering the case when $t \rightarrow \infty$ and assuming $\rho_0 = 0$, equation (5.14) becomes:

$$\frac{n_{new}}{n_0} = \left(-\frac{Q_{new}}{\rho} \right) \left(-\frac{\rho}{Q_0} \right) = \frac{Q_{new}}{Q_0} \quad (5.15)$$

This result is rather intuitive: if the source doubles, it is expected that the power will double too. If $\rho_0 \neq 0$ the result is:

$$\frac{n_{new}}{n_0} = \left(-\frac{Q_{new}}{\rho + \rho_0} \right) \left(-\frac{\rho}{Q_0} \right) = \frac{Q_{new}}{Q_0} \left(\frac{\rho}{\rho + \rho_0} \right) \quad (5.16)$$

For the case $l \rightarrow 0$, the prompt jump approximation, all the terms in equation (5.14) should be simplified by setting $t=0$ and $l \rightarrow 0$. The most remarkable facts are that the two exponentials $e^{\rho_1 t}$ and $e^{\rho_2 t}$ goes to 1 and to 0 respectively.

In the case $\rho_0 = 0$, equation (5.14) becomes:

$$n_{new} = \frac{n_0 \beta}{\beta - \rho} + \frac{Q_{new}}{\beta - \rho} = \frac{n_0}{\beta - \rho} \left(\beta - \rho \frac{Q_{new}}{Q_0} \right) \quad (5.17)$$

If a reactivity step $\rho_0 \neq 0$ is provided, (5.17) changes into:

$$\frac{n_{new}}{n_0} = \frac{1}{\beta - (\rho + \rho_0)} \left(\beta - \rho \frac{Q_{new}}{Q_0} \right) \quad (5.18)$$

Equations (5.16) and (5.18) are the most general expressions for the power ratio for $t \rightarrow \infty$ and $l \rightarrow 0$ respectively.

Equation (5.14) shows that several parameters determines the evolution of neutrons population in the reactor and the asymptotes expressed by equations (5.16) and (5.18) underlines the key role played by a few of them, especially by the sub-criticality level.

In fact, while for critical assemblies the prompt jump is a function of β and of the reactivity step (equation (3.14)), in sub-critical systems it also depends on the state of sub-criticality.

These preliminary considerations can be extended and improved by analysing some transients under different conditions, which means for different values of the parameters. In the rest of the section the simplest transient, which is the doubling of the neutrons source strength at time $t=0$, will be analyzed.

In the system under study reference value for the parameters are [D'Angelo, 2003]:

- $\beta=0.0035$
- $l= 4.2*10^{-7} s$
- $\lambda = \left(\frac{1}{\beta} \sum_i \frac{\beta_i}{\lambda_i} \right)^{-1} = 0.0897 s^{-1}$ where λ_i and β_i are the values for the six groups model.

Sub-criticality level

The power response after doubling the source is studied for different level of sub-criticality, from 0.995 to 0.95. Since the neutron generation time is very small, the important part of the transient is the first tens of microseconds.

Fig 5.1 shows that a higher k implies a lower prompt response and a slower transient, because delayed neutrons have more importance and the external source is weaker: the system still shows some “critical behaviour”. On the contrary, for $k=0.95$, the prompt response is about 90% of the whole transient, showing a decreased importance for delayed neutrons at this sub-criticality level: the transient is now mostly driven by the source.

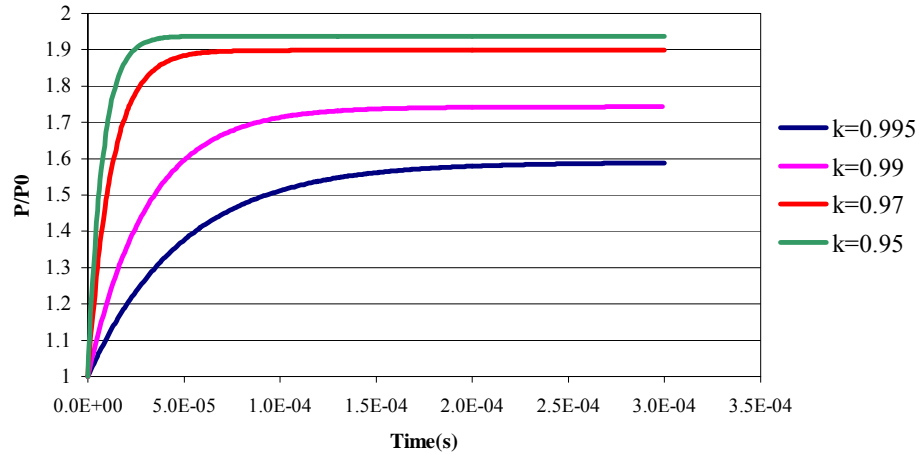


Fig 5.1: transient beginning at four sub-criticality levels

After the prompt response, the system evolves much slowly; Fig 5.2 helps understanding how time scale is important to enlighten different phenomena: at the scale of seconds no difference can be seen in the initial growth between the prompt jump approximation and the complete solution, because the transient is too long. Nevertheless, Fig 5.2 still shows the different magnitude of the prompt jump for different sub-criticality levels and how the system slowly evolves towards the asymptotic value.

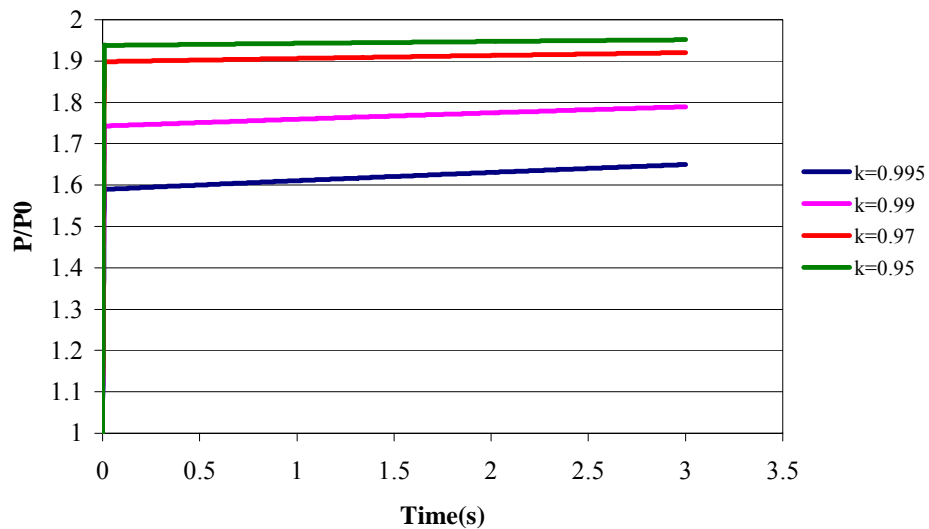


Fig 5.2: first 3 seconds of transient at four different sub-criticality levels

A plot of the complete transient gives the asymptote for $t \rightarrow \infty$ and represents a

further validation of equation (5.14). Results show a good agreement not only for the doubling of the source, but also for a reactivity step insertion and for both. An example for the doubling of the source is shown in Fig. 5.3.

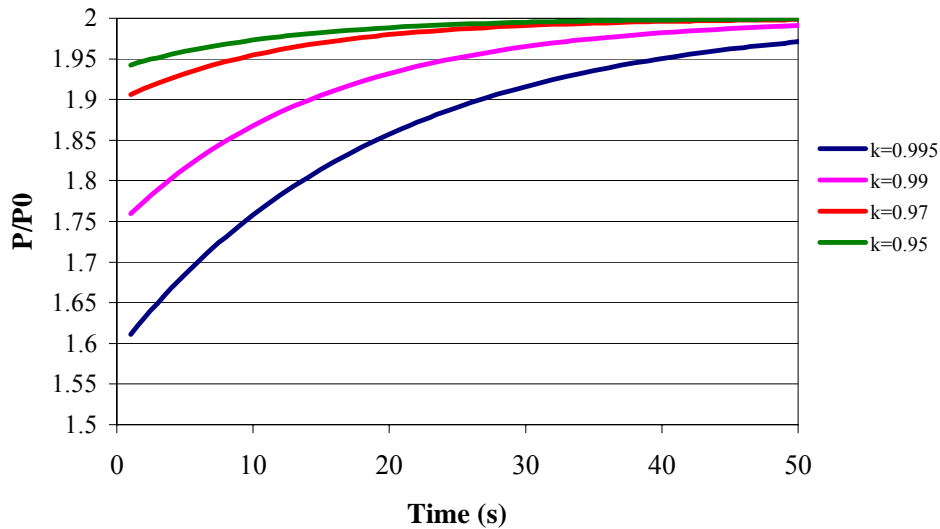


Fig 5.3: asymptotic power response at four different sub-criticality levels

Delayed neutrons fraction β

Since different fuel mixtures can be used in a sub-critical system, the delayed neutrons fraction varies inside a certain range, which is normally lower than the value for Uranium-235 in critical reactors ($\beta=0.0065$). In fact Plutonium and MA, which are used as a fuel in ADS, have a β fraction much lower than Uranium. In critical system this fact can cause control problems that would not occur in an ADS, because the system is driven by the source.

Fig 5.4 shows how the response changes over the whole transient by varying β . The k value is set to 0.98 while reference values are assumed for the other parameters.

A low β makes the transient faster and the prompt response higher, because the delayed neutrons fraction is smaller.

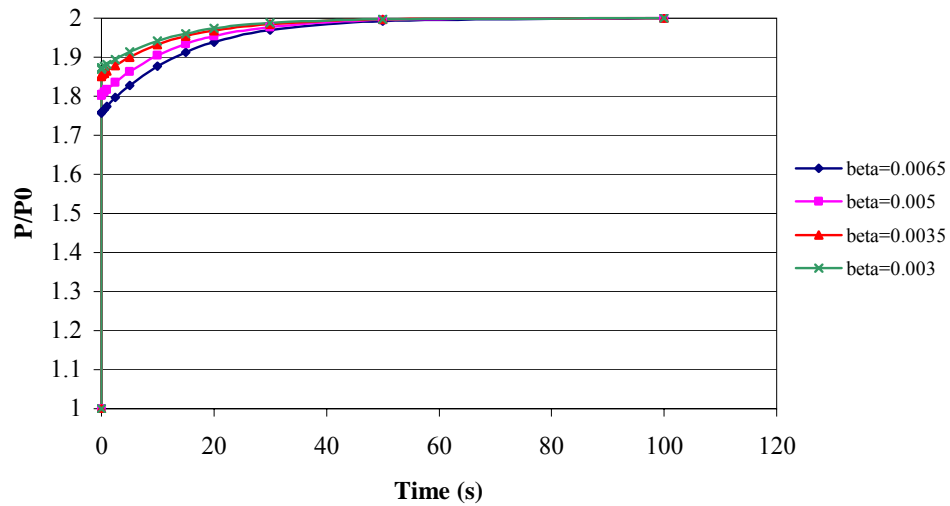


Fig 5.4: influence of β in the power response

Precursors decay constant λ

The decay constant λ is inversely proportional to the mean precursors generation time: it expresses how fast the precursors decay.

λ depends on fission fragments yields: therefore, it is not expected to change so much in an ADS when the fuel composition is varied. Higher λ means faster production of delayed neutrons, thus faster transients.

Since λ is only referred to delayed neutrons production, the value of the prompt response is not influenced. A plot for $k=0.98$ and reference values for the other parameters is shown in Fig 5.5.

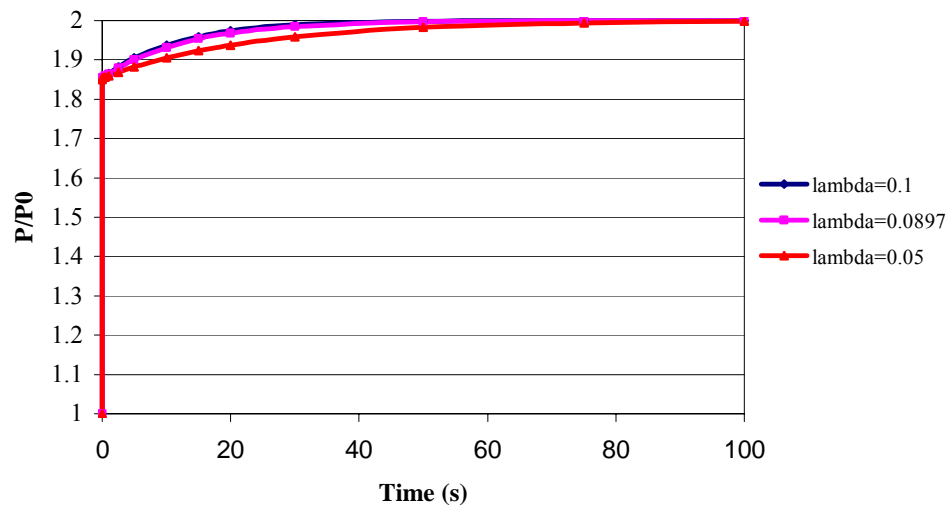


Fig 5.5: influence of λ in the power response

Neutrons generation time l

In fast systems the neutrons generation time can vary from 10^{-6} to 10^{-8} seconds.

If $l < 10^{-5}$ it can be shown that, assuming reference value for all the other parameters, more than 70% of the power change is done almost instantaneously (less than 1 ms) while for larger values the prompt response is less important.

Since ADS is always a fast system, l is always smaller than 10^{-5} . The “prompt response” is thus very important.

Non-dimensional analysis

Equation (5.14) has been derived and discussed assuming all the parameters to be independent from each other.

The reader may wonder if the parameters β , λ and l are truly independent or if it possible to identify a unique quantity whose variation is representative for all the parameters.

A non-dimensional formulation of the point kinetic system might provide the answer. β , λ and l are physically very different, being the first two related to fission products, and thus to delayed effects, and the last one to neutrons generation time.

Nevertheless, the product λl is dimensionless and a careful analysis on equation (5.14) shows that the coefficients of the exponentials always contain the term λl and never any of the two separated.

Despite this, the two decaying exponentials depend separately on λ and l and this remains true even if an exact expression for the root of the characteristic equation is used. Therefore, the three parameters are both physically and “formally” independent.

In Fig. 5.1-5.5 the power response has been scaled by the reference power P_0 , which is the steady state power level at a certain sub-criticality level and consequently with source strength Q_0 .

It is important to prove that the power ratio is a function of the source strength ratio and not of Q_0 . In other words, if the same source variation is given to systems at different steady state power level but with the same sub-criticality level the response will be the same.

A non-dimensional formulation of point kinetics is:

$$l \frac{d\bar{n}}{dt} = (\rho - \beta)\bar{n} + \beta\bar{c} - \rho\bar{Q} \quad (5.19)$$

$$\frac{1}{\lambda} \frac{d\bar{c}}{dt} = \bar{n} - \bar{c} \quad (5.20)$$

where:

$$\bar{n} = n / n_0$$

$$\bar{c} = c / c_0$$

$$\bar{Q} = Q_{new} / Q_0$$

and the usual relations between the steady state values of neutrons and precursors density and of the source strength have been used.

Considering the simple case of a step-wise change in the source strength at time $t=0$, in the Laplace domain the result is:

$$\bar{N} = \frac{1}{sl} \frac{ls^2 + (l\lambda + \beta - \rho B)s - \rho\lambda B}{(s - \omega_1)(s - \omega_2)} \quad (5.21)$$

where $B = Q_{new}/Q_0$ and the other terms are defined as in equation (5.9).

Equation (5.21) highlights the dependence of the non-dimensional power only on the non-dimensional source, and thus on the source ratio.

5.2 The Prompt Jump approximation

Equation (5.12) shows how complex is the complete mathematical solution for the simplest case of a step-wise change in the neutrons source strength. This equation expresses both the advantage and the disadvantage in finding analytical solutions: the possibility of having an agile, readable and understandable tool is limited to a few cases.

In chapter 3.4 it has been shown how a first order equation describing the evolution of the neutron density in the prompt jump approximation can be derived. The basic assumption in this procedure is the possibility to neglect time derivatives in the point kinetic system.

Equation (3.20) has been derived without any further assumption on the source or on the reactivity level, so it remains valid for the sub-critical case.

If the source is changed step-wise from q_0 to q_{new} , the new approximated power level is:

$$n_{new} = \frac{\lambda c_0 + lq_{new}}{\beta - \rho} \quad (5.22)$$

Using the definition $lq = Q$ and the relation $Q_0 = -\rho n_0$, equation (5.22) is equal to (5.17), that represents the new power level in the prompt jump approximation. The validity of this method is thus proved.

Equation (3.21), that we recall for completeness, can now be solved in the sub-critical case:

$$(\beta - \rho) \frac{dn_1}{dt} - \left(\lambda \rho + \frac{d\rho}{dt} \right) n_1 = \lambda l q + l \frac{dq}{dt} \quad (3.21)$$

The solution of this equation, once the type of source is defined, gives the power evolution in the PJ: this means that the initial value for n_1 is given by the prompt jump approximation. A comparison between this solution and the complete one shows how good this approximated model is: the two solutions, after a sufficiently large time, should converge to the same value.

Neglecting feedback, the equation is simplified into:

$$(\beta - \rho) \frac{dn_1}{dt} - \lambda \rho n_1 = \lambda l q + l \frac{dq}{dt} \quad (5.23)$$

Considering the special case of doubling of the source at time $t=0$, for positive time the equation (5.23) becomes:

$$(\beta - \rho) \frac{dn_1}{dt} - \lambda \rho n_1 = \lambda l q_{new} \quad (5.24)$$

where $n_1(t=0)$ is the value of the prompt jump given by equation (5.17).

The solution of the equation is:

$$n_1(t) = \left(n_1(0) + \frac{l q_{new}}{\rho} \right) e^{\frac{\lambda \rho t}{\beta - \rho}} - \frac{l q_{new}}{\rho} \quad (5.25)$$

which represents the evolution of neutron population in the prompt jump approximation and for a step-wise change in the source.

Another interesting case is represented by a ramp-wise variation in the source strength.

It is assumed that the source is varying between a value q_0 and q_{new} in a certain time t' , according to the relation:

$$q_{new}(t) = q_0 (1 + at) \quad (5.26)$$

where $t < t'$ and a is a number.

In this case equation (5.23) should be used and it can be solved using Laplace Transform method. This procedure is general, and the source profile only determines the type and the complexity of the final solution.

A few steps lead to:

$$N(s) = \frac{l}{\beta - \rho} \frac{(\lambda + s)}{\left(s - \frac{\lambda \rho}{\beta - \rho} \right)} Q(s) + \frac{n_1^* - \frac{l q_0}{\beta - \rho}}{\left(s - \frac{\lambda \rho}{\beta - \rho} \right)} \quad (5.27)$$

where n_1^* is the value of the neutron population in the prompt jump approximation.

Substituting the expression for the Laplace transform of a ramp, equation (5.27) becomes:

$$N(s) = \frac{l q_0}{\beta - \rho} \frac{(\lambda + s)}{\left(s - \frac{\lambda \rho}{\beta - \rho} \right)} \left(\frac{1}{s} + \frac{a}{s^2} \right) + \frac{n_1^* - \frac{l q_0}{\beta - \rho}}{\left(s - \frac{\lambda \rho}{\beta - \rho} \right)} \quad (5.28)$$

This equation can be rearranged into:

$$N(s) = \frac{lq_0}{\beta - \rho} \frac{s^2 + (\lambda + a)s + \lambda a}{s^2 \left(s - \frac{\lambda \rho}{\beta - \rho} \right)} + \frac{n_1^* - \frac{lq_0}{\beta - \rho}}{\left(s - \frac{\lambda \rho}{\beta - \rho} \right)} \quad (5.29)$$

With an inverse Laplace Transform and a few steps the final expression for the neutron density evolution in the prompt jump approximation is derived:

$$n_1(t) = -q_0 l \left[\left(\frac{\lambda + a}{\lambda \rho} + \frac{a(\beta - \rho)}{\lambda \rho^2} \right) \left(1 - \exp\left(\frac{\lambda \rho t}{\beta - \rho} \right) \right) + \frac{at}{\rho} \right] + n_1^* \exp\left(\frac{\lambda \rho t}{\beta - \rho} \right) \quad (5.30)$$

These approximated results are now analyzed in comparison to the complete solution provided in the previous section.

Equation (5.25) is first compared with the complete solution expressed by equation (5.12) at different sub-criticality levels. It can be shown that for high k the two solutions reaches the same value after about 200 μ s while for lower k the transient is faster and the convergence is reached after about 50 μ s.

Equation (5.25) fully describes the transient apart for the first instants where a relevant difference with the complete solution is present.

An example for $k=0.97$ is shown in Fig 5.6.

For large time both the solutions converge to the same steady value.

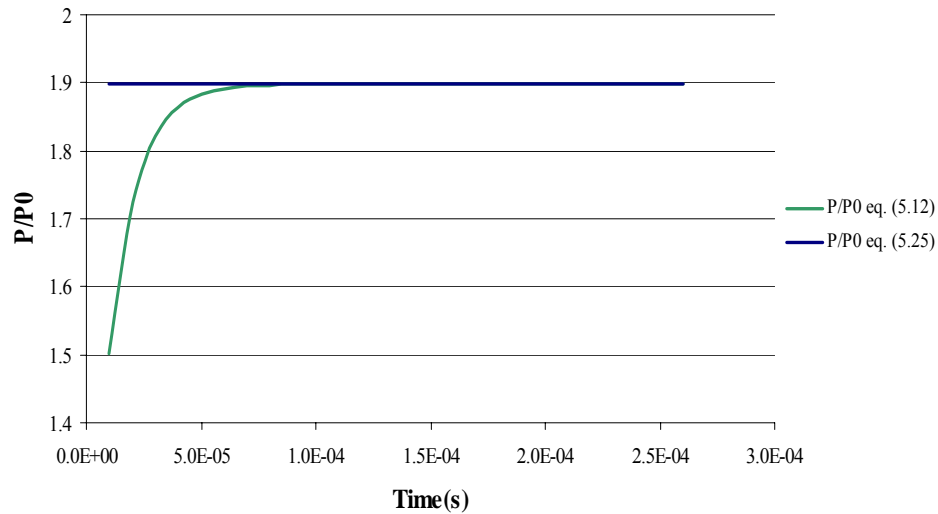


Fig 5.6: comparison between equation (5.12) and (5.25) for $k=0.97$

For the ramp case, the solution of the point kinetic system (5.1) and (5.2) becomes very complex to obtain by analytical means.

Therefore, since it has been proved that the approximated equation (5.23) gives good results for a step-wise change in the source, the ramp case can be treated under this approximation using equation (5.30).

As a first example, a fast ramp leading to a source doubling in 10^{-4} s can be analyzed.

Equation (5.30) should be used for $t < 10^{-4}$ while for $t > 10^{-4}$ the source strength is kept to the final value. The problem is thus reduced to the constant source one and a modified form of (5.25) may be employed: after the ramp being finished, the source has been increased to the value q_{new} . Equation (5.25) becomes:

$$n_1(t) = \left(n_1(0) + \frac{lq_{new}}{\rho} \right) e^{\frac{\lambda\rho(t-t')}{\beta-\rho}} - \frac{lq_{new}}{\rho} \quad (5.31)$$

where at $t = t'$ the ramp is finished.

Since the time scale of the ramp profile is very short, results are very similar to the step-wise case except for the fact that the power changes according to the fast ramp profile and not almost instantaneously, as described by equation (5.25). Additionally, at this time scale it is not possible to see how power evolves after the ramp has been finished.

The same procedure can be employed if the doubling of the source occurs in 1 second, and thus the ramp is much slower.

Since the time scale is now longer, the differences between the PJ approximation and (5.30)-(5.31) are more evident, as it can be seen in Fig 5.7.

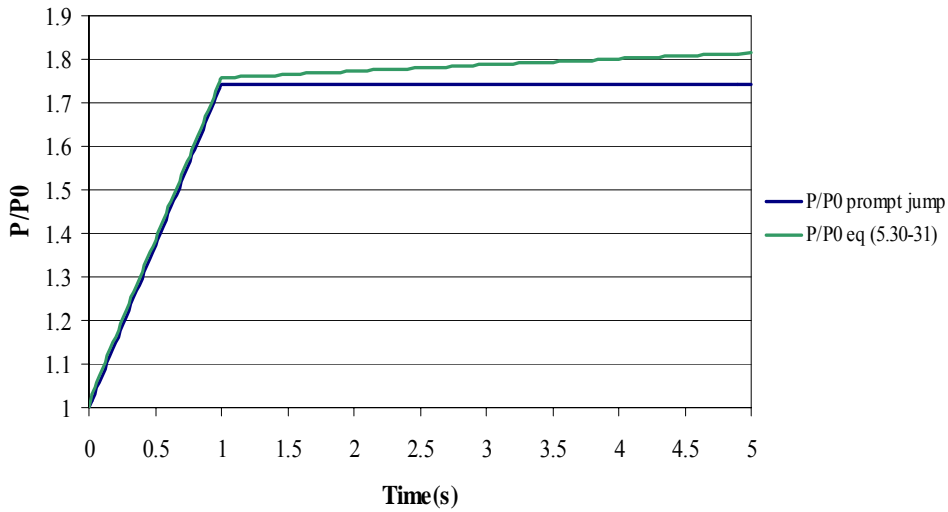


Fig. 5.7: response to a slow ramp (1s) at $k=0.99$

In addition, it is interesting to point out that when the source has reached its final value the equation describing the transient changes from (5.30) to (5.31). The value $n_1(t = 1s)$ is given by (5.30) and represents the neutrons population after the ramp has been completed. This is thus the constant value that has to be used in the “constant source” approximated solution.

Fig 5.8 compares the first 5 sec of the transient shown in Fig 5.7 with a step-wise increase of the source by a factor of two. In the former case only the approximated method can be used, while in the latter both the exact and the approximated solution can be employed. The most remarkable result is that after the source has been doubled the power level evolves almost in the same way.

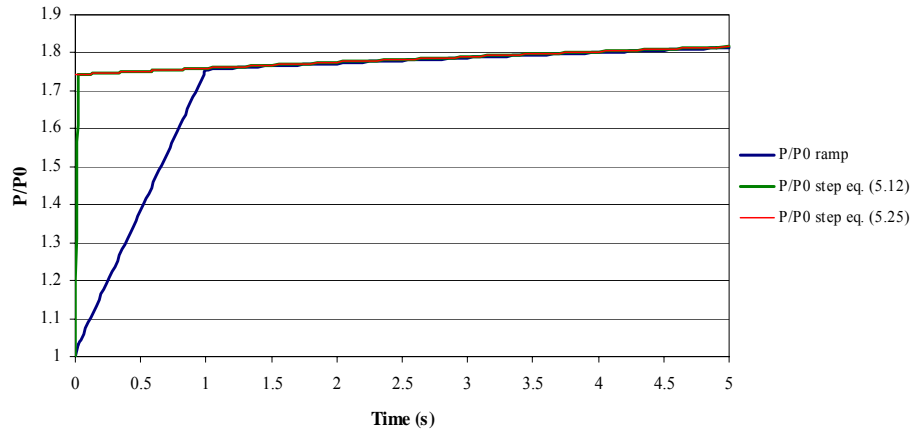


Fig 5.8: comparison between ramp and step input response; $k=0.99$

5.3 The Fuchs Model for sub-critical systems

The Nordheim-Fuchs model, already described for critical systems in chapter 3.7, will be now considered in the sub-critical case.

In this model all the neutron sources except the production of prompt neutrons are neglected, so in the dynamic system the term λc can be retained.

The equation to solve is then:

$$\frac{dn}{dt} = \frac{\rho - \beta}{l} n + q \quad (5.32)$$

As a preliminary analysis, it is expected this approximation to be valid for very short and large power excursion, when it is acceptable to neglect the production of delayed neutrons.

Equation (5.32) can be solved employing Laplace transforms for a general source profile q :

$$N(s) = \frac{Q}{s - \frac{\rho - \beta}{l}} + \frac{n_0}{s - \frac{\rho - \beta}{l}} \quad (5.33)$$

where Q is the Laplace Transform of the source q .

If the source, originally at constant value q_0 for a system in steady state conditions, changes step-wise to a new level q_{new} at time $t=0$, the final result is:

$$n(t) = \left(n_0 + \frac{q_{new} l}{\rho - \beta} \right) e^{\frac{\rho - \beta}{l} t} - \frac{q_{new} l}{\rho - \beta} \quad (5.34)$$

Since in sub-critical systems ρ is negative and the studied transients concern changes in the source strength, the exponential in (5.34) is negative and goes to 0 for very

large time; the asymptote is then:

$$n_{asympt} = -\frac{q_{new}l}{\rho - \beta} \quad (5.35)$$

The asymptotic power in this approximation thus depends on the reactivity, which means on the sub-criticality level expressed by k . The asymptotic power is different from the one given by equation (5.15): as already foreseen, the Fuchs approximation cannot be used for the whole transient.

A comparison between the exact equation and the Fuchs approximation for different transients and different value of k has been made.

If the source strength is doubled, the Fuchs model is satisfactory only for low reactivity level ($k < 0.97$) and for a few tens of microseconds ($< 50\mu\text{s}$). Discrepancies at the tail remain around 5-7%, as it can be seen in Fig.5.9.

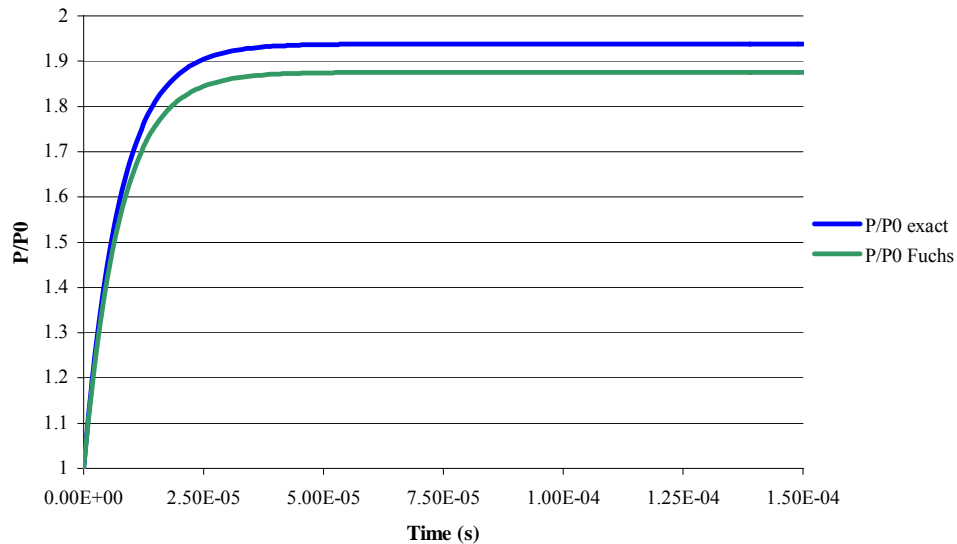


Fig 5.9: comparison between Fuchs model and exact solution when the source strength is doubled; $k=0.95$

When the source is set at 4 times the initial value, the Fuchs model is more accurate and for lower k level and $t < 50\mu\text{s}$ the differences at the tail are within 1-2%. In this case delayed neutrons have almost no importance.

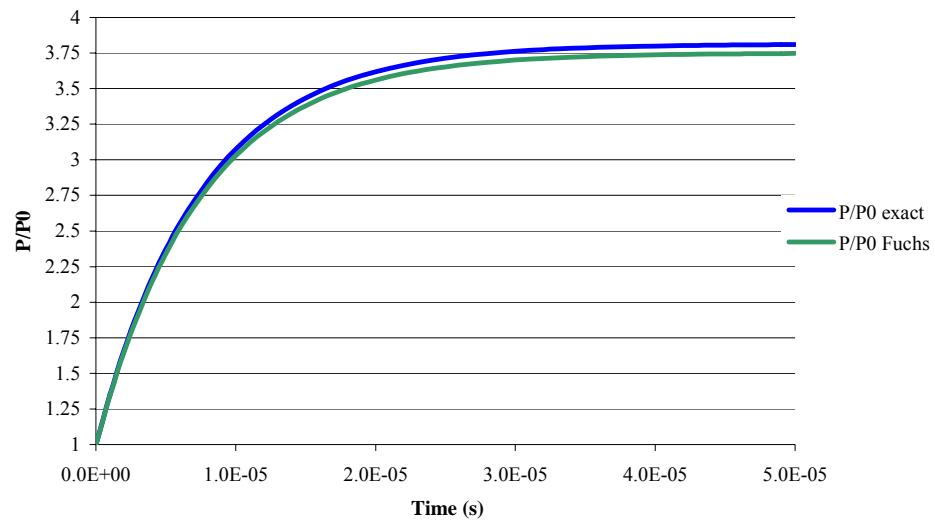


Fig 5.10: comparison between Fuchs model and exact solution when the strength of the source becomes four times bigger; $k=0.95$

Chapter 6 *Stability analysis of sub-critical systems*

This chapter presents an extensive study on the stability of the ADS, using linear stability theory.

In chapter 5 it has been shown that the strength of the external neutrons source is the most important parameter in driving the dynamics of the ADS; therefore this study will focus on the system response to source fluctuations.

Stability analysis is presented in the following sections according to an increasing level of complexity, from the simplest model of the core to a multi-delayed feedback model. This approach allows a comparison between analytical results and simulations. In addition, results obtained under different approximations can be compared and it is thus possible to evaluate if a simple model gives satisfactory results.

6.1 Reactor core transfer function

In this section the forward-loop transfer function is studied in the case of one group of delayed neutrons.

As worked out in chapter 3.5, the response to a source fluctuation is given by:

$$\delta N(s) = \frac{l \left[\delta n(0) + \sum_i \frac{\lambda_i \delta c_i(0)}{s + \lambda_i} + \delta Q(s) \right]}{ls + \beta - \rho_0 - \sum_i \frac{\beta_i \lambda_i}{s + \lambda_i}} \quad (3.30)$$

Looking at the steady-state portion of the response and considering the one group model, equation (3.30) becomes:

$$G(s) = \frac{\delta N(s)}{\delta Q(s)} = \frac{l}{ls - \rho_0 + \beta - \frac{\lambda \beta}{s + \lambda}} \quad (6.1)$$

This response is valid for any type of source fluctuation.

Equation (6.1) can be better written as:

$$G(s) = \frac{(s + \lambda)}{s^2 + \left(\lambda + \frac{\beta - \rho_0}{l} \right) s - \frac{\rho_0 \lambda}{l}} \quad (6.2)$$

$G(s)$ represents the open loop transfer function for a sub-critical system driven by a neutron source in the presence of source oscillations. Since the system is sub-critical, the reactivity ρ_0 is always negative and never 0.

Considering different frequency ranges, $G(s)$ can be further simplified, as already described in chapter 4.3.

For very low frequency ($s \ll \lambda$), equation (6.1) is approximated by:

$$G(s) = \frac{l}{ls - \rho_0 + \beta - \frac{\lambda\beta}{\lambda}} = \frac{l}{ls - \rho_0} = \frac{1}{s - \rho_0/l} \quad (6.3)$$

The Bode diagram is a flat line till the negative pole $s = \rho_0/l$, followed by a descent with a slope of 20db/decade.

In the high frequency range ($s \gg \lambda$), equation (6.1) becomes:

$$G(s) = \frac{l}{ls - \rho_0 + \beta - \frac{\lambda\beta}{s}} = \frac{s}{s^2 + \frac{\beta - \rho_0}{l}s - \frac{\lambda\beta}{l}} \quad (6.4)$$

$G(s)$ has a zero in the origin and two poles, one close to the origin and the other at higher frequency; a sketch is drawn in Fig 6.1.

A good approximated value for the high frequency pole is: $s \approx (\rho_0 - \beta)/l$.

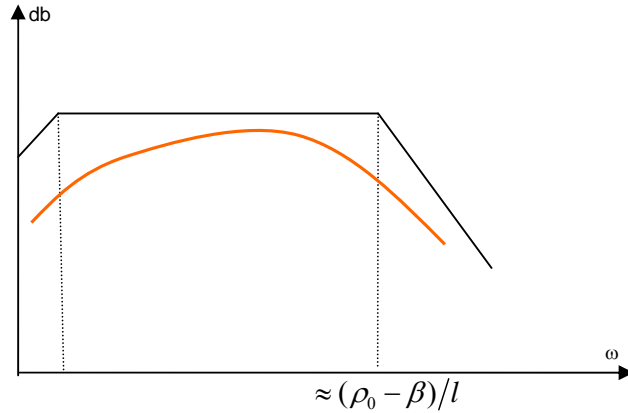


Fig 6.1: Bode diagram for high frequency

The last case is the Prompt Jump approximation: when l is very small the transfer function can be written in the simpler form:

$$G(s) \approx \frac{1}{\frac{\beta - \rho_0}{l} - \frac{\lambda\beta}{l(s + \lambda)}} = \frac{s + \lambda}{\frac{\beta - \rho_0}{l}s - \frac{\rho_0\lambda}{l}} \quad (6.5)$$

The pole, at frequency $s = \rho_0\lambda/(\beta - \rho_0)$, is quite close to the zero, at frequency $s = -\lambda$.

For typical values of the parameters it will further be proved that the pole is at lower frequency than the zero. Anyway, just by looking at this simplified formulation, it is evident that $|\rho_0/(\beta - \rho_0)| < 1$; hence the pole is at lower frequency.

The asymptotic Bode diagram, representing the low frequency part of the response is:

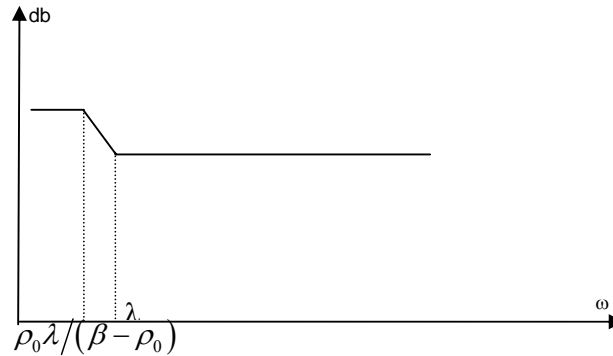


Fig 6.2: Bode diagram in the prompt jump approximation, assuming the pole to be at lower frequency than the zero

To study the stability of this system the sign of the poles of $G(s)$ should be defined in the suitable range in which the parameters can vary. For this reason it is important to know the order of magnitude of all the parameters.

The following values can be assumed:

- Reactivity ρ_0 : it is negative and, for $0.95 < k < 0.995$, $-10^{-2} < \rho_0 < -10^{-3}$
- Delayed neutron fraction $\beta \approx 10^{-3}$
- Precursors decay constant $\lambda \approx 10^{-1}$
- Neutron generation time $l \approx 10^{-7}$

Substituting into equation (6.2) it is found that:

- $\lambda + \frac{\beta - \rho_0}{l} \approx \frac{\beta - \rho_0}{l} \approx 10^4 \rightarrow 10^5$, so the term λ is negligible
- $-\frac{\rho_0 \lambda}{l} = 10^3 \rightarrow 10^4$ and positive

Equation (6.2) shows that one zero is at $s = -\lambda = -0.0897$ while the two poles are given by the solutions of the equation:

$$s^2 + \left(\lambda + \frac{\beta - \rho_0}{l} \right) s - \frac{\rho_0 \lambda}{l} = 0 \quad (6.6)$$

or of the simplified form:

$$s^2 + \left(\frac{\beta - \rho_0}{l} \right) s - \frac{\rho_0 \lambda}{l} = 0 \quad (6.7)$$

The result from equation (6.6) is:

$$s_{1,2} = \frac{-\left(\lambda + \frac{\beta - \rho_0}{l} \right) \pm \sqrt{\left(\lambda + \frac{\beta - \rho_0}{l} \right)^2 + \frac{4\rho_0 \lambda}{l}}}{2} \quad (6.8)$$

Equation (6.8) shows that for typical values given to the parameters, the poles have negative real part and the square root is positive. Both the poles are thus real and negative, so the system is always stable.

Considering that:

$$\frac{4\rho_0\lambda}{l} \ll \left(\lambda + \frac{\beta - \rho_0}{l} \right)^2$$

one pole is very close to zero and the other has a very large absolute value.

From the point kinetics system expressed by equations (3.3) and (3.4) it can be noticed that, provided n_0 to represent the power, the source does not, because it would not be dimensionally coherent. In fact the source q has the same dimensions as n/l . If the source is redefined as in chapter 5.1:

$$\bar{q} = ql \quad (6.9)$$

the source and the power are now dimensionally coherent and the transfer function is modified just by the factor $1/l$. The stability analysis is not changed, but with this choice the response to variations in the source strength is a power fluctuation.

The new transfer function is thus:

$$G(s) = \frac{1}{l} \frac{(s + \lambda)}{s^2 + \left(\lambda + \frac{\beta - \rho_0}{l} \right) s - \frac{\rho_0 \lambda}{l}} \quad (6.10)$$

A typical value for the source strength is between 10 and 20 MW. Assuming proton energy of about 1 GeV, this corresponds to a proton current between 10 and 20 mA [Roadmap, Enea, 2001].

The same analysis can be obtained in Matlab using the code written below:

```
%transfer function for subcritical reactor
%definition of the parameters
lambda=0.0897;
beta=0.0035;
l=4.2e-7;
k=0.98; %possible value of k; for ADS 0.95<k<0.995
rho=(k-1)/k
a=lambda+(beta-rho)/l; %coefficient of s
b=-lambda*rho/l; %coefficient of s^0

%transfer function
G=tf([1/l lambda/l],[1 a b])
rlocus(G) %plot the root locus
[p z]=pzmap(G)
format long; %position of poles and zeros
```

The Bode diagrams and the step-input response can be plotted using the functions: $Bode(G)$ and $step(G)$.

Simulations confirm that the system is always stable.

As an example, the root-locus, the Bode diagrams and the step-input response are plotted for $k=0.98$.

The root locus plot gives:

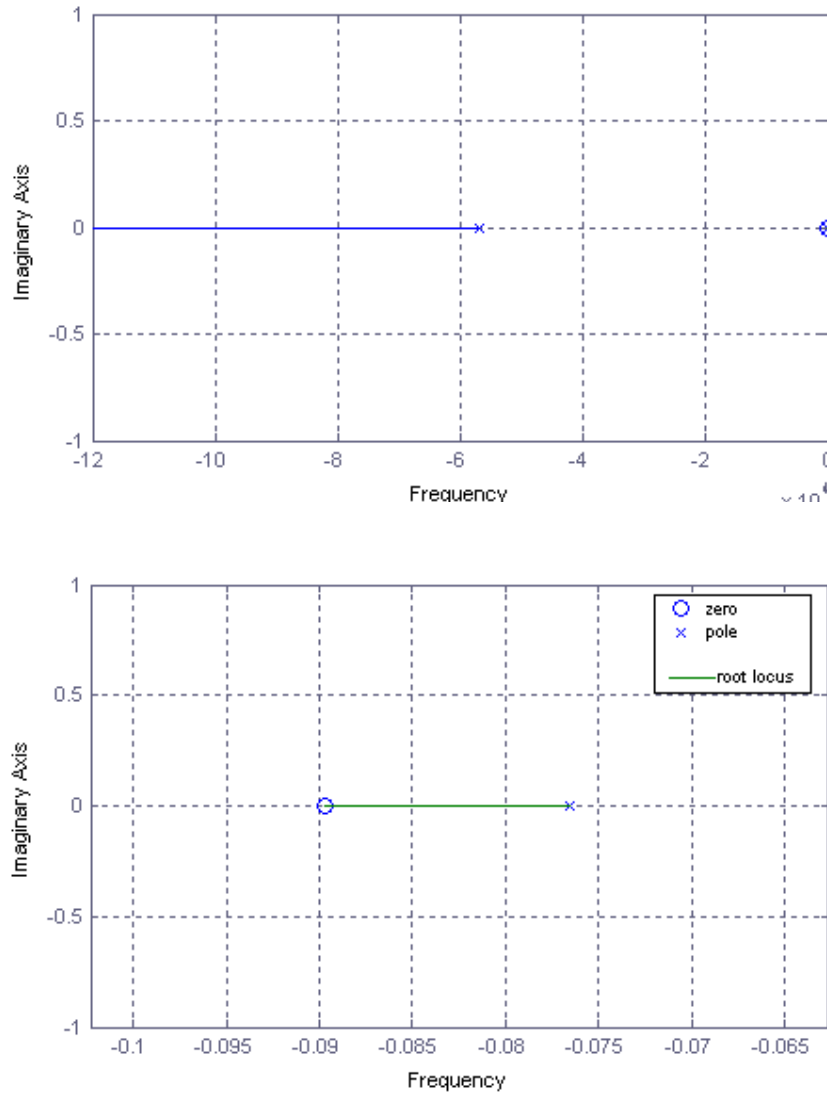


Fig 6.3: root locus plot at $k=0.98$ (up) and zoom in on the pole and zero close to the origin

The most important values are:

- $\rho = \rho_0 = -0.0204081$ reactivity level
- $G(s) = \frac{2.38 \cdot 10^6 s + 2.136 \cdot 10^5}{s^2 + 5.692 \cdot 10^4 s + 4359}$
- zero: $s = -0.0897$
- poles: $s = -5.69224 \cdot 10^4$ and $s = -0.076568$

If k has a lower value, the root locus plot is the same but the low frequency pole and the zero are even closer. Since the poles always stay on the negative real axis, the system is stable even if the gain is varied.

The Bode diagrams in Fig 6.4 show that the phase never crosses -180^0 : the system is always stable, its phase margin is 90^0 and the gain margin is infinite.

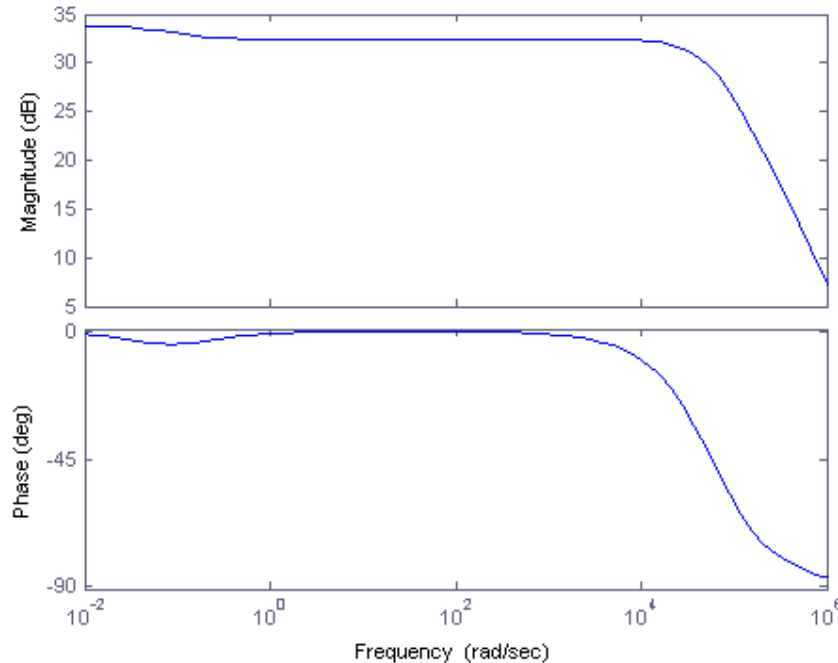


Fig 6.4: Bode diagrams at $k=0.98$

The magnitude of the oscillations can be derived using the well known relation:

$$A(\text{db}) = 20 \text{Log}_{10}(M)$$

where A is the amplitude in decibel and M is the amplitude in W .

Amplitude of 1MW for the source oscillations is a reasonable value, because for $0.95 < k < 0.99$ it is 5-10% of the total power. If $k=0.98$, the system reacts with oscillations about 32db (40MW) wide; since the total power is $1500 \text{MW}_{\text{th}}$ [Rubbia et al, 1995], this is less than 3%.

If $k=0.95$ is chosen, calculations show that fluctuations are only about 1.2% of the power. Considering that the source strength is proportional to the sub-criticality level, the source is stronger and the fluctuations of 1MW are thus less significant.

If the experimental XADS is considered, its smaller size requires a less intense proton beam and thus the magnitude of the source oscillations should be scaled down by a factor of about 10. Typical source fluctuations will therefore be about 0.1MW wide.

The analysis is completed by looking at the step-input response, from which it is possible to know the time scale of the transient. Fig 6.5 shows the response of the system for $k=0.98$ and for $k=0.95$ to a source step of 1MW at time $t=0$. After a fast increase in the power the system approaches an asymptotic level.

The sub-criticality level determines the size of the initial fast increase and the time scale of the transient. At lower k the relative magnitude of the initial jump is higher and the transient is faster because the source is more important.

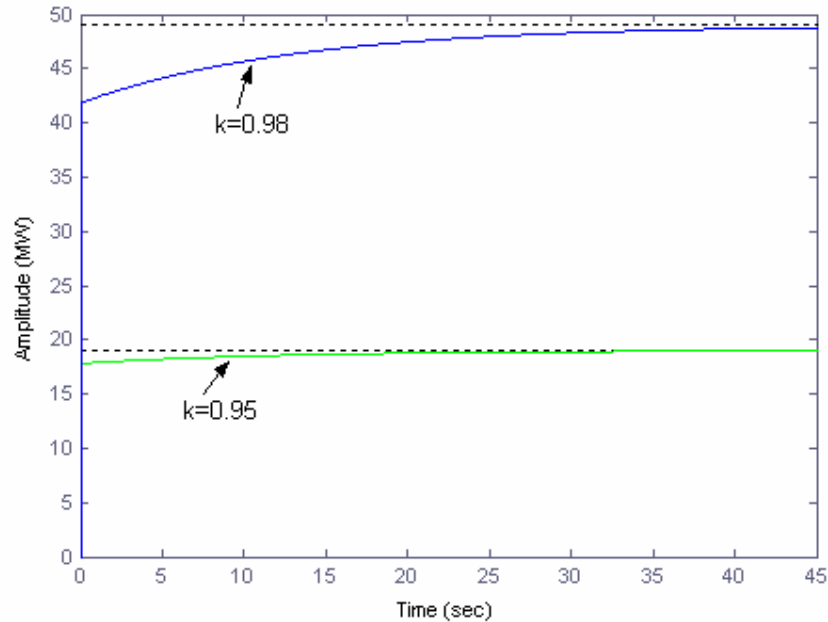


Fig 6.5: response to a step at two reactivity level: $k=0.98$ and $k=0.95$

The validity of the approximations given by equations (6.4) and (6.5) can be tested in Matlab comparing the complete model with the two approximations “high frequency” and “prompt jump”.

At low frequency, there is optimal accordance between the complete model and the prompt jump approximation (PJ); sometimes it is said that the PJ is the low frequency part of the full response.

At high frequency the use of equation (6.5) gives good result only considering that the validity of this equation is limited to high frequencies. In fact, as shown in Fig 6.6, the root locus shows a positive pole very close to zero.

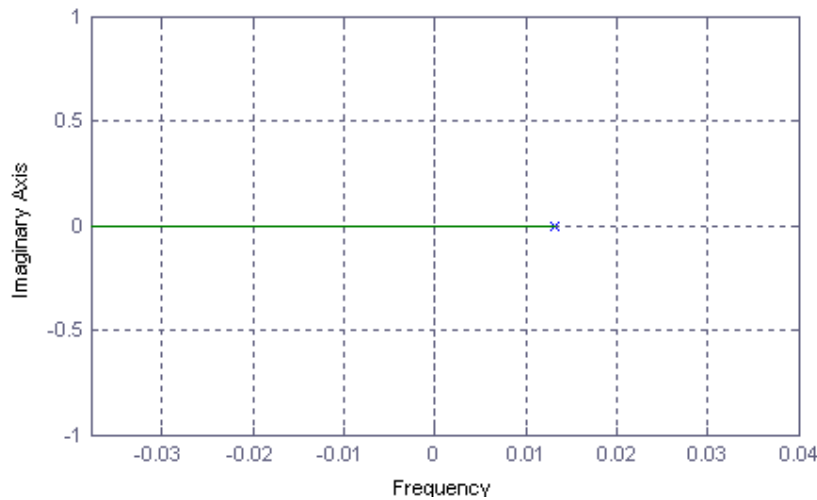


Fig 6.6: low frequency part of the root-locus for equation (6.4)

6.2 Six groups approximation

An analytical study of the stability of the ADS core is possible only in the one group approximation, because the equations are easy to solve. The important result from the previous section is the stability of the ADS core and its smooth response to source perturbations.

The aim of this section is a stability analysis of the core using the more accurate six groups approximation.

The data for the six groups of delayed neutrons are reported in Table 6.1.

Group, i	β_i (* 10^{-5})	λ_i
1	8.6	0.0129
2	73	0.0313
3	65.5	0.1346
4	126.7	0.3443
5	58	1.3764
6	18.2	3.7425
Total:	350	0.0897

Table 6.1: β_i and λ_i in the six groups approximation [D'Angelo, 2003]

The reactor transfer function is expressed by:

$$G(s) = \frac{\delta N(s)}{\delta \bar{Q}(s)} = \frac{1}{ls + \beta - \rho_0 - \sum_i \frac{\beta_i \lambda_i}{s + \lambda_i}} \quad (6.11)$$

where \bar{Q} is the Laplace transform of $\bar{q} = ql$.

The sum in equation (6.11) is over six groups, so $G(s)$ has 7 poles and 6 zeros. Since most of them are very close to each other, the Root locus plot does not provide clear information: the stability is thus studied using a “poles-zeros map” or the Bode Diagrams.

The results shown in the following figures are based on the Matlab code in Appendix A₁ and consider the parameter k to vary inside the suitable range for ADS.

It is also interesting to see how the response varies if the neutron generation time l is changed or if the multiplication factor approaches 1, making the system nearly critical.

Bode diagrams

The Bode diagrams give the response of the system to sinusoidal oscillations of the source of any frequency and of amplitude 1. Since the phase never crosses -180° , stability is assured.

The typical response shows a plateau value until the high frequency pole, than a decrease with a slope of -20db/decade ; higher k implies higher magnitude of the oscillations. The example at $k=0.98$ shown in Fig 6.7 highlights that the system reacts with oscillations of almost constant amplitude for a wide frequency range of the perturbing input. Study on accelerators show that all the possible source fluctuations are well within this range [Roadmap, Enea, 2001].

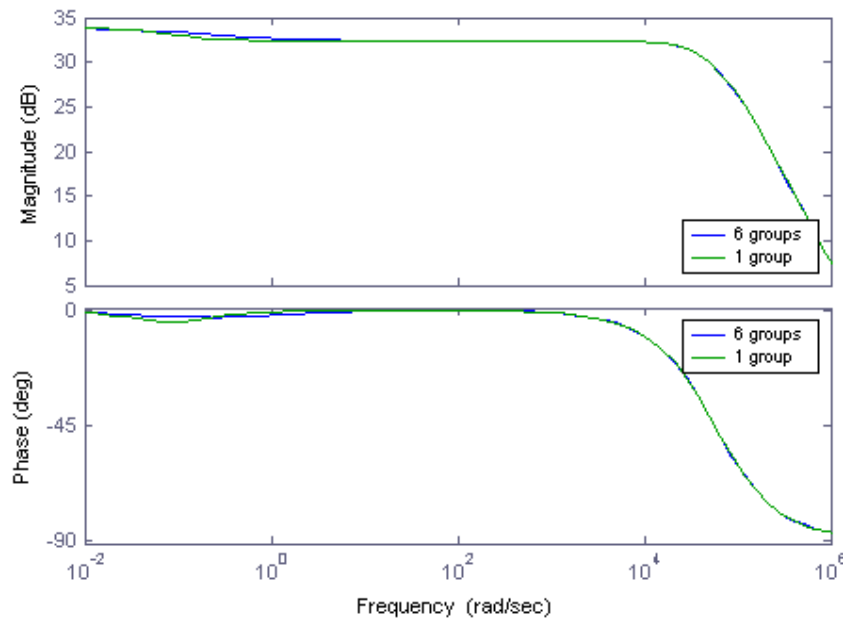


Fig 6.7: Bode diagrams at $k=0.98$

If the system is nearly critical ($k > 0.999$) the low frequency part of the response changes, showing wider oscillations as in Fig 6.8: this is due to significant changes only in the low frequency poles and zeros. Such a high k would imply relevant control problem because the system could be easily made critical, thus vanishing all the advantages of having a sub-critical system.

For this reason the case $k \rightarrow 1$ is analysed as a limiting case.

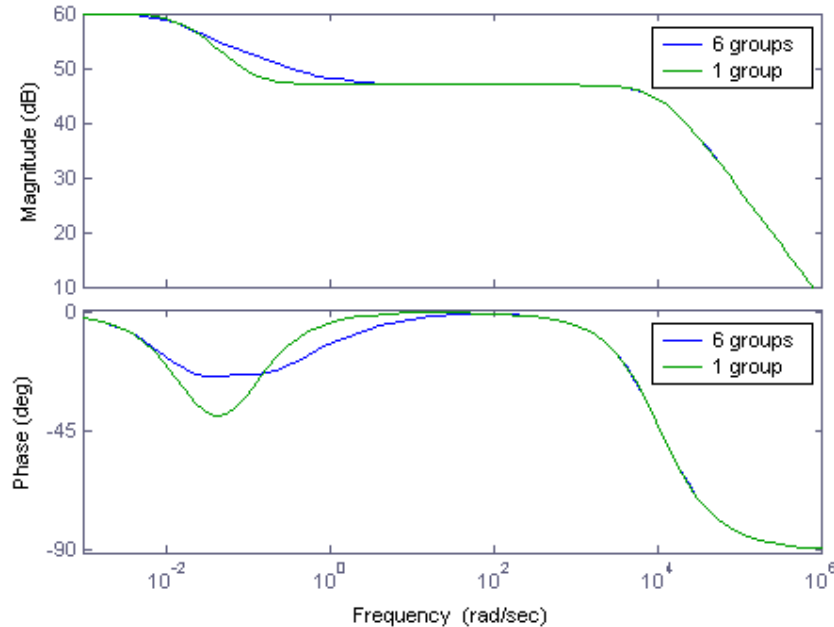


Fig 6.8: Bode diagrams at $k=0.999$

Fig 6.7 and 6.8 also compare the two approximations with one and six groups of delayed neutrons. Fig 6.8 shows that in a nearly critical case delayed neutrons play a major role and thus the difference is more evident. This is true only at low frequency because at higher frequency, and thus for fast transients, delayed neutrons can be neglected, as proposed in the Fuchs model.

Poles-zeros map

As expected from the previous paragraph, the system is intrinsically stable since all the poles and zeros are real and negative.

If k increases the absolute values of poles and zeros are lower, with the low frequency poles very close to zero, but they never become positive. A decrease in l makes the system less fast and it also causes lower absolute values for the poles. Provided that the poles are always negative, variations in their value only affect the time scale of the response and the position of the cut-off frequency, but not the stability of the system.

Step response

If the source strength is varied step-wise, the system reacts with a fast “jump” in the power level followed by a slower increase to a slightly higher plateau value. An example is given in Fig 6.9.

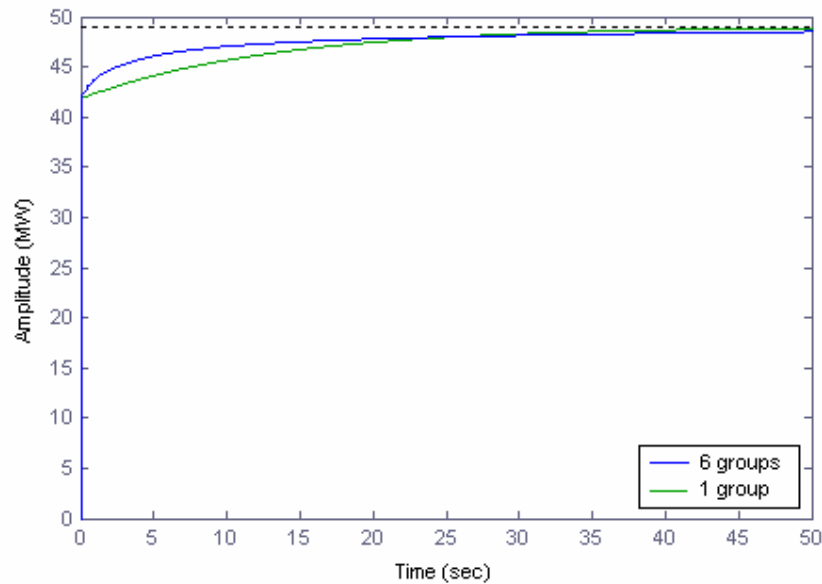


Fig 6.9: step response at $k=0.98$

Lower k implies a faster transient because delayed neutrons play a minor role. Higher k level holds a higher asymptotic value, but the power does not rise exponentially as in critical reactors. A decrease in l towards thermal reactors produces slower transients to the same asymptotic value.

Ramp response

System response to a ramp-wise variation in the source strength of any slope and length is studied. An example is given in Fig 6.10.

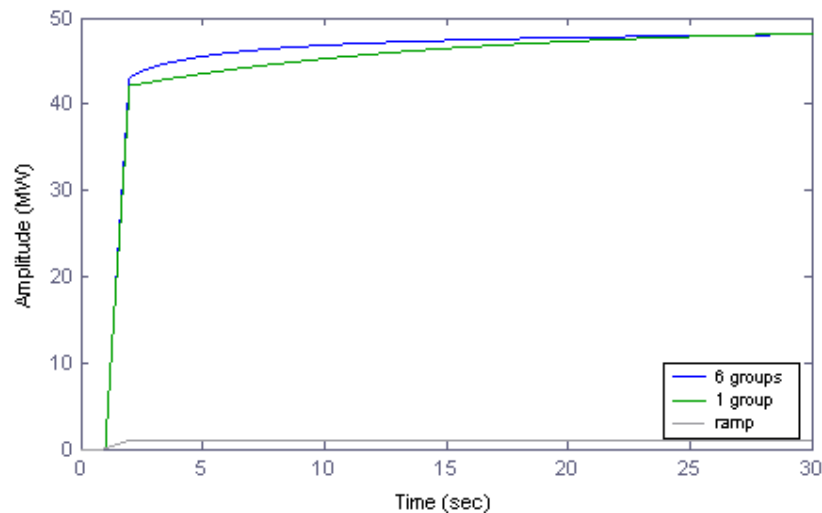


Fig 6.10: response to a 1s ramp leading to a 1MW change in the source at $k=0.98$

The response is similar to a step, but the initial part is smoother and follows the ramp shape.

As previously emphasized, if k is settled to a lower value, like 0.95, the response is faster, the magnitude lower and the one and 6 groups approximations almost equal.

Ramp-wise variations in the source strength are very interesting because they can simulate typical ADS transients, like the reactor start-up.

Pulse

A pulse of any amplitude can be generated at any time. Since the system is fast, the response to even very short pulse is significant, and more relevant for higher k value. However, studies on accelerators show that the fastest variations are in the order of milliseconds, and thus this value will be the lowest limit for the neutrons source. [Roadmap, Enea, 2001]

If l decreases by about three orders of magnitude the system is not fast enough and the response to the same pulse is almost negligible.

In any case, overpower excursions in the neutrons source up to 25-30% of the steady state value do not cause dramatic effects in the response from the stability point of view.

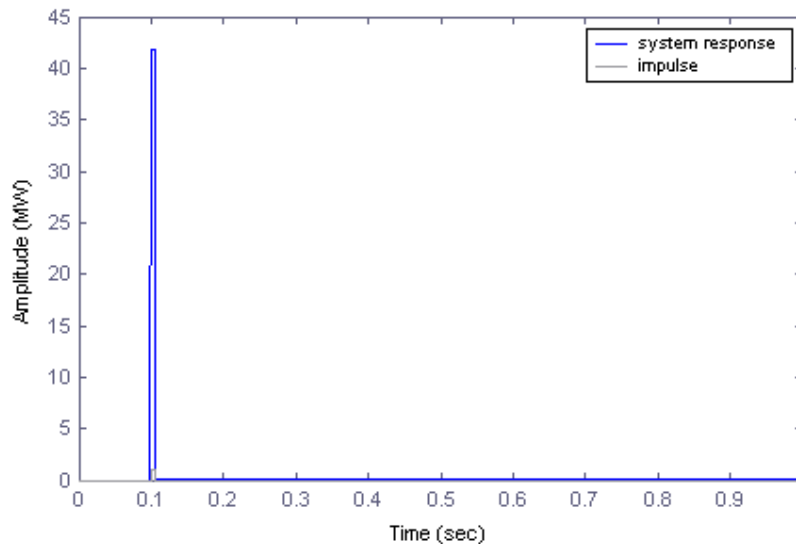


Fig 6.11: impulse (5 ms) response at $k=0.98$

In chapter 5 the dynamic behaviour of ADS when the source strength is varied has been studied analytically while in this chapter 6 the response to source fluctuations has been studying by means of simulation programs. The results are now compared.

The doubling of the source analyzed in chapter 5 can be translated in terms of source fluctuations by giving two steps of magnitude one, well spaced in time so that when the second step is given the transient due to the first one is concluded. This signal can be called a “doubling of the perturbation”.

Fig 6.12 shows the complete transient when $k=0.97$: a very good accordance with the analytical solutions is found for the whole transient.

Furthermore, comparison with the 6 groups approximation highlights that, being the difference within 1%, the analytical model still provides good results, and thus appears to be of major interest.

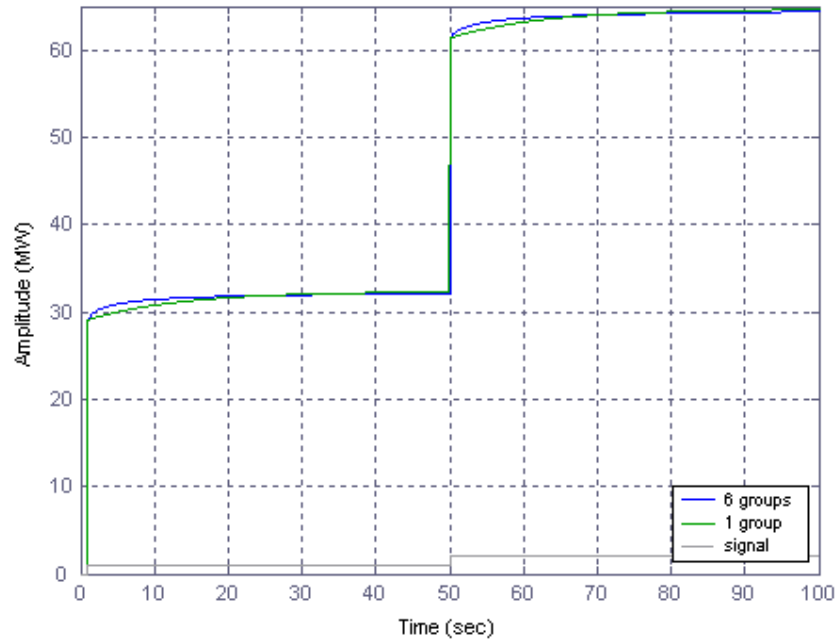


Fig 6.12: doubling of the perturbation in the source when $k=0.97$

6.3 Temperature Feedback

The stability analysis performed in the previous sections has shown that the ADS core is stable and smoothly reacts so several kinds of perturbations in the source strength. Should wide oscillations have been present, it would have been necessary to change the “neutronic design”.

The stability analysis is now completed by adding feedback to the system: an overall negative feedback coefficient will increase the stability of ADS while the presence of some positive effects would determine a possible unstable behaviour under certain conditions.

Feedback acts when a change in some parameters determines a change in the power level. If the power rises, the temperature of the fuel and of the coolant increases: this causes different effects in the fuel, the coolant and the external structure, normally perceived by an increase or a decrease in the reactivity level. For this reason, many feedback effects can be described in terms of temperature changes.

A sum of all these effects is not enough to determine whether the total coefficient is positive or negative, since each of them has a characteristic time constant that influences the stability behaviour of the reactor.

Normally it is not necessary to introduce a time constant for each effect because it is accurate enough to divide the feedback into two categories: prompt effects, mainly involving the fuel, and delayed ones, concerning the coolant.

In the ADS model under study the time constant associated with delayed effects is very large because the coolant flow is driven by natural circulation and it thus has a low average speed.

A simple model to study feedback is the “Lumped Model”, already presented in chapter 4.4 for critical systems.

The core assumption is to consider the reactor to be a unique block, with a shape of the temperature distribution throughout the whole system as in the steady state. The reactor has a characteristic average temperature T and temperature variations due to any kind of perturbation are adequately represented by assuming a single averaged coolant temperature T_c and using Newton’s law of cooling. No distinction between prompt and delayed effects is made, so that all the reactivity coefficients are added together. An average time for heat transfer to the coolant τ can be calculated.

The feedback transfer function is:

$$H(s) = \frac{\alpha K}{s + \gamma} \quad (4.18)$$

where α is the total temperature feedback coefficient taken with opposite sign.

Since the model is the same as in Fig 4.1, the characteristic equation is:

$$1 + G(s)H(s) = 0 \quad (4.2)$$

The parameter K is the reciprocal of the reactor heat capacity. As the reactor is composed by fuel, coolant and structure material, K is calculated by doing a weighted average for a specific reactor composition.

According to the available data [Rubbia et al, 1995], [Schikorr, 2001], it can be assumed the reactor to be formed by 53% molten lead coolant, 32% fuel and 15% structure material (steel).

The values for the specific heat are:

- $C_{lead} = 1.5495 * 10^6 \frac{J}{m^3 K}$ [Rubbia et al, 1995]
- $C_{fuel} = 2.92 * 10^6 \frac{J}{m^3 K}$ [Schikorr, 2001]
- $C_{steel} = 3.53 * 10^6 \frac{J}{m^3 K}$

The value for K is thus:

$$K \approx 0.437 * 10^{-6} \frac{m^3 K}{J}$$

Considering that different fuel mixtures can be used and that slightly different designs have been proposed, K can easily change within 5-10% percents. However, simulations will show that variations of K of this order of magnitude are not relevant and thus a very accurate estimate of the parameter is not necessary.

The coefficient γ is the reciprocal of the mean time for heat transfer to the coolant τ and it is assumed to be an average time constant driving the whole process.

τ is calculated as the ratio between the heat capacity of the core and the product of the heat capacity of the coolant and the coolant flow rate [Hainoun et al, 2004].

The same core composition as in the previous point is assumed and standard values for the density are chosen (for the fuel $d = 8.5 \text{ g/cm}^3$).

Applying the aforementioned relation τ is found to be around 2.35 s; consequently:

$$\gamma = 0.425 \text{ s}^{-1}$$

Detailed simulations validated by experimental results for critical fast reactors show that the value proposed is of the correct order of magnitude [Hummel, 1970].

Results will show that even τ is not a critical parameter for the system and thus variations up to a factor of 2 or 3 do not change system response significantly.

From equation (4.2) it is evident that for dimensionality reasons the product $G \cdot S$ must be non-dimensional but if equation (4.18) is multiplied by equation (6.2) this is not the case. The feedback transfer function $H(s)$ is generally obtained as a “power function” and its dimensions are the reciprocal of a power density.

In sub-critical systems source fluctuations have dimension of power density, as expressed by the relations:

$$\bar{q} = |n_0 \rho| \quad (6.12)$$

For this reason the Transfer Function $G(s)$ does not have dimension of a power density leading to the incoherence found in equation (4.2).

The solution is suggested by equation (6.12) itself: the power density n_0 is introduced and the feedback transfer function becomes:

$$H(s) = \frac{\alpha K n_0}{s + \gamma} \quad (6.13)$$

Typical values for the power density are:

- $n_0 = 523 * 10^6 \frac{W}{m^3}$ [Rubbia et al, 1995]
- $n_0 = \frac{P_{th}}{V_{fuel}} \approx 423 * 10^6 \frac{W}{m^3}$ [Schikorr, 2001]

For the experimental LBE-Cooled XADS by Ansaldo the power density is only :

$$n_{0,XADS} = 227 \frac{MW}{m^3}$$

The last coefficient to be calculated in equation (4.18) is α ; it consist in a summation of all the feedbacks listed below.

Doppler effect ($\alpha_{Doppler}$)

The reactivity effect resulting from Doppler broadening of fission and capture resonances arises from a competition between fission, capture and leakage processes, the last being negligible in ADS. The effect is prompt and negative and its value is:

$$\alpha_{Doppler} = -1.44 * 10^{-5} \text{ } ^\circ\text{C}^{-1} = -1.44 \text{ pcm}/^\circ\text{C} \quad [\text{Rubbia et al, 1995}]$$

Coolant density (α_{cool})

An increase in the power level determines an increase in the coolant temperature and thus a decrease in its density. A less dense coolant shows less moderation and absorption.

If coolant boiling point is reached, void formation must also be considered. The use of molten lead, with its very high boiling point ($\approx 2020\text{K}$), makes void formation to occur after the integrity of reactor core is lost: this kind of event is beyond design basis accident analysis.

If sodium coolant is chosen, void formation could happen leading to a strong positive feedback.

α_{cool} exhibits a spatial dependence and it is often positive in the core centre and negative in the outer parts but, since point kinetics has been used, an average value over the whole volume is calculated.

α_{cool} is expressed in terms of temperature by the following relation:

$$\alpha_{cool} = \frac{d\rho}{dT} = \left(\frac{\Delta\rho}{\Delta\text{Density}} \right)_{cool} \left(\frac{\Delta\text{Density}}{\Delta T} \right)_{cool} \quad (6.14)$$

Substituting numerical values:

$$\alpha_{cool} = -1.37 * 10^{-6} \text{ } ^\circ\text{C}^{-1} = -0.137 \text{ pcm}/^\circ\text{C} \quad [\text{Rubbia et al., 1995}]$$

It is important to notice that α_{cool} is one order of magnitude smaller than $\alpha_{Doppler}$ and that its effect is delayed, because it regards coolant flow.

Motion of fuel and structure

Besides Doppler effect, temperature changes due to power excursions affect the reactivity by thermal expansion, which changes the geometry of the reactor and the density of the material.

A temperature increase causes the fuel to expand radially and axially. This expansion may result in a compression and eventually ejection of fission gasses (e.g: Na) with a consequent void formation.

The suggested overall value is:

$$\alpha_{fuel-ex} = -0.25 * 10^{-5} \text{ } ^\circ\text{C}^{-1} = -0.25 \text{ pcm}/^\circ\text{C} \quad [\text{Schikorr, 2001}]$$

Heating of the coolant is also perceived by the structural material, which is itself heated and expanded. This effect is delayed and globally positive but not very relevant. Its value can be inferred from fast reactor and it is:

$$\alpha_{structure-ex} \approx 0.05 - 0.1 \text{ pcm}/^\circ\text{C} \quad [\text{Hummel, 1970}]$$

Another effect connected with fuel motion is fuel rods bowing: this is due to a temperature gradient in the radial direction, which can be caused by a gradient in the neutron flux across the rod, differences in coolant temperature across a subassembly or in the heat conduction across structural members.

Fuel bowing consists in a larger expansion of the rod in one side compared to the other. The rods can be bended towards or outwards the core centre, causing an increase or a decrease in the reactivity.

This phenomenon is limited and kept under control by using different kind of supports and fuel assemblies. Considering that bowing effect is inversely proportional to the size of the reactor and the ADS under study is big compared to normal fast systems it will not play an important role.

Nevertheless, this effect is simulated by a reactivity insertion up to some tens of *pcm*, as it can be inferred from simulation on existing fast reactors [Hummel, 1970].

Cladding material removal from the core

Steel combined with Zirconium is often used as cladding material: its melting temperature is about 1450 K. Since the boiling point of Lead is much higher, the cladding material fails before coolant boiling and fuel melting occur.

Additionally, since clad density is lower than coolant density, the molten material tends to move away. This process causes a strong positive insertion of reactivity, which has been evaluated to be up to about 2000 *pcm* in case of complete clad melting [Schikorr, 2001].

This process is rather different from the other temperature feedback effects because it happens only if the cladding temperature exceeds the melting value. The system normally operates far below the critical points but in case of severe accident conditions the cladding material will be the first to fail.

Neglecting the distinction between prompt and delayed effect and adding all the parameters it is found:

$$\alpha = -(\alpha_{Doppler} + \alpha_{cool} + \alpha_{fuel-ex} + \alpha_{structure-ex}) = 1.727 * 10^{-5} \text{ } ^\circ\text{C}^{-1} \quad (6.15)$$

6.4 Six groups and lumped model

This section considers the six groups approximation and the lumped model for feedback. Since the model does not separate prompt from delayed effects and assumes the reactor to be a unique block, the validity of the model could be questioned. However, the use of a simple model gives an immediate understanding in the physics of the system and in the role played by feedback and the sub-criticality level.

A first insight on the stability of the system can be gained analytically using the one group approximation.

The equation $G^*H=0$, which is important to plot the Root Locus is:

$$\frac{\alpha Kn_0}{l} \frac{s + \lambda}{(s + \gamma) \left[s^2 + \left(\lambda + \frac{\beta - \rho_0}{l} \right) s - \frac{\rho_0 \lambda}{l} \right]} = 0 \quad (6.16)$$

This equation has one zero in $s = -0.0897$ and three poles, one in $s = -\gamma$, one at very high frequency and the last one very close to 0: since the Root Locus is always in the left half plane, the system is stable.

In Fig 6.13 an example of the low frequency part of the Root locus plot is given for $k=0.98$.

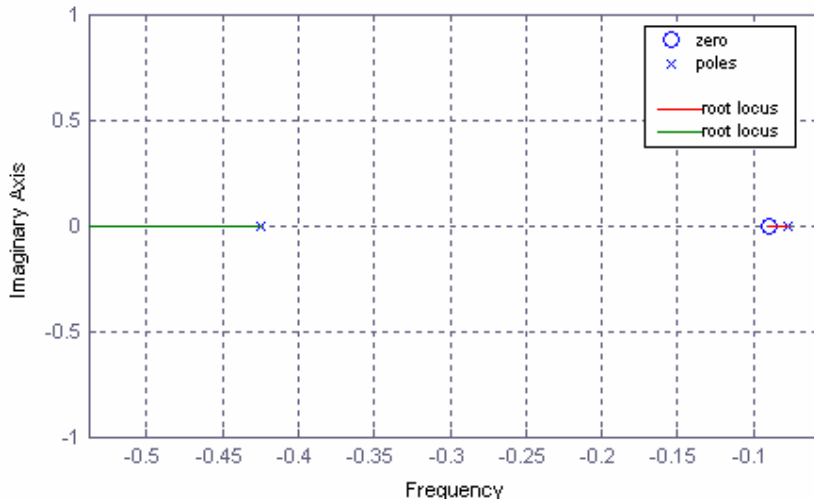


Fig 6.13: low frequency part of the root locus for $k=0.98$

The equation for the system with feedback is (4.1), which becomes in this case:

$$Y(s) = \frac{G(s)}{1 + G(s)H(s)} = \frac{(s + \lambda)(s + \gamma)}{l(s + \gamma)(s^2 + as + b) + \alpha Kn_0(s + \lambda)} \quad (6.17)$$

where a and b are the coefficient of s and s^0 respectively as in equation (6.10).

Equation (6.17) has two negative zeros at the frequency $s = -\gamma$ and $s = -\lambda$ and three poles.

The problem is now studied in the six groups approximation; the Matlab code used for this analysis is in Appendix A2.

The reference power level n_0 is taken from the Conceptual design by Rubbia. Using the function “*poles-zeros map*”, it is possible to analyze how poles and zeros modify their position by changing one or more parameters and if there is any instability risk.

Sub-criticality level k

Within the range that is mostly chosen for ADS ($0.97 < k < 0.985$) the poles are always real and negative.

If $k > 0.995$ two poles are complex conjugate, but still with a negative real part. The system exhibits an oscillatory behaviour for that particular frequency but such a high reactivity level vanishes the advantages of choosing a sub-critical assembly.

Heat capacity K and power density n_0

If the fuel mixture and the reactor composition and geometry are changed, variations in the K value up to 10% and in n_0 up to 20% are reasonable and possible. This will not cause any significant change in the poles-zeros plot but an increase in the power density will probably more easily lead to criticality.

Time constant for heat transfer τ

An increase/decrease in τ means a slower/faster heat transfer rate to the coolant; for γ , which is the reciprocal of τ , the previous relation is valid reversed.

Calculations show that if $0.8 < \gamma < 1.2$ [1/s] and both K and n_0 are increased by respectively 10% and 20% two complex conjugate negative poles appear for $k > 0.99$. For γ values around 1 this is true for $k > 0.977$. Such a γ can be reached if the system has a higher coolant flow rate, together with a decrease in the core specific heat and in the core mass.

Reactivity feedback coefficient α

The reactivity feedback coefficient is of course an important parameter in driving the transients. Since ADS is sub-critical, a stronger positive reactivity insertion is necessary to overcome both the negative feedback and the sub-criticality level.

For $k = 0.99$ a positive insertion of $4 \text{ pcm}/^\circ\text{C}$ is enough to lead to instability while for $k = 0.97$ this value is enhanced to $8 \text{ pcm}/^\circ\text{C}$; the temperature considered is the average reactor temperature as proposed in the lumped model.

If γ decreases to 0.35 [1/s], which means lower heat transfer rate, and the power density is increased by 20% the reactivity insertion leading to instability would be 3 and $6 \text{ pcm}/^\circ\text{C}$ respectively.

As described in chapter 6.3, a particular fuel rods design can cause a positive reactivity feedback due to bowing: in this case, the insertion of a few tens of pcm

must be considered. If $k > 0.99$ the risk of reaching criticality can be present. Therefore, special attention in the fuel rods design is necessary.

These considerations assure the stability of the system in most of the conditions, but they do not give complete information about the system response. For this reason, the rest of this section studies the response to several perturbations in the source. The value $k=0.98$ proposed by Rubbia in his conceptual design is chosen.

The Bode diagrams in Fig 6.14 show the results expected from the poles and zeros map: the system is stable with a phase margin of 90^0 and an infinite gain margin.

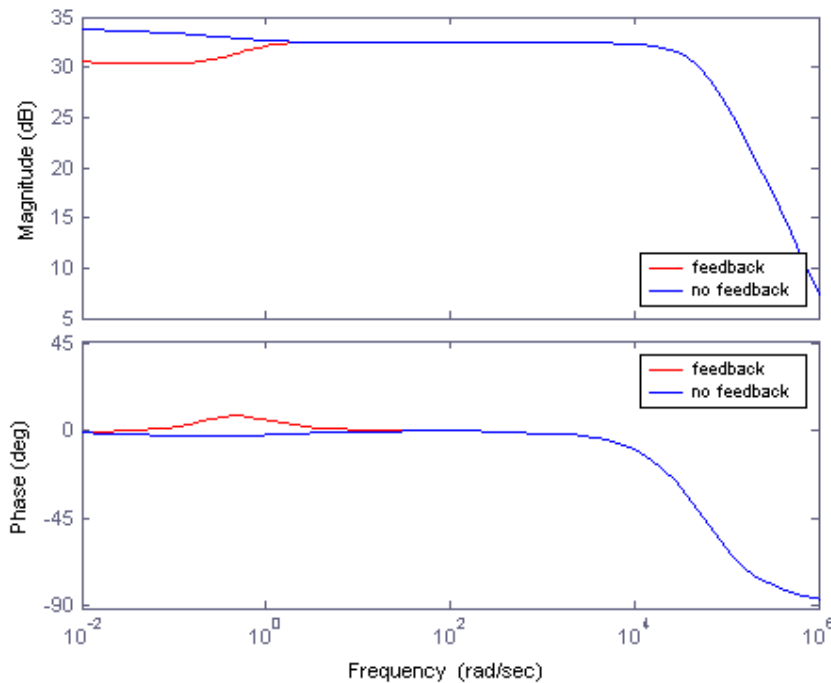


Fig 6.14: Bode diagram at $k=0.98$

The magnitude of the response shows a plateau value for a quite wide range of frequency ($10-10^4$) of the perturbing input. At low frequency a slightly lower value is observed while at high frequency the amplitude quickly drops.

The figure also highlights that feedback causes a lowering in the amplitude at low frequencies.

Since the source power at $k=0.98$ is about 12.5 MW [Rubbia et al, 1995] and the amplitude of the oscillations is 1MW, source variations represent 8% of the total power. Fig. 6.14 shows that the system reacts with fluctuations about 32.5db (42 MW) wide in the plateau at medium frequency and about 30.5db (33 MW) wide in the low frequency range (<1 rad/s): these values represent respectively 2.8% and 2.2% of the thermal power.

Fig 6.15 and 6.16 describe the system response when at time $t=0$ the source strength is increased step-wise by 1MW. After a rapid increase in the power level, the

response is different in the presence of feedback. For this case, the power drops towards a lower asymptotic value. Fig 6.16 describes how the feedback acts at the beginning of the transient.

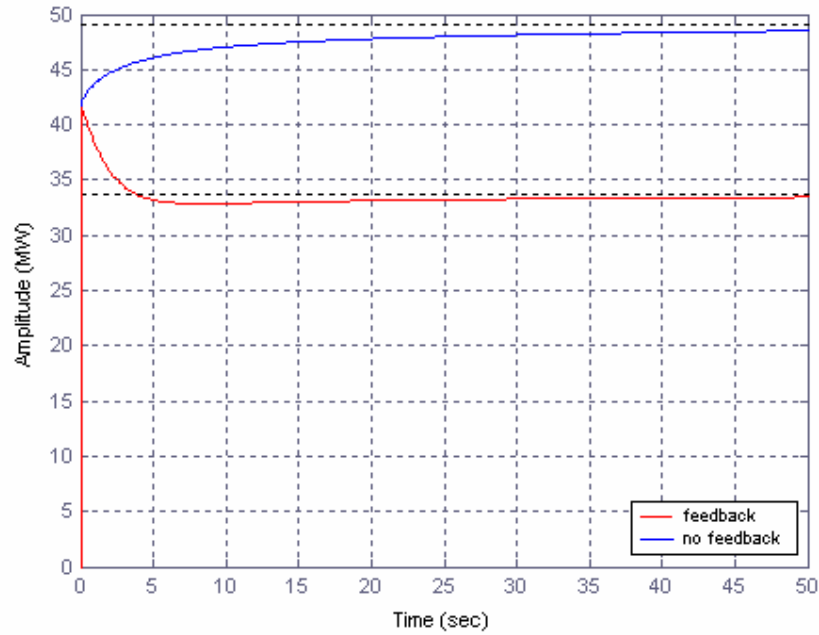


Fig 6.15: response to a step-wise variation in the source at $k=0.98$

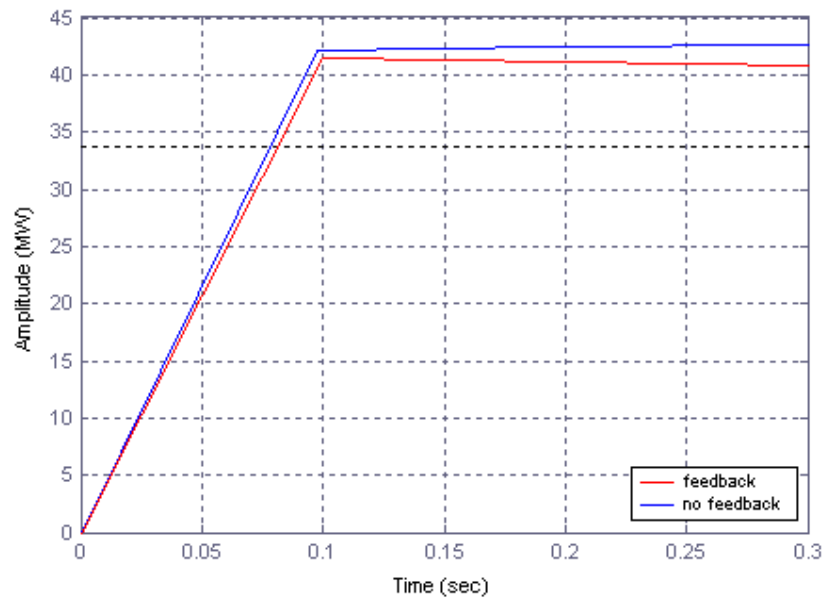


Fig 6.16: first 0.3s in the response to a stepwise variation in the source at $k=0.98$

Further calculations have shown how the parameters influence the transient response; the most important results are summarized below:

- If k increases, which means that the system is closer to criticality, the negative feedback is more important because the initial high power excursion will be damped in a few seconds.
- An increase in γ , which means that the heat transfer is larger, lowers the importance of feedback, because the negative feedback has less time to act.
- If feedback is positive but not enough to lead to instability, the power will still rise to an asymptotic value while if instability occurs it will rise exponentially.

A typical source transient is described by a ramp. Fig 6.17 shows the response of the ADS when the source strength is varied by 1 MW in 1 second. The ramp is slow enough to give to the feedback enough time to lower the initial power peak.

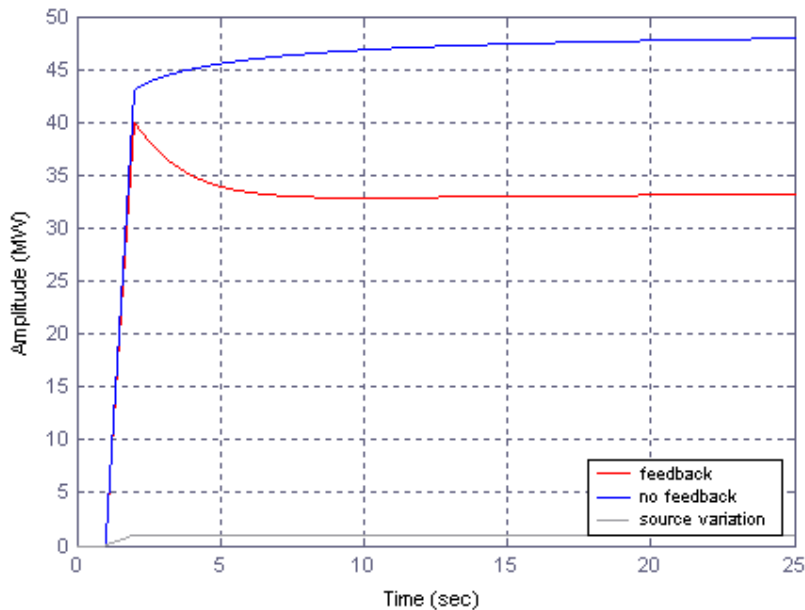


Fig 6.17: response to a ramp-wise variation in the source at $k=0.98$

The importance of the negative feedback in reducing the magnitude of the system response can be better understood if a sequence of changes in the source is considered. This can happen in accidental conditions but also when the source level has to be adjusted to meet some requirements, like a specified power level.

An example is shown in Fig 6.18. The equilibrium of ADS is first perturbed with a 1s ramp that increases the source strength by 1 MW followed after some seconds by a slower ramp (5s) of 1 MW more.

Since the feedback acts twice, the final power variation is much lower.

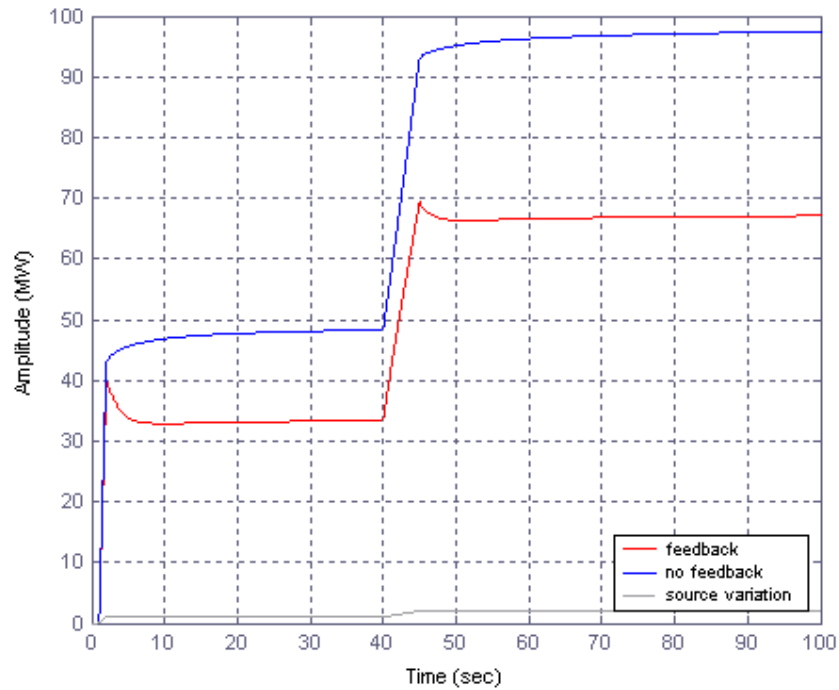


Fig 6.18: response to a double ramp in the source at $k=0.98$

Finally the response to a pulse is studied.

If a 5ms impulse is given, as was done in the absence of feedback (Fig 6.11), the difference between the two cases is less than tenths of MW during the whole transient and it is thus negligible. Feedback cannot act because the time scale is very short; even a positive feedback coefficient does not affect the response significantly.

6.5 The feedback transfer function with delay

The lumped model proposed in chapter 6.3 can be improved if prompt and delayed feedback effects are separated. In this section the feedback transfer function with delays is derived by solving the heat balance equations for the different parts of the system.

The reactor is composed by fuel rods, coolant and structural material and the fuel promptly responds to power changes. Considering that the steady state is changed by small perturbations, the starting point is the system:

$$\begin{aligned}\frac{d(\delta T_f)}{dt} &= K_f \delta P - \gamma_f \delta T_f \\ \frac{d(\delta T_c)}{dt} &= \gamma_c \left[\delta T_f(t - \Delta t_{cool}) - \delta T_c \right] \\ \frac{d(\delta T_{str})}{dt} &= \gamma_{str} \left[\delta T_c(t - \Delta t_{cool-str}) - \delta T_{str} \right]\end{aligned}\quad (6.18)$$

where:

$\delta T_f, \delta T_c, \delta T_{str}$ are temperature variation in the fuel, coolant and structure;

K_f is the heat capacity of the fuel;

$\gamma_f, \gamma_c, \gamma_{str}$ are the reciprocal of time constants for fuel, coolant and structure

Employing Laplace Transform and the relation between temperature and reactivity ($\delta \rho = \alpha \delta T$), after a few steps the following transfer functions are derived:

$$\begin{aligned}H(s)_{prompt} &= \frac{\delta \rho_{pr}}{\delta P} = \frac{-\alpha_{prompt} K_{fuel}}{s + \gamma_f} \\ H(s)_{cool} &= \frac{\delta \rho_{cool}}{\delta P} = \frac{-\alpha_{cool} K_{fuel} \gamma_c e^{-s \Delta t_{cool}}}{(s + \gamma_f)(s + \gamma_c)} \\ H(s)_{str} &= \frac{\delta \rho_{str}}{\delta P} = \frac{-\alpha_{structure-ex} K_{fuel} \gamma_c \gamma_{str} e^{-s(\Delta t_{cool} + \Delta t_{cool-str})}}{(s + \gamma_f)(s + \gamma_c)(s + \gamma_{str})}\end{aligned}\quad (6.19)$$

The overall feedback transfer function is:

$$H(s) = n_0 \left(H(s)_{prompt} + H(s)_{cool} + H(s)_{str} \right) \quad (6.20)$$

where n_0 is the specific power density.

The values for all the parameters in equation (6.19) are calculated using data from the previous sections and from the literature.

The more precise data available for fast reactors can be used either when the data for ADS is missing or to check if the values calculated by the author for ADS are within the correct order of magnitude.

Fuel data

The reactivity coefficient α_{prompt} , the fuel heat capacity and the characteristic time constant γ_f are now calculated.

An increase in the power level, due to an increase in the number of fissions, suddenly causes the fuel to heat up.

The related feedback effects are the Doppler and the fuel expansion; they are both prompt and negative and they can thus be summed into an overall prompt feedback coefficient:

$$\alpha_{prompt} = \alpha_{Doppler} + \alpha_{fuel-ex} = -1.69 pcm / ^\circ C$$

The reciprocal of the fuel heat capacity is simply:

$$K_{fuel} = \frac{1}{C_{fuel}} = 0.342 * 10^{-6} \frac{m^3 \text{ } ^\circ C}{J}$$

For the characteristic time constant, data on fast critical reactor suggest $\gamma_f \approx 0.3 - 0.5 s^{-1}$ [Hummel, 1970]. An estimate for the ADS under study is based on the relation:

$$\tau_f = \gamma_f^{-1} = \frac{C_{fuel}}{h} \quad (6.21)$$

where C_{fuel} is the heat capacity of the fuel and h is an overall heat transfer coefficient between the fuel and the heat sink, which is now the coolant.

The data available from papers suggest slightly different values depending on system design and characteristics, but generally slightly higher than those proposed for critical fast systems. A final estimate of $\tau_f = 4s$ seems in accordance with the available data; the reciprocal value is:

$$\gamma_f = 0.25 s^{-1}$$

Coolant data

As derived in chapter 6.3 the delayed reactivity feedback coefficient is:

$$\alpha_{cool} = -0.137 pcm / ^\circ C$$

The coolant flow is driven by natural circulation and its average velocity through the core is thus very low. The initial value of 1.5 m/s proposed by Rubbia has to be reduced to limit corrosion problems and to take into account that when an accident occurs the lack of the driving force causes the coolant flow to slow down. A value of about 1m/s is currently proposed.

Since the core is 25m high [Ceballos, 2004], the delay is estimated as:

$$\Delta t_{cool} \approx 30s$$

The characteristic time constant for the coolant is estimated considering the ratio between C_{fuel} and C_{lead} and the value already found for the fuel. The result is:

$$\gamma_c = 0.47s^{-1}$$

Structure data

The structural material expansion gives a positive feedback worth:

$$\alpha_{structure-ex} = 0.1 \text{ pcm}/^{\circ}\text{C}$$

Besides the delay already calculated for the coolant, a few more seconds have to be added; a reasonable value is:

$$\Delta t_{cool-str} = 3s$$

The characteristic time constant is calculated following the same procedure described for the coolant. The result is:

$$\gamma_{str} = 0.21s^{-1}$$

The complete system with delayed feedback is always described by the characteristic equation (4.2) but the presence of delays, which is reflected by exponential functions, may lead to computational problems. Matlab, for example, does not handle delayed feedback: hence, some approximations have to be introduced.

The most used approximation to solve this kind of problems is the Pade's approximation; it transforms an exponential into a transfer function and it thus provides an easy way to solve the problem. Additionally Pade's approximation often gives more accurate results compared to other approximations, like Taylor's.

The second order approximated transfer function given below is accurate enough for the problem under study:

$$e^{-s\Delta t} \approx \frac{\Delta t^2/12 s^2 - \Delta t/2 s + 1}{\Delta t^2/12 s^2 + \Delta t/2 s + 1} \quad (6.22)$$

The use of an approximation in presence of other simulation software that can handle time delay is questionable. This choice is justified considering the magnitude of feedback effects and the accuracy of the approximations.

The values calculated in chapter 6.3 shows that delayed feedback coefficients are smaller compared to the prompt one.

In addition the value for the delays and for the characteristic time constants in equation (6.19) are not accurate while Pade's approximation is very good.

These considerations suggest that the results using Pade's approximation will not substantially differ from the one using the exact exponential function. This choice would have been questionable if experimental data for the parameters were available.

6.6 Six groups approximation and delayed feedback

This final section concerning stability analysis and response to source fluctuations describes the behaviour of ADS when the 6 groups approximation and the feedback model introduced in the previous section are used.

Poles-zeros map shows that the system is stable because for any value of the reactivity all the poles have negative real parts. Nevertheless, a few of them are imaginary. Since all the poles and zeros are clustered around the origin, the Root locus plot does not give so much information.

Calculations prove that, being the only positive feedback a lot delayed, safety is further enhanced because the negative prompt feedback acts first. However, the difference is not so relevant because the positive feedback coefficient is small.

Stability can be also analyzed using Nyquist plot, which substitutes the Bode diagrams when a delay is present. In fact Bode diagrams are constructed for polynomial transfer functions in the Laplace domain (like trigonometric functions) while the Laplace Transform of a delay is an exponential function.

Since Pade's approximation has been used, the exponential function has been expanded in power and thus the criterion for the applicability of the Bode Diagrams is satisfied. Therefore, both methods can be used to study the stability of the ADS.

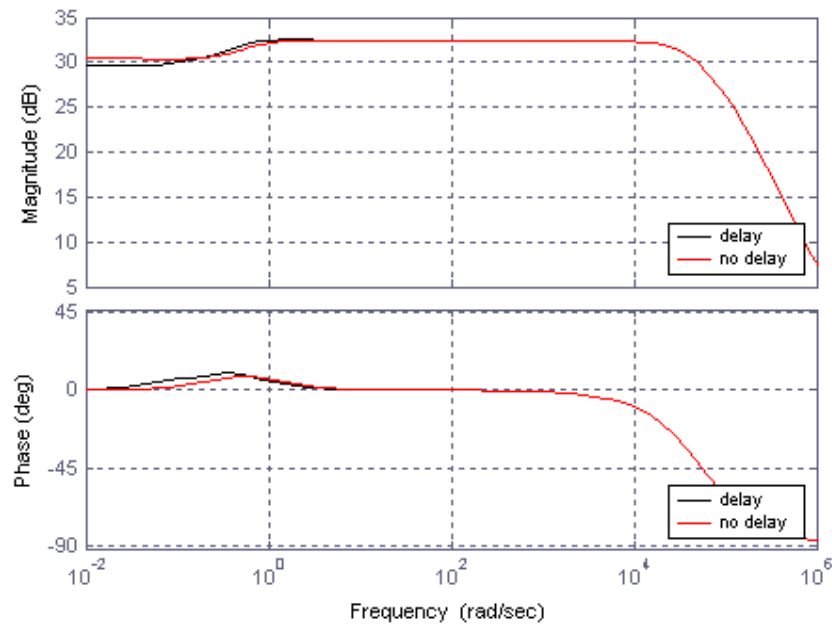


Fig 6.19: Bode diagrams at $k=0.98$

Fig 6.19 shows that the difference between the approximations with or without delay is small and only concerns the low frequency part. The differences diminish at low k .

The response to a 1 MW step-wise increase in the source strength, plotted in Fig 6.20, shows that, since the prompt negative feedback is lower in the delayed case, the initial amplitude of the response is a little higher.

The difference in the asymptotic value is due to the different values for the characteristic times; in the delayed case the heat transfer coefficient between fuel and coolant is assumed slower than the overall value calculated in the lumped model.

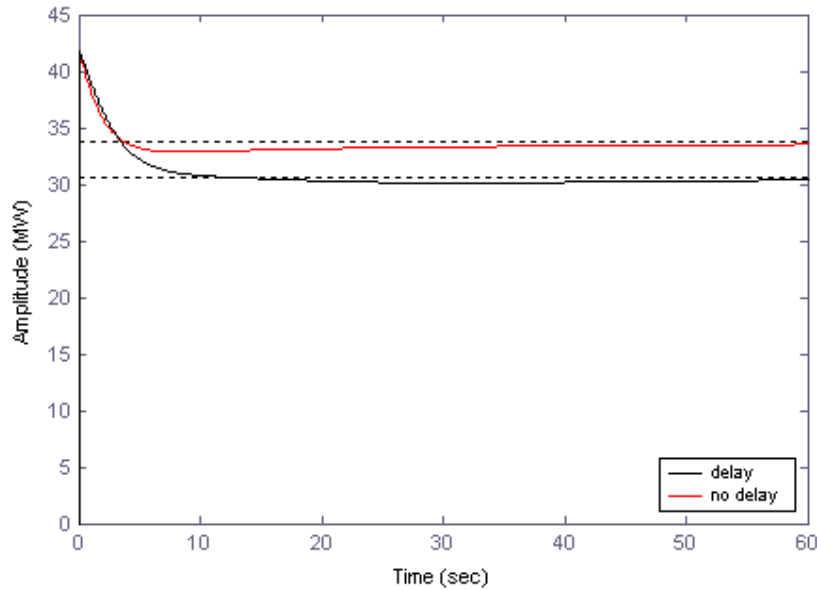


Fig 6.20: step input response at $k=0.98$

Further calculations show that variations in the characteristic times correspond to changes in the asymptotic power level. If the characteristic time τ is faster, the asymptotic value is higher while a slower coefficient implies lower power variations.

Similar results are obtained when the source varies ramp-wise, as described in Fig 6.21.

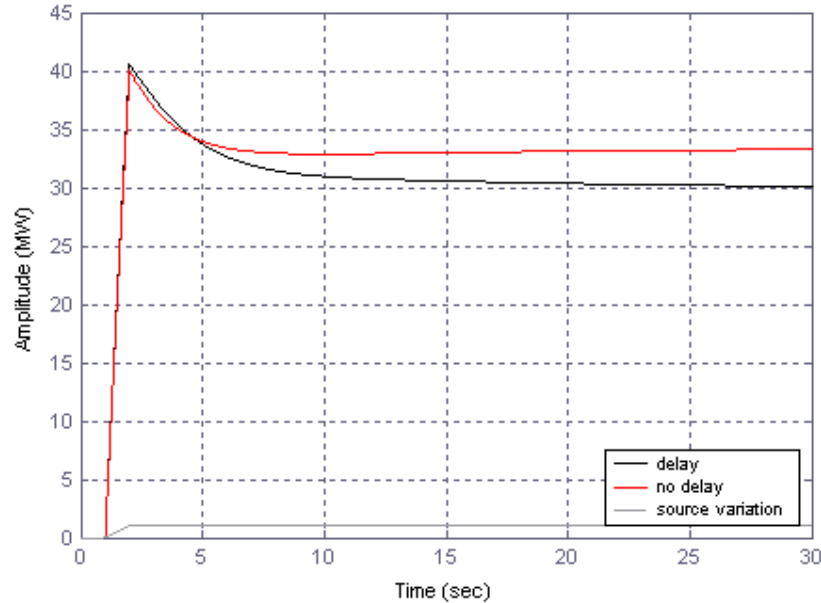


Fig 6.21: response to a ramp wise variation of 1 MW in the source strength at $k=0.98$

The response to an impulse shows again that no distinction can be made between the two approximations, since the feedback is basically not acting at these very short time scales.

The previous considerations have shown that ADS is stable in normal operation conditions and that the system reacts to several types of variation in the source strength with power oscillations of relative smaller magnitude.

The analysis is now completed studying ADS behaviour in a few accidental conditions, when a consistent amount of reactivity is injected into the system.

Clad melting

In chapter 6.3 it has already been mentioned that partial or total clad melting is one of the worse scenario foreseeable for ADS.

Preceding studies have modelled this accident with a linear reactivity insertion up to 2000pcm in an arbitrarily chosen temperature interval of 200 degrees above the clad melting temperature [Schikorr, 2001].

The effect is delayed and the time lag is at least of the same magnitude as the structure material expansion. This estimation is conservative, because an increase in the fuel temperature will initially be compensated by the heating of the coolant until, at a certain point, the clad melting temperature will be reached.

An average conservative estimate of the delayed feedback coefficient is:

$$\alpha_{clad} = 9\text{pcm} / ^\circ\text{C}$$

The Nyquist plot in Fig 6.22 shows that the system is still stable if $k=0.95$; an unstable behaviour is present for $k>0.951$.

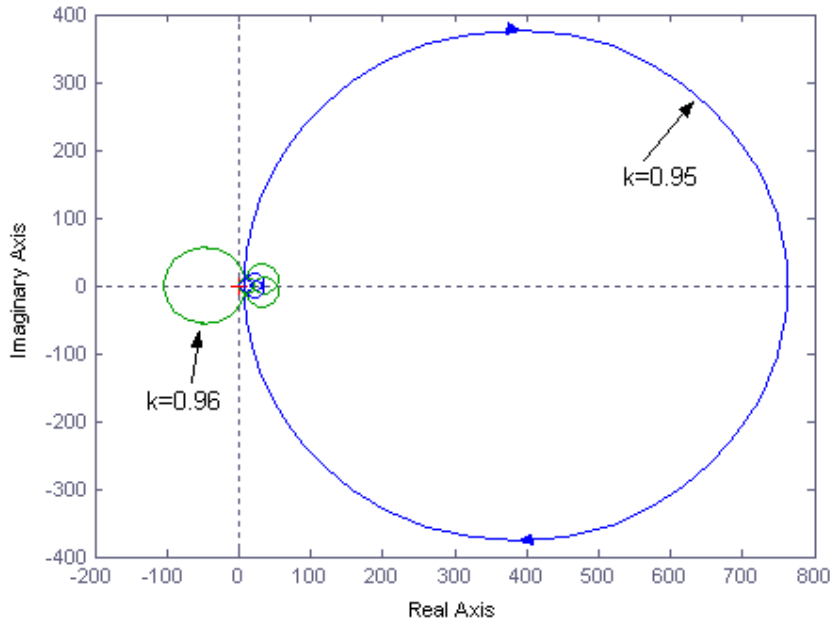


Fig 6.22: Nyquist diagram for $k=0.95$ and $k=0.96$ when a delayed insertion of $9\text{pcm}/^\circ\text{C}$ is considered: the green plot shows instability

Furthermore, if the power density is decreased by 20% the stability boundary is enhanced up to $k=0.96$.

The characteristic times for heat transfer play an important role; if the transfer coefficient is made 20% faster, the previous values are increased to $k=0.958$ and $k=0.966$ respectively. These values mostly depend on thermo dynamical properties of materials and on the geometry of the design.

Since the values attributed to the parameters are not always accurate and not proved by experiments, it is not possible to define the critical value for k precisely.

Despite this limitation, the results show that even under severe accident conditions ADS can exhibit a stable behaviour at quite high sub-criticality level.

Moreover, the frequently chosen value of $k=0.98$ can be taken at BOL (beginning of life) and it lowers during fuel lifetime.

The results presented so far describe ADS as a stable system at quite high sub-criticality level (~ 0.96) and at reference power density, in agreement with the value currently proposed [Schikorr, 2001; Rubbia, 1995].

Nevertheless, it cannot be denied that at lower sub-criticality level the instability risk under severe accidental conditions is present.

Therefore, it is important to study the typical time scale of ADS response when instability is present, to understand whether the system is controllable or not.

This is done giving a step-wise change in the source strength, which is the most severe way to perturb the system.

Fig 6.23 and 6.24 describes some typical transients.

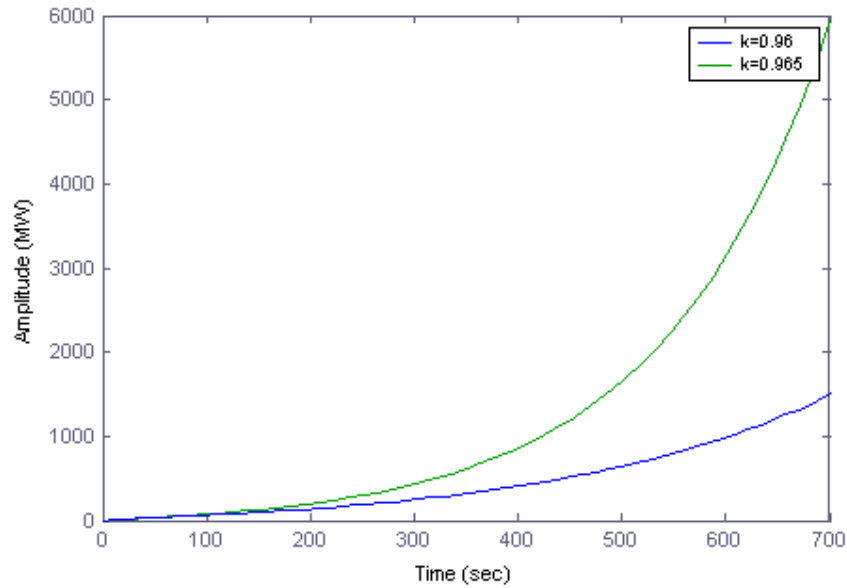


Fig 6.23: step response under unstable conditions

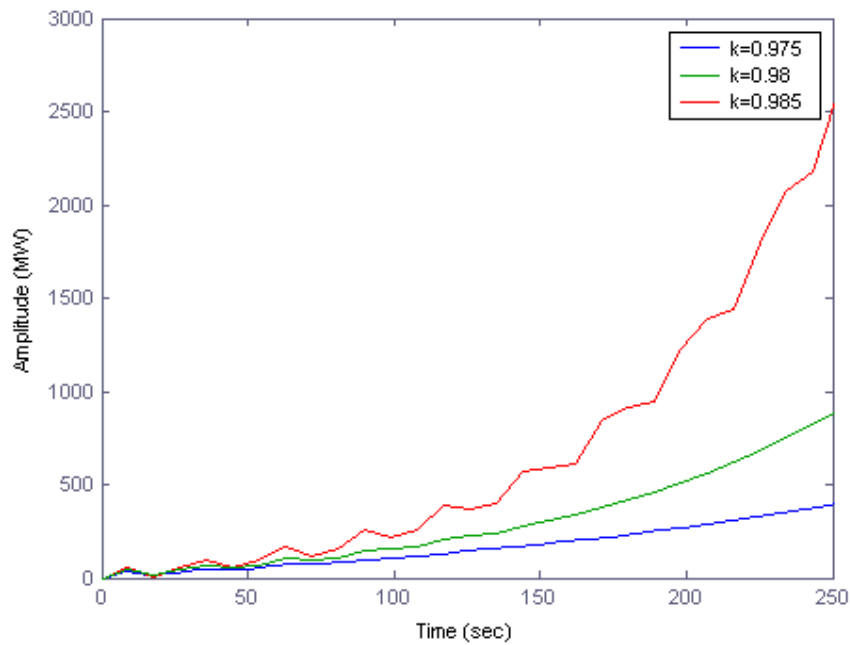


Fig 6.24: step response under unstable conditions when the power density and the characteristic time for heat transfer are lowered by 20%

From these two figures it is evident that the system, even if unstable, can be controlled because it takes some time before the power increases exponentially.

Some actions could thus be taken within that period.

At $k > 0.98$ control becomes more problematic, especially at high power density.

Prompt and delayed reactivity insertions

Besides clad melting, several other situations may lead to a variation of the working conditions.

For example, depending on design specifications, fuel rods bowing can be perceived as a positive prompt effect. Gaseous fission fragments can be released when the integrity of the cladding material is not perfect, causing a positive reactivity insertion due to voiding. In addition, any external cause can be translated in a positive or negative reactivity insertion but these effects are normally small.

A prompt and delayed positive reactivity insertion can simulate these effects. For simplicity, the delay is assumed the same as the coolant and the reactivity is worth $1\text{pcm}^{\rho}C$.

Fig 6.25 shows that the stability is guaranteed in both cases but the magnitude of the fluctuations differs at intermediate frequency.

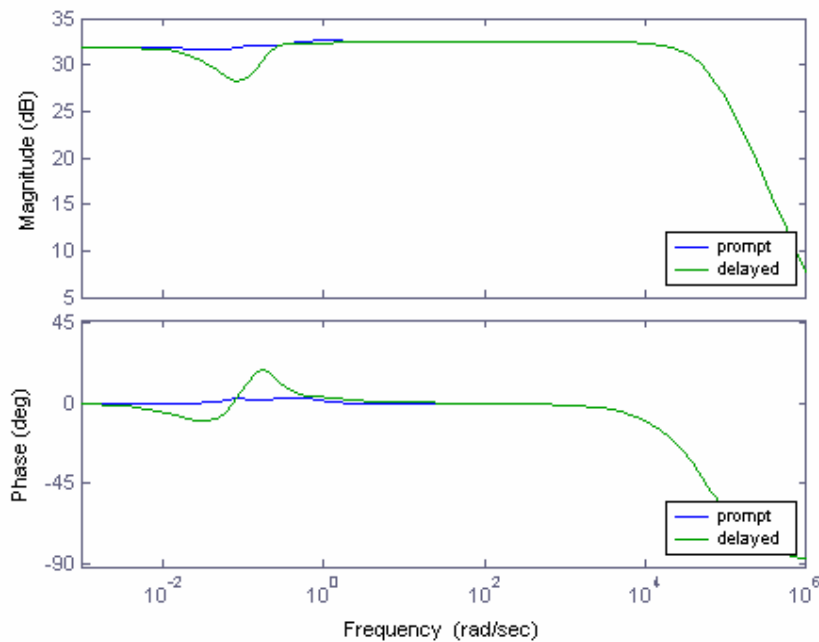


Fig 6.25: Bode diagrams for a prompt or delayed reactivity insertion of $1\text{pcm}^{\rho}C$; $k=0.98$

In Fig 6.26 the response to a step-wise change in the source is given. In case of delayed reactivity insertion, the power drops significantly after the prompt response because of the stronger prompt negative feedback.

Since the magnitude of the reactivity change is the same in both cases, the reactor approaches the same new steady state power level.

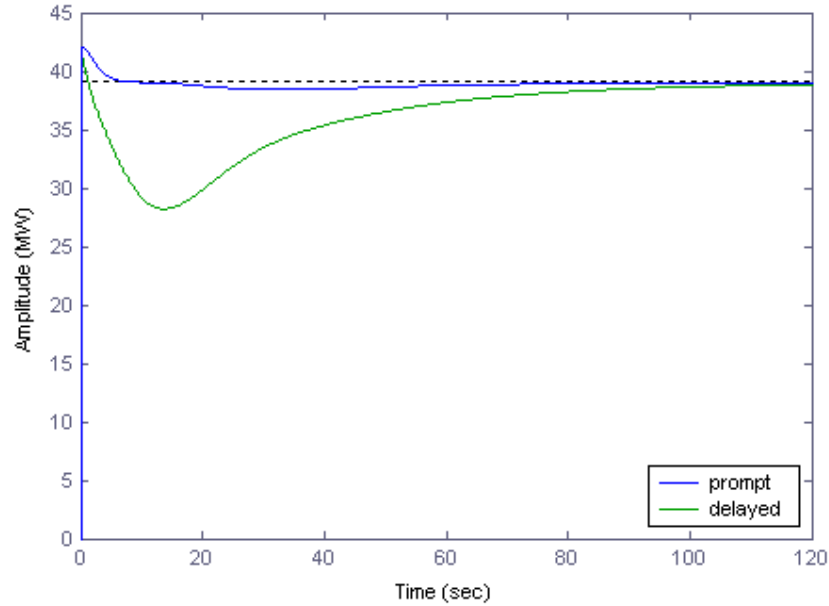


Fig 6.26: step-input response for a prompt or delayed reactivity insertion of $1\text{pcm}/^\circ\text{C}$; $k=0.98$

6.7 Stability analysis in case of reactivity fluctuations

This section briefly describes ADS behaviour in presence of reactivity fluctuations. Provided that the source strength is the most relevant parameter in driving the system, the interest in reactivity fluctuations is justified by some effects related to heat removal system.

Since the heat is removed by natural circulation, simulations have shown that when the source is shut down the lack of the driving force for natural circulation will lead to oscillations in the flow rate and hence in the temperature of fuel, cladding and structures. These thermal oscillations can be perceived by the system as reactivity fluctuations [Ceballos,2004].

Reactor response to reactivity fluctuations is given by the equation:

$$G(s) = \frac{\delta N(s)}{\delta R(s)} = \frac{n_0}{ls + \beta - \rho_0 - \sum_i \frac{\beta_i \lambda_i}{s + \lambda_i}} \quad (4.7)$$

where n_0 is the steady state power density and ρ_0 is the sub-critical reactivity level. Equation (4.7) has been derived under the assumptions of small reactivity oscillation ($|\delta n| \ll n_0$), to neglect higher order terms.

For this reason, the validity of the equation is limited to fluctuations with amplitude varying from some pcm up to a few tens of pcm .

The feedback transfer function is expressed by equation (6.20) considering that, for dimensional coherence, the term n_0 must be neglected.

The poles and zeros map shows that the poles are always real and negative: the system is stable.

Additionally, all the zeros and poles are at low frequency except for a high frequency pole, which determines a cut off in the amplitude of the response.

The Nyquist plot in Fig 6.27 confirms the previous results.

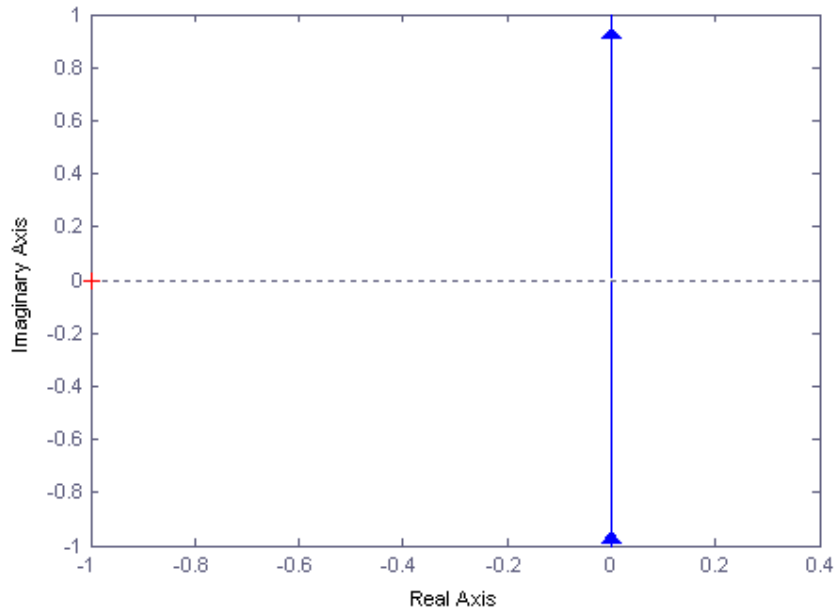


Fig 6.27: Nyquist plot in case of reactivity fluctuations at $k=0.98$

Loss of coolant or defects in the cladding material can be modelled by a step-wise or ramp-wise change in the reactivity level.

Fig 6.28 shows the response to a 10 pcm step-wise reactivity insertion. After a rapid increase in the power level, the presence of an overall negative feedback makes the reactor power to approach a lower asymptotical value. As in the case of source fluctuations, a higher sub-criticality level causes a lower power peak.

Fig 6.29 gives the response to a ramp-wise reactivity change for different sub-criticality level. The difference between Fig 6.28 and Fig 6.29 mostly concerns the time scale: for the ramp case the transient is longer.

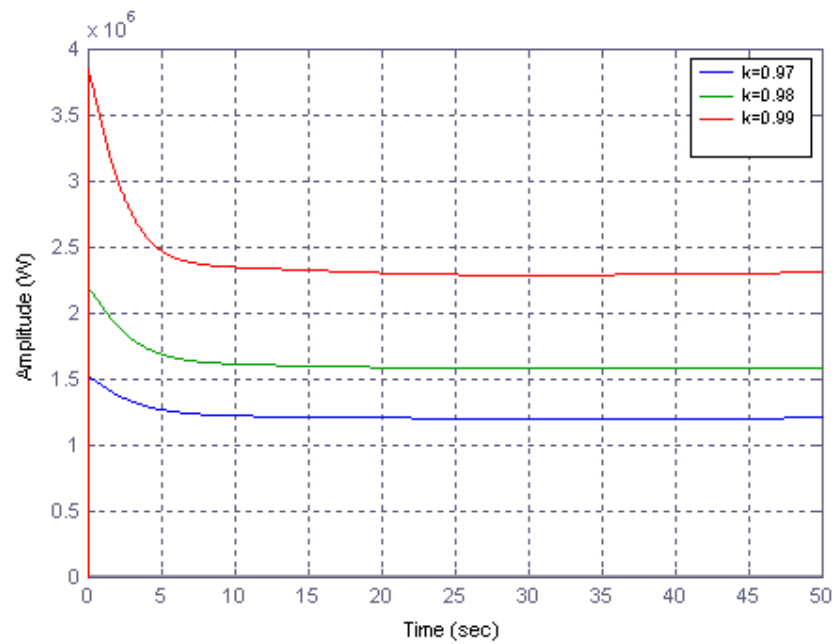


Fig 6.28: response to a 10 pcm step-wise reactivity insertion

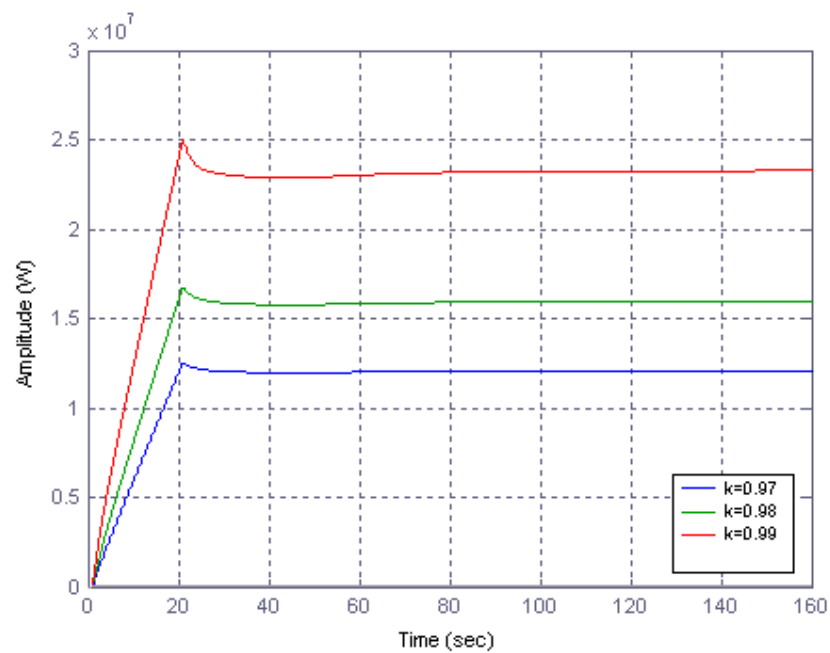


Fig 6.29: response to a ramp-wise reactivity insertion of 100 pcm in 20s

This thesis has studied ADS from two different perspectives: in chapter 5 the dynamic behaviour of the system has been analyzed analytically when the source strength is varied step-wise or according to a ramp profile while chapter 6 presents a stability analysis of the ADS under source fluctuations, using linear stability theory. The system under study is a 1500 MW_{th} lead cooled ADS, driven by natural circulation, with dimensions and power density typical of an industrial facility. However, this work does not focus on a specific design but tries to broaden the perspective by identifying which are the most important parameters and by studying their influence in the characteristic response.

The solution of Point Kinetics in the one group approximation shows that the response of ADS to source variations is typical of a sub-critical system. The magnitude of the source variation determines the new asymptotic power level. Since the ADS is sub-critical, the power cannot grow exponentially unless the system is made critical by a positive reactivity insertion.

The most important parameter is the sub-criticality level, expressed by the multiplication factor k . Results have shown that lower k , which means higher sub-criticality level and stronger source, causes a higher initial prompt response and a faster transient because delayed neutrons are not important: the transient is mainly driven by the source. Lower k also guarantees a higher safety margin. Since the source is stronger, it is more difficult to have a reactivity insertion strong enough to lead to criticality.

Changes in the fuel composition, which cause variations in the delayed neutrons fraction β and in the decay constant for precursors γ , influence the response. However, their effect is limited to 5-10% during the transient and does not affect the asymptotic power level.

A non-dimensional analysis of the system has shown that the parameters β, λ and l are both physically and “formally” independent. In addition, the power ratio is always a function of the source strength ratio.

The stability analysis has shown that a sub-critical system is an interesting option because the reactor core is always stable at any sub-criticality level. In addition, if the coolant is LBE and the fuel rods design is properly assessed, the feedback coefficient is always negative and thus the stable behaviour of the system is enhanced.

In normal operating conditions the only positive feedback coefficient, due to structural material expansion, is small and delayed. Hence, it does not influence the response of the system significantly.

Criticality can be reached in severe accidents like clad melting or unexpected positive reactivity insertions. Under normal conditions a positive effect from fuel rod bowing can lead to criticality only if the system is slightly sub-critical.

The value for k currently proposed by the majority of the research groups is around 0.98-0.97 at the beginning of life (BOL). Fuel burnup lowers this value by some percents, leading to $k \approx 0.96$ or less at the end of the fuel cycle.

Under accident condition a sufficiently low k can avoid criticality to be reached. Values below 0.95 at BOL would probably solve most of the problems but they would require too high proton current from the accelerator.

Values between 0.96 and 0.97 still give very high safety margin because even if instability occurs the time scale is large enough to allow effective actions.

Therefore, the ADS should work in a range for k between 0.95 and 0.97. The results found in this thesis prove that this choice would guarantee a stable behaviour during the whole fuel cycle and controllable power increase when instability is reached in the most severe accident conditions

In a ADS for industrial use the power density n_0 is significantly larger than in the experimental XADS. However, careful assessment in the design can reduce the original value proposed by Rubbia and thus enhance the stability range under severe accident conditions.

The characteristic time for heat transfer, which depends on material and thermo-hydraulic properties, is another important parameter that influences the system response. It has been shown that under accident conditions a faster heat transfer coefficient improves the stability range because the positive feedback has less time to act.

Recommendations for further research

The Point Kinetics model used in this thesis does not consider spatial effects. Since in the ADS the neutrons source is concentrated in the middle of the core, the flux profile is not uniform and spatial effects can be relevant. Therefore, this work could be improved considering a better analytical description of sub-critical systems.

The stability and parametric analysis has lead to the identification of the most important parameters and of some critical conditions for the system. Further work has to consider numerical simulations to study specific transients and determine when the limit temperatures of fuel, coolant and structure are exceeded.

Appendix: Matlab codes

Appendix A₁: 6 groups model

% Definition of the parameters

```
clear all;
```

```
beta1=8.6e-5;  
beta2=7.3e-4;  
beta3=6.55e-4;  
beta4=1.267e-3;  
beta5=5.8e-4;  
beta6=1.82e-4;
```

```
beta=350e-5;
```

```
lambda1=0.0129;  
lambda2=0.0313;  
lambda3=0.1346;  
lambda4=0.3443;  
lambda5=1.3764;  
lambda6=3.7425;
```

```
lambda=0.0897;
```

```
k=0.98;          % k can vary within the range 0.95<k<0.99
```

```
rho=(k-1)/k
```

```
l=4.2e-7;
```

```
G1=tf([beta1*lambda1],[1 lambda1]);  
G2=tf([beta2*lambda2],[1 lambda2]);  
G3=tf([beta3*lambda3],[1 lambda3]);  
G4=tf([beta4*lambda4],[1 lambda4]);  
G5=tf([beta5*lambda5],[1 lambda5]);  
G6=tf([beta6*lambda6],[1 lambda6]);
```

% Definition of the summation term

```
G_sum=G1+G2+G3+G4+G5+G6;
```

% Definition of the other part of the denominator

```
Gd=tf([1 (beta-rho)],[1]);
```

% Definition of the denominator

```
G_den=Gd-G_sum;
```

% Definition of the forward-loop transfer function

```
G=inv(G_den);
```

% poles-zeros map, Bode diagrams, step response are plotted using the user-defined functions. Variations of any type in the source strength can also be generated by creating the desired signal.

Appendix A₂: 6 groups model with prompt or delayed feedback

```
% Definition of the parameters
clear all;

beta1=8.6e-5;
beta2=7.3e-4;
beta3=6.55e-4;
beta4=1.267e-3;
beta5=5.8e-4;
beta6=1.82e-4;

beta=350e-5;

lambda1=0.0129;
lambda2=0.0313;
lambda3=0.1346;
lambda4=0.3443;
lambda5=1.3764;
lambda6=3.7425;

lambda=0.0897;

k=0.98;      % k can vary within the range 0.95<k<0.99
rho=(k-1)/k;
l=4.2e-7;

G1=tf([beta1*lambda1],[1 lambda1]);
G2=tf([beta2*lambda2],[1 lambda2]);
G3=tf([beta3*lambda3],[1 lambda3]);
G4=tf([beta4*lambda4],[1 lambda4]);
G5=tf([beta5*lambda5],[1 lambda5]);
G6=tf([beta6*lambda6],[1 lambda6]);

% Definition of the summation term
G_sum=G1+G2+G3+G4+G5+G6;

% Definition of the other part of the denominator
Gd=tf([1 (beta-rho)],[1]);

% Definition of the denominator
G_den=Gd-G_sum;

% Definition of the reactor transfer function
G=inv(G_den);

% CASE 1: lumped model; no delayed feedback
alfa=1.727e-5;
K=0.437e-6;
gamma=0.425;

% Feedback transfer function
H=tf([n0*K*alfa],[1 gamma]);

% System transfer function
GH=feedback(G,H);
```

```

% CASE 2: Prompt and delayed feedback
alfa_pr=1.69e-5;
alfa_cool=-0.863e-5;
alfa_str=-0.1e-5;
K_fuel=0.342e-6;
n0=523e6;
gamma_fuel=0.25;
gamma_cool=0.47;
gamma_str=0.21;

% Delays for coolant and structures
d_c=30;
d_s=3; d_t=d_c+d_s;

% Feedback Transfer Function
% Fuel
H_f = tf([alfa_pr*K_fuel*n0],[1 gamma_fuel]);

% Coolant
H_c=tf([alfa_cool*gamma_cool*K_fuel*n0],[1 (gamma_fuel+gamma_cool)
gamma_fuel*gamma_cool]);
% Second order Pade's approximation
D_c=tf([(d_c^2)/12 -d_c/2 1],[(d_c^2)/12 d_c/2 1]);
H_c_d=H_c*D_c;

% Structure
H_str=tf([alfa_str*gamma_cool*gamma_str*K_fuel*n0],[1 (gamma_fuel+gamma_cool+gamma_str)
((gamma_fuel*gamma_cool)+gamma_str*(gamma_fuel+gamma_cool))
gamma_fuel*gamma_cool*gamma_str]);
% Second order Pade's approximation
D_str=tf([(d_t^2)/12 -d_t/2 1],[(d_t^2)/12 d_t/2 1]);
H_str_d=H_str*D_str;

% Overall Feedback Transfer Function
H_t=H_f+H_c_d+H_str_d;

% System in the feedback configuration
S=feedback(G,H_t)

% poles-zeros map, Bode diagrams, step response are plotted using the user-defined functions.
Variation of any type in the source strength can also be generated by creating the desired signal.

```

References

- [1] D.L Hetrick, *Dynamics of Nuclear Reactors*, American Nuclear Society, 1993
- [2] G.I. Bell, S. Glasstone, *Nuclear Reactor Theory*, Van Nostrand Reinhold Company, 1970
- [3] H.H. Hummel, D. Okrent, *Reactivity Coefficients in Large Fast Power Reactors*, American Nuclear Society, 1970
- [4] A. Hitchcock, *Nuclear Reactor Stability*, Temple Press, 1960
- [5] Rubbia, Rubio, Buono, Carminati, Fietier, Galvez, Geles, Kadi, Klapisch, Mandrillon, Revol and Roche, *Conceptual Design of a fast neutron operated energy amplifier*, CERN/AT/95-44, 1995
- [6] *A European Roadmap for Developing Accelerator Driven System (ADS) for Nuclear Waste Incineration*, ENEA, 2001
- [7] W.M. Schikorr, *Assessments of the kinetic and dynamic transient behaviour of subcritical systems (ADS) in comparison to critical reactor systems*, Nuclear Engineering and Design 210 , 2001.
- [8] H. Nifenecker, S. David, J.M. Loiseaux and O. Meplan, *Basics of accelerator driven subcritical reactors*, Nuclear Instruments and Methods in Physics Research A 463, 2001, pg 428-467
- [9] H.Conde', *Introduction to ADS for Waste Incineration and Energy Production*, Dept of Neutron Research, Uppsala University, Sweden, 2002
- [10] L. Mansani, R. Monti, P. Neuhold, *Proposed sub-criticality level for an 80 MW_{th} Lead-Bismuth-cooled ADS*, Ansaldo Nuclear Division, Genova, Italy, 2002
- [11] J.Carlsson, H.U.Wider, *Safety Aspects of Larger Heavy Metal-Cooled Accelerator Driven System*, Joint Research Centre of the EC, Petten, 2003
- [12] L. Cinotti, B. Giraud, H. Ait Abderrahim, *The XADS Designs in the 5th FP*, 2003
- [13] C. Ceballos, D. Lathouwers, A. Verkooijen, *Study of transients in a natural circulation liquid metal cooled ADS*, 6th International Conference on Nuclear Thermal Hydraulics (NUTHOS-6), Nara, Japan, October 2004
- [14] *Proceedings of an Information meeting on Accelerator-Breeding*, Brookhaven National Laboratory, January 18-19 1977, BNL Report CONF-77010

- [15] *Energy for Tomorrow's World*, World Energy Council (WEC), 1993
- [16] A.D'Angelo, F.Gabrielli, *Benchmark on Beam Interruptions in an Accelerator Driven System*, 2003, NEA/NSC/DOC 17, Issy-les-Molineaux, France
- [17] A. Hainoun, I. Khamis, G. Saba, *Dynamic analysis of the closed loop transfer function in the miniature neutron source reactor (MNSR)*, Nuclear Engineering And Design, 2004
- [18] A.Gandini, M. Salvatores, *The Physics of Subcritical Multiplying Systems*, Journal of Nuclear Science and Technology, Vol.39, No.6, June 2002
- [19] <http://www.vibrationdata.com/Laplace.htm>
- [20] <http://www.mathworld.wolfram.com/LaplaceTransform.html>
- [21] <http://www.mathworks.com>